Phase diagram and correlation exponents for interacting fermions in one dimension

Eugene B. Kolomeisky

Laboratory of Atomic and Solid State Physics, Cornell University, Ithaca, New York 14853-2501

Joseph P. Straley

Department of Physics and Astronomy, University of Kentucky, Lexington, Kentucky 40506-0055

A theory is given for the ground-state properties of short-ranged interacting spin-$\frac{1}{2}$ fermions moving in a periodic potential, based on a combination of renormalization-group ideas, the harmonic (Luttinger) liquid approach, and the symmetry properties of the Hubbard model, for a wide range of interactions and arbitrary fillings. For rational filling factors the outcome depends nontrivially on the parity of the order of the $2k_F$ umklapp scattering: even values fall into a universality class characterized by a separation of charge and spin degrees of freedom in the long-wavelength limit, while the action for the case of odd orders does not have this property, thus leading to distinct phase diagrams. It is argued that even when the long-wavelength action does exhibit a spin-charge separation it is not always an accurate approximation, particularly for the case of strong repulsion between electrons of the same spin. This leads to a classification of the possible ground states, associated correlation exponents, and phase transitions. The translational correlation exponents upon approaching insulator phases (existing at exact commensuration) by changing electron density can be related to the fractional charge of the solitons, using the Landauer rule.

CONTENTS

 0034-6861/96/68(1)/175(40)/$13.00

I. INTRODUCTON

A. Introduction and motivation

The static and transport properties of a one-dimensional system of electrons moving in a periodic potential are determined by the interplay between three conflicting forces.

The first is the system's quantum nature (i.e., the uncertainty principle), which pushes it towards disorder and lack of any correlation among the particles. Even in higher dimensionality, where quantum fluctuations are expected to be less important, they still are more important than the interactions, so that the Landau Fermi-liquid theory successfully represents much of the physics. One-dimensional many-body problems are more complex (Emery, 1979a; Solyom, 1979)—indeed, an interacting system does not properly have a Fermi surface at all (Luttinger, 1963; Gutfreund and Schick, 1968)—but, parts of the Fermi language remain useful.

The second determining force is the interaction between the particles, which will be different for particles of the same spin and particles of different spin. Under this heading we can include the Pauli exclusion principle, whose effect in one dimension can be imitated by a contact interaction between particles of the same spin. The interparticle interactions make the system behave more like an elastic fluid (the Luttinger liquid) with a low-energy excitation spectrum of acoustic type; it becomes almost meaningful to talk about interparticle spacings. The interactions between particles of different spins can further lead to correlations in the spin density, so that in various limits we may have an uncorrelated fluid, a "superconductor" composed of pairs of opposite spin, or an "antiferromagnet" with spin orientation alternating along the line.[1]

The presence of an external periodic potential further complicates the problem. If the interparticle spacing is commensurate with the period of the potential, the properties of the system can be greatly modified; with sufficiently weak quantum fluctuations the particles will be completely localized and an insulator results. Even in the conducting phase there is a decrease in the conductance near commensuration. Repulsive interparticle forces will facilitate the ability of the external potential to localize the particles, because they tend to make the particle spacing more uniform and thus accentuate the periodicity.

The spin-up and spin-down electrons are physically identical and have the same interactions with particles of the same spin. The interparticle interaction between the two degenerate systems is never a small perturbation, and the resulting eigenstates are the sum and difference of the two fields. Thus the natural variables for the problem are the charge density ($\uparrow+\downarrow$) and spin density ($\uparrow-\downarrow$). For a translationally invariant system, this separation of spin and charge is a rigorous property. However, a periodic potential can destroy this separation, notably when the spin ordering is incommensurate with the periodicity of the potential, or when the interaction between particles of the same spin is very strong. However, in most cases of interest, the spin and charge fields are uncoupled, and the original problem is split into two simpler ones.

A great deal of the description of the interacting quantum fluid can be given in terms of the parameters g_C^* and g_S^*. These are defined as the exponents that characterize the algebraic decay of the two-point correlation functions due to charge ("C") and spin ("S") fluctuations (this will be discussed further in Sec. I.F). They can be computed from the parameters of the harmonic description of the system: the mass density, compressibility, and susceptibility; and they are conveniently thought of as measures of the degree of quantum fluctuation in the system.

1. Exact solutions

Exact solutions have played an important role in furthering our understanding of the properties of one-dimensional systems. Several solutions are particularly relevant to the present discussion:

(a) Gaudin (1967, 1983) and Yang (1967) calculated the ground-state energy, spectrum, and wave functions for the continuum Hubbard model (fermions with a delta-function interaction between opposite spins) by means of the Bethe ansatz. They found that this model leads to a metal for repulsive interactions and a superconductor for attractive interactions.

(b) Lieb and Wu (1968) gave the equivalent treatment for the lattice version of the same problem (fermions with interaction between particles of opposite spin on the same site), which is then the simplest model for the effect of a periodic external potential. They found that attractive interactions always lead to a superconductor, and that repulsive interactions lead to a metal, except at half-filling, where an antiferromagnetic insulator results. There are no phenomena associated with other rational fillings.

(c) Luther and Emery (1974) found that the spin part of a translationally invariant model allowing for interaction between particles of the same spin could be solved by transforming it into a "superconductor" model (free-fermion-like excitations with filled and empty bands, separated by a gap) for a special ratio of the unlike-spin/like-spin interaction, which corresponds to a particular value of g_S. We shall refer to this set of parameters as the Luther-Emery line.

(d) Emery, Luther, and Peschel (1976) considered the lattice version with a half-filled band and showed

[1]We hasten to note that this characterization in terms of spatial ordering of the spin does not confer all the other properties associated with antiferromagnetism and superconductivity in higher dimensionality; in what follows we shall encounter insulating "superconductors" and perfectly conducting "antiferromagnets".

that an analogous solution can be obtained for the charge degrees of freedom for a particular value of g_C. The corresponding phase is an antiferromagnet.

(e) Pokrovsky and Talapov (1979) solved exactly a model of the commensurate-incommensurate transition in two dimensions at finite temperature. This is related to the metal-insulator transition in a one-dimensional quantum system, through the path-integral representation of the quantum problem. Their solution describes the behavior along the Luther-Emery line at and away from half-filling.

(f) Schulz (1980) calculated the density correlations near the commensurate-incommensurate transition (i.e., near the metal-insulator transition of a fractionally filled band, in the quantum context).

(g) Haldane (1982) solved the one-dimensional quantum sine-Gordon theory with nonzero soliton density. His solution gives a general description of the metal-insulator transition and contains the solutions of Luther and Emery, Pokrovsky and Talapov, and Schulz as special cases.

(h) Efetov and Larkin (1975) found an exact solution for a lattice model of attractive fermions (with attraction between particles of the same spin, in addition to a large negative Hubbard interaction) at half-filling for a special value of the intraparticle interaction that corresponds to g_C=4. This is a conductive phase.

(i) Emery (1976) related a generalized Hubbard model in the limit of strong Hubbard attraction to the exactly solved (Luther and Peschel, 1975) quantum XXZ spin-chain problem and was able to calculate the exponent g_C^* for a range of nearest-neighbor attraction, reproducing the result of Efetov and Larkin as a special case. These models always yielded conducting phases, with g_C^* approaching 2 (the free-fermion value) in the Hubbard limit.

(j) Fowler (1978) extended Emery's connection to the case of nearest-neighbor repulsion and showed that the resulting phases are all insulators with an energy gap that, for small nearest-neighbor interactions, behaves in a way typical of a Kosterlitz-Thouless transition. Together with Emery's work, this suggests that the Hubbard model is a marginal case and lies along the boundary between metal and insulator for an attractive Hubbard interaction.

(k) Luther (1976, 1977) has argued that, for a repulsive interspin interaction, there is again a relationship with the quantum XXZ chain, yielding an antiferromagnet at half-filling with any interaction strength.

(l) Schulz (1990) solved exactly a quarter-filled generalized Hubbard model with infinite Hubbard repulsion and showed that there is a transition from the metal to the insulator phase for sufficiently repulsive nearest-neighbor interactions. He also calculated g_C^* in the conducting phase as a function of nearest-neighbor interaction.

2. Phenomenological approaches

At the time that exact solutions were being formulated, important advances were made with phenomenological approaches.

Perturbative renormalization-group analysis has been very useful in indicating that one-dimensional many-body problems have behavior quite different from that implied by the Landau Fermi-liquid theory (Emery, 1979a; Solyom, 1979).

Much of the current activity in the field is related to the elucidation of another phenomenological idea, the "harmonic" (or Luttinger) liquid. First put forward in the 1970s (Popov, 1972; Efetov and Larkin, 1975) and then emphasized by Haldane (1980, 1981a–1981c), it allows us to calculate explicitly the correlation exponents—which to a considerable extent characterize the macroscopic properties of the quantum fluid—without directly evaluating the corresponding correlation functions.

Schulz (1990, 1991) applied this approach to the simplest nontrivial lattice model of interacting spin-$\frac{1}{2}$ fermions, the Hubbard model, and thereby provided us with a detailed description of the crossover between weak and strong interactions as well as of the metal-insulator transition that occurs at half-filling. Another important step was made by Giamarchi (1991), who argued that the results for the exponents of the correlation functions of the Hubbard model in the vicinity of half-filling are generic features of any Luttinger liquid.

Conformal field theory (Bogoliubov and Korepin, 1988, 1989; Frahm and Korepin, 1990, 1994; Kawakami and Yang, 1990) has also been applied to this problem, with similar results.

3. An overview of the present approach

Our discussion will be more closely allied with the phenomenological approaches, though our theory is certainly influenced by knowledge of the exact results. We shall attempt to convince the reader that there is a great deal of universality in one-dimensional models, an idea pioneered by Luther and Peschel (1975). The starting point and the derivation of the basic equations is similar to the approach of Emery (1979b).

As already noted, the interacting electron system is best represented in the long-wavelength limit in terms of fields representing the fluctuations in the spin and charge densities. In the vicinity of rational filling k/l (where k/l is an irreducible fraction), the most important processes are $2lk_F$ and $4lk_F$ umklapp scattering, where k_F is the Fermi wave vector. When l is even, the spin and charge degrees of freedom are decoupled, and the theory reduces to a pair of independent sine-Gordon models. This model can be studied using perturbative renormalization, and we shall adopt the renormalization language generally.

The simplest case is half-filling ($l=2$), because the Hubbard model has a particle-hole symmetry, which further simplifies the phase diagram. The renormalization-group diagram describing the flow of the charge degrees of freedom is so constrained by the symmetry of the problem that we think we understand it completely for a wide range of interactions. Comparison of this diagram with various exact results puts them in appropriate places in the flow. The Hubbard model itself is a marginal case, dividing the regime of insulating and conducting phases, so that any generalization that suppresses quantum fluctuations (e.g., a short-ranged repulsive interaction between particles of the same spin) leads to an insulator, while a generalization that increases the quantum fluctuations (e.g., an attractive short-range interaction) will yield a conductor. For this reason we shall dedicate considerable effort to the characterization of this model in the limits of large and small Hubbard interaction. Then the behavior of generalizations of the Hubbard model can be predicted rather simply. The behavior of the correlation functions near half-filling can also be understood phenomenologically by introducing a condition cutting off the flow on a length scale corresponding to the average distance between the vacancies or extra particles.

The vicinity of other rational filling factors k/l is more complex. For even l, there continues to be a separation of charge and spin degrees of freedom, but for odd l the separation is not achieved and the problem falls into a different universality class, which we discuss in Sec. V.C. Even when the spin-charge separation does exist, the corresponding action is still not accurate enough to describe physical systems with strong repulsion between electrons of the same spin. We shall identify these new contributions and find a corresponding set of exponents. All this puts some limitations on the existing results (Giamarchi, 1991) and classifies possible phases, phase transitions, and types of critical singularities that can be found in generic interacting spin-1/2 fermionic systems in one dimension.

B. The model

In one dimension the distinction between bosons and spinless fermions is not as significant as it is in higher dimensionality, because we cannot go from a configuration to one with exchanged particles without having two particles at the same point in space at some intermediate stage. If we restrict ourselves to the sector in which the particles are in order along the line ($x_1 \leqslant x_2 \leqslant \cdots \leqslant x_M$), the Pauli exclusion principle reduces to a boundary condition specifying the vanishing of the wave function whenever two particles are at the same coordinate. It follows that, for any interacting fermion problem, there is a corresponding interacting boson problem (for example, free fermions correspond to hard-core point bosons) that has many of the same physical properties. In what follows we shall use this correspondence to treat the system in the bosonic representation. However, we shall keep the language of the fermionic representation, since this is the problem of interest.

Introduction of spin does not greatly complicate the problem. For any choice of the axis of quantization, the fermionic wave function has a representation in terms of the coordinates of the two populations of "spin-up" and "spin-down" particles; the number of particles of each type is fixed whenever the total spin is a good quantum number.

We may then introduce the basic model for this paper: two sets of particles, possibly with different (spin-dependent) like-spin and unlike-spin interactions, moving in an external potential. Restricting ourselves to two-body forces, we can write the action as follows:

$$A=\int dt\Bigg\{\sum_{j=1}^{N}\left[\frac{m}{2}\left(\frac{dx_j}{dt}\right)^2-\mu\right]+W\sum_{i<j}^{N}\delta_a(x_i-x_j)+\sum_{j=1}^{N}V(x_j)+\sum_{j=1}^{N}\left[\frac{m}{2}\left(\frac{dy_j}{dt}\right)^2-\mu\right]+W\sum_{i<j}^{N}\delta_a(y_i-y_j)+\sum_{j=1}^{N}V(y_j)+U\sum_{i,j}^{N}\delta_a(x_i-y_j)\Bigg\}, \tag{1.1}$$

where t is the imaginary time variable, N is the number of particles of each spin direction (the total is $2N$ particles), m is the particle mass, the x's and y's stand for the coordinates of the particles of the two types, μ is their common chemical potential, W is the amplitude of the interaction between like spins, $V(x)$ is a spin-independent external potential of period b: $V(x+b)=V(x)$, U is the amplitude of the unlike-spin (Hubbard) interaction, and the notation $\delta_a(x)$ refers to any well-localized function with characteristic size a that reduces to the mathematical δ function as $a\to 0$. The wave function in path-integral representation corresponding to the action (1.1) can be viewed as a classical partition function for a collection of $2N$ interacting line objects running along the t direction (the world lines of the two different kinds of particles) subjected to an external potential with the chemical potential controlling the average line (particle) density $n=N/L$, where L is the size of the system. The role of temperature in the equivalent classical two-dimensional problem is played by Planck's constant.

As already noted, this action describes bosons of two different types, but can be interpreted as describing spin-1/2 fermions if we choose the "on-site" part (the part having true delta-function form) of the like-spin interaction to be infinite. For instance, noninteracting free fermions are described by hard-core bosons, which is the case $W=\infty$, $a=0$, $V=0$, and $U=0$; the continuum version of the Hubbard model is given by $W=\infty$, $a=0$, $V=0$, and finite U. The absolute value of the wave function for fermions with a short-ranged attractive interaction between particles of the same spin is indistinguishable from the wave function for bosons with finite W outside the range of the interaction; in this sense the two systems are equivalent insofar as their density correlations are concerned. Exchange symmetry means that we need

to know only the wave function in one region $x_1 \leqslant x_2 \leqslant x_3 \cdots \leqslant x_N$. The fermionic wave function necessarily vanishes at the boundaries, but for attractive fermions can be rapidly varying close to them, with an effective boundary condition that mimics soft-core repulsive bosons. In the resulting "bosonic" picture we always have $W>0$ to prevent collapse of the ground state.

C. Reduction to a field theory

The derivation of a long-wavelength continuum version of the original microscopic action (1.1) is analogous to that of Kolomeisky (1993) and is given in the Appendix. Here we only outline the main steps.

The displacements of the particles of each population with respect to their classical positions will be represented by the fields $u_\uparrow(x,t)$ and $u_\downarrow(x,t)$, where the arrows indicate the spin directions. The interaction terms between particles of the same type (the W terms) will be treated in the harmonic liquid approximation, which represents the interactions between the particles by a compliance. This gives a nonlinear two-component field theory, in which the fields $u_\uparrow$ and $u_\downarrow$ are coupled both through the U terms and through the harmonic part of the long-wavelength action, which contains their mixed spatial derivatives.

The harmonic part of the action can be diagonalized by the introduction of new variables C describing the center-of-mass motion of the spin populations, and S describing the relative displacement of one spin population with respect to the other:

$$C=\frac{u_\uparrow+u_\downarrow}{2}, \quad S=\frac{u_\uparrow-u_\downarrow}{2}. \tag{1.2}$$

As the nomenclature suggests, this corresponds to the transformation to the charge- and spin-density operators that diagonalize quantum Hamiltonians in other approaches (Emery, 1979a, 1979b; Solyom, 1979); the variable C describes the center-of-mass motion of the two populations and represents fluctuations in the charge, while S describes the relative displacements of one spin population with respect to the other and is then a spin degree of freedom.

The external potential is expanded into a Fourier series (see Appendix), and approximations are made appropriate to the assumption that we are concerned with the effects of fluctuations having wavelengths long compared to the interparticle distance n^{-1}. We also assume that the filling factor is close to an irreducible fraction $nb=k/l$, which then selects the terms arising from a particular Fourier component k of the potential and a particular order l of umklapp scattering as being particularly important. Then the action takes the form

$$A=A_{\text{harmonic}}+A_{\text{correlation}}+A_{\text{external}}, \tag{1.3a}$$

where

$$A_{\text{harmonic}}=\frac{1}{2}\int dxdt(\mu_S\dot{S}^2+K_S S'^2+\mu_C\dot{C}^2+K_C C'^2), \tag{1.3b}$$

$$A_{\text{correlation}}=\Gamma_1\int dxdt\ \cos 4\pi nS, \tag{1.3c}$$

$$A_{\text{external}}=\begin{cases}\Gamma_2\int dxdt\ \cos 2\pi(\rho x-nlC)+\Gamma_3\int dxdt\ \cos 4\pi(\rho x-nlC) & \text{for } l \text{ even}\\ \Gamma_2\int dxdt\ \cos 2\pi(\rho x-nlC)\cos 2\pi nS+\Gamma_3\int dxdt\ \cos 4\pi(\rho x-nlC) & \text{for } l \text{ odd}\end{cases} \tag{1.3d}$$

where $\rho=|nl-k/b|$.

We claim that this is the correct form for the long-wavelength action regardless of the strength of the short-range interactions, and that it can be written down at the outset. The harmonic part comes from the assumption that each spin population can be regarded to be a harmonic fluid and that the interaction between spin populations is short ranged. The structure of the nonlinear terms is dictated by symmetry considerations.

1. The harmonic terms

A_{harmonic} describes a pair of translationally invariant fluids. The dots and primes in Eq. (1.3b) represent time and space derivatives. The effective mass density μ_C and the reduced mass density μ_S are simply related to the particle density and mass. The other two parameters characterizing the harmonic fluids are the compliances K_C and K_S, which are determined by the unlike-spin and like-spin interactions.

The macroscopic properties of the system may also be described in the harmonic approximation, as long as $A_{\text{correlation}}$ and A_{external} are irrelevant, by an action of the same form with renormalized parameters μ_C^*, μ_S^*, K_C^*, and K_S^* that take into account the effects of $A_{\text{correlation}}$ and A_{external} (as well as the effects of terms that have already been dropped). Here there is an additional physical interpretation: K_C^* and K_S^* determine the change in free energy caused by changes in mass density

and spin density, and they are proportional to the reciprocal of compressibility and the susceptibility, respectively. In the absence of an external potential, translational symmetry implies that

$$\mu_C^* = 2\ \text{mn}. \tag{1.4a}$$

For the continuum Hubbard model [the $W=\infty$, $a=0$ case of Eq. (1.1)], the values of the phenomenological constants appearing in Eq. (1.2) are

$$\mu_C = \mu_S = 2\ \text{mn}, \tag{1.4b}$$

$$K_C = 2\pi^2\hbar^2 n^3/m(1+mU/\pi^2\hbar^2 n), \tag{1.4c}$$

$$K_S = 2\pi^2\hbar^2 n^3/m(1-mU/\pi^2\hbar^2 n), \tag{1.4d}$$

valid in the limit that $|U| \ll \pi^2\hbar^2 n/m$.

These relationships and the generalization to the case of finite W are derived in the Appendix.

2. Correlations between opposite spins

The $A_{\text{correlation}}$ describes an important effect of the unlike-spin interaction: it causes correlations in the relative positions of particles of the two spins. The coupling constant Γ_1 takes the value $\Gamma_1 = 2n^2 U$ in the limit of weak Hubbard interaction and $a=0$, and in general has the same sign as U; then for a repulsive Hubbard interaction the second term is minimized if $2nS$ takes on half-integer values (antiferromagnetic order), and for an attractive Hubbard interaction $2nS$ takes on integer values, representing a tendency for particles of opposite spin to pair. Thus the effect of this term will be to attempt to bring about an ordering of the field S, which will be signaled by the appearance of a gap in its spectrum.

3. Effect of the external potential

A_{external} describes the most important consequences of the external potential. The potential will be most effective when the average spacing of the particles is commensurate with one of its Fourier components; when these are not exactly the same there will be a finite density of discommensurations. This is measured by the parameter $\rho = |nl - k/b|$, where the index l is the order of $2k_F$ scattering and k is the index of the Fourier component; at commensuration, $nb = k/l$ and $\rho = 0$. In writing A_{external} we have displayed the terms for just one l and k; there is actually an infinite set of these, but the relevant term has small ρ. The precise values of the coefficients Γ_2 and Γ_3 are not important, except that we shall need to know that, in the limit of weak Hubbard interaction U, the parameter Γ_2 is proportional to U for $l>1$ and approaches a constant as $U \to 0$ and $l=1$, while the parameter Γ_3 is always proportional to U (see Appendix).

4. Separation of spin and charge

The variables C and S represent the charge and spin degrees of freedom, which are not coupled by A_{harmonic} or $A_{\text{correlation}}$. As explained above, this is a natural consequence of the symmetry between up and down spin in a translationally invariant theory. However, A_{external} can couple them when l is odd. The origin of the differing forms for even and odd l (Schulz, 1994; Kolomeisky and Straley, 1995) is explained in Fig. 1: when l is odd (as in the case of the one-third filled band), the external potential provides a bias favoring paired order over antiferromagnetic order of the spins; in contrast, when l is even (as in the case of the half-filled band), these two orderings are treated equivalently and there apparently is no coupling between the spin and charge degrees of freedom. This separation of spin and charge degrees of freedom greatly simplifies the problem when l is even. Indeed, for l even, the Γ_3 term of A_{external} can be dropped, since it will always be less relevant than the Γ_2 term. However, there are higher-order terms that have been dropped from Eq. (1.3d) that do couple the fields. These terms may invalidate the spin-charge separation in the strong-coupling limit.

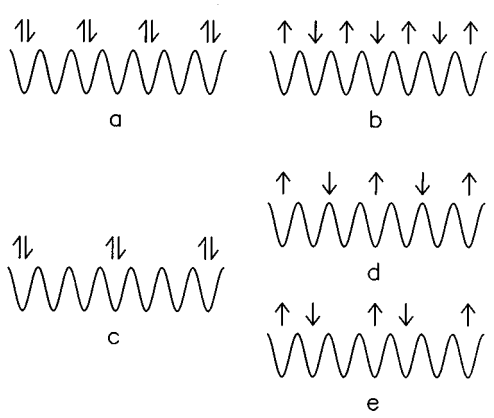

FIG. 1. Sketches of various extremal configurations of interacting one-dimensional spin-$\frac{1}{2}$ fermions in a periodic potential for the cases of $\frac{1}{2}$ (a and b) and $\frac{1}{3}$ (c–e) filled bands in the classical limit. The particles are represented by arrows indicating the spin direction, and the potential is shown by the solid curves. For the case of interspin attraction, the ground-state configurations (a and c) are insensitive to the parity of the denominator of the filling factor. For the case of interspin repulsion, the ground-state configuration is antiferromagnetic for the half-filling (b). For the case of $\frac{1}{3}$ filling, the ground-state configuration is not antiferromagnetic (d); instead it is dimeric (e).

For odd l the two fields are explicitly coupled; these cases will have to be treated separately. This arises in particular for the filled band, but also, for example, in the $\frac{1}{3}$-filling case.

5. Why the harmonic theory is the appropriate model in one dimension

The field theory expressed in Eq. (1.3) starts from an elasticity theory: the description is in terms of the sound and spin waves of the system. This might be regarded as an unusual place to start; certainly in three dimensions we would expect that single-particle degrees of freedom were more important, and indeed the theory for that

TABLE I. Various choices for correlation exponents and their notations used in the literature.

	This paper	Kane and Fisher, 1992a	Emery, 1979a, 1979b	Solyom, 1979	Schulz, 1990, 1991; Giamarchi, 1991
Charge exponent	g_C	g_ρ	$2\theta_c$	$2\gamma_\rho$	$2K_\rho$
Spin exponent	g_S	g_σ	$2\theta_s$	$2\gamma_\sigma$	$2K_\sigma$

case is written that way. However, in the present case we can give arguments why (1.3) is an adequate model and an appropriate long-wavelength description.

A single-particle excitation is, to first approximation, a motion of a single particle, ignoring the presence of the others. However, in a one-dimensional fermionic system, this description is useless, at least on scales exceeding the mean interparticle spacing, because the particles cannot pass each other at all. Thus the collective modes are a better description.

In higher dimensions the particles may or may not be able to move around each other, and then we can have liquids as well as solids. In one dimension the particles cannot freely move past each other, and as a result the possible condensed phases are closer to being solids.

Any system will have sound waves, because these are the Goldstone modes that correspond to the breaking of translational symmetry. We know that this description is incomplete in higher-dimensional systems whenever transverse phonon modes are absent, as they are in fluids and gases. In one dimension, however, the compressional modes necessarily exist, and these exhaust the one degree of freedom each particle has: the single-particle motions are already implicitly included in our description.

D. The correlation exponents

Two important dimensionless combinations can be formed from the parameters of the harmonic part of the action (1.3b):

$$g_S=\frac{\pi\hbar(2n)^2}{\sqrt{\mu_S K_S}}, \tag{1.5a}$$

$$g_C=\frac{\pi\hbar(2n)^2}{\sqrt{\mu_C K_C}}. \tag{1.5b}$$

We shall refer to these generically as g_ν ($\nu = C,S$). The parameter $2n$ that appears in Eq. (1.5) is the total electron density. With the bare μ's and K's these characterize the degree of quantum fluctuation in the spin and charge subsystems. For sufficiently large g_ν, $A_{\text{correlation}}$ and A_{external} are irrelevant (as are the higher-order irrelevant operators, which are not written down). We define renormalized parameters g_ν^*, μ_ν^*, and K_ν^* that characterize the long-distance behavior in that case (Popov, 1972; Efetov and Larkin, 1975; Haldane, 1980, 1981a–1981c). Our definition for g_ν (other than the notation) coincides with that of Kane and Fisher (1992a). Essentially the same exponents (1.5) have appeared by other names in previous approaches, as described in Table I.

If one or both collective modes of the system are gapless, they can be characterized by the corresponding sound velocities,

$$c_\nu^{*2}=K_\nu^*/\mu_\nu^*, \quad \nu=C,S. \tag{1.6}$$

Therefore the correlation exponents and the associated long-wavelength properties of the spin-$\frac{1}{2}$ quantum fluid are determined by the renormalized parameters μ_ν^* and K_ν^* whenever the corresponding mode is gapless. In this case the form of A_{harmonic} (1.3b) as well as the physical meaning of the fields S and C (1.2) imply that the parameter K_S^* is determined by the susceptibility of the system, while K_C^* is governed by the compressibility:

$$K_C^*=2n^2\frac{\partial\mu}{\partial n}\equiv(2n)^2\frac{\partial\mu}{\partial(2n)}, \tag{1.7}$$

where the second representation is again in terms of the total particle density $2n$. These formulas were used by Schulz (1990, 1991) to extract g_C^* from the exact solution of the Hubbard model (Lieb and Wu, 1968).

The model (1.1) contained the parameters m, U, W, $n=N/L$, a, and an amplitude and period for the potential $V(x)$. In going to the long-wavelength action (1.2), the first five determine the four microscopic values for μ_ν and K_ν according to Eqs. (1.4a)–(1.4d). If the measurable properties of the system are such that spin and charge degrees of freedom do not interact on a macroscopic scale, then each subsystem that is a harmonic liquid is described completely in terms of its renormalized parameters μ_ν^*, K_ν^*. The mean interparticle distance n^{-1} sets a "microscopic" scale in the problem, and the combinations $n\sqrt{\mu_\nu^*/K_\nu^*}$ set "elementary" time scales. These two are of secondary importance to the equilibrium properties of the system, as they just specify what units are being used. On the other hand, the only dimensionless combinations that can be comprised out of μ_ν^*, K_ν^*, n, and Planck's constant $\hbar$ have the form (1.5a), (1.5b). These will play a central role in determining the macroscopic properties of the system. This argument also suggests that the combinations (1.5a), (1.5b), which comprise the *bare* parameters of the problem, will be important in determining the role of the nonlinear terms of the action (1.3). Renormalization theory will provide the prescription for determining how the microscopic values of g_C and g_S combine with the nonlinear part of the action to determine the measurable exponents g_C^* and g_S^*.

1. One-point density correlations

We show now how to relate the parameters g_ν (1.5) with the properties of the density correlations of the

quantum liquid. Other correlation functions can be also readily found (Emery, 1979a; Solyom, 1979). The method we are using is a generalization of a similar calculation of correlations in classical two-dimensional crystals (Landau and Lifshitz, 1980).

Let us define $d_0(x)$ as the density function characterizing each spin population without quantum fluctuations. Under these circumstances the particle positions are frozen in an equidistant periodic configuration, and the function $d_0(x)$ can be decomposed into a Fourier series:

$$d_0(x)=\sum_G d_G e^{iGx},\quad G=2\pi nr,\quad r=0,\pm1,\pm2,\ldots. \tag{1.8}$$

Here the G's are the reciprocal lattice "vectors"; the Fourier coefficient $d_{G=0}$ is just the average particle density n. Taking into account the zero-point motion leads us to the result that the particles forming a one-dimensional lattice undergo dynamical fluctuations described by the fields $u_\downarrow$ and $u_\uparrow$ [see Appendix, and Eq. (1.2)]. Since $u_\downarrow$ and $u_\uparrow$ are slowly varying as functions of position ($|u_\downarrow'|,|u_\uparrow'|\ll 1$), the dynamical density functions can be found from Eq. (1.8) by taking into account the local shifts from the equidistant positions:

$$d_\uparrow(x,t)=d_0[x-u_\uparrow(x,t)]=\sum_G d_G \exp iG(x-u_\uparrow)$$
$$=\sum_G d_G e^{iGx}e^{-iG(C+S)}, \tag{1.9}$$

$$d_\downarrow(x,t)=d_0[x-u_\downarrow(x,t)]=\sum_G d_G \exp iG(x-u_\downarrow)$$
$$=\sum_G d_G e^{iGx}e^{-iG(C-S)}, \tag{1.10}$$

where $d_\uparrow$ and $d_\downarrow$ are density functions corresponding to the two spin populations, and we used the definitions (1.2).

The averaging of Eqs. (1.9) and (1.10) over quantum fluctuations can be performed by a Gaussian averaging procedure, because the probability distributions for the fluctuating fields C and S will be given by actions quadratic in C and S with (or without) gaps in every case we shall consider. Then

$$\langle d_\uparrow(x,t)\rangle=\langle d_\downarrow(x,t)\rangle$$
$$=\sum_G d_G \exp\left(-\frac{G^2}{2}(\langle C^2\rangle+\langle S^2\rangle)\right)e^{iGx}, \tag{1.11}$$

where $\langle\cdots\rangle$ is the average over zero-point motion. When the spectrum has a gap, the average of the square of the corresponding field is finite; for a gapless spectrum the average is infinite. When both spectra have gaps, the effect of quantum fluctuations leads to a Debye-Waller factor $\exp[-(G^2/2)(\langle C^2\rangle+\langle S^2\rangle)]$: long-range crystalline order is not destroyed by quantum effects.

When the system has a gapless mode, the corresponding mean value $\langle C^2\rangle$ or $\langle S^2\rangle$ is infinite: the Debye-Waller factor is zero for $G\neq0$, and only the term with $G=0$ contributes. Then Eq. (1.11) reduces to the homogeneous density

$$\langle d_\uparrow(x,t)\rangle=\langle d_\downarrow(x,t)\rangle=n. \tag{1.12}$$

In this case quantum fluctuations destroy the long-range crystalline order in one dimension—a situation that is closely analogous to the destruction of the long-range order by thermal fluctuations in classical two-dimensional systems of continuous symmetry (Landau and Lifshitz, 1980; Mermin and Wagner, 1966; Mermin, 1967; Hohenberg, 1967).

2. Two-point density correlations

The averaged density functions (1.12) do not suffice to characterize the phases in which there is a gapless mode. In these cases we have to look at the second moments of Eqs. (1.9) and (1.10). Several correlation functions can be constructed.

First, there is the function $\langle d_\uparrow(x_1,t_1)d_\uparrow(x_2,t_2)\rangle$ that characterizes correlations inside one of the spin populations. From the Fourier expansion (1.9) one gets

$$\langle d_\uparrow(x_1,t_1)d_\uparrow(x_2,t_2)\rangle=\sum_{G,G'} d_G d_{G'} e^{iGx_1+iG'x_2}$$
$$\times\langle e^{-iGC_1-iG'C_2}\rangle$$
$$\times\langle e^{-iGS_1-iG'S_2}\rangle. \tag{1.13}$$

When C or S is gapless, the averaging of the corresponding exponential gives zero except for the terms $G=-G'$ (Landau and Lifshitz, 1980). Then we get instead of (1.13)

$$\langle d_\uparrow(x_1,t_1)d_\uparrow(x_2,t_2)\rangle=\sum_G |d_G|^2 e^{iG(x_1-x_2)}$$
$$\times\langle e^{-iG(C_1-C_2)}\rangle\langle e^{-iG(S_1-S_2)}\rangle. \tag{1.14}$$

First, we assume that we are inside the gapless or normal-metal phase. Calculating the averages in (1.14) with the help of the harmonic part of the action (1.3) with renormalized μ_ν^* and K_ν^*, we get

$$\langle d_\uparrow(x_1,t_1)d_\uparrow(x_2,t_2)\rangle - n^2 \propto \frac{\cos 2\pi n(x_1-x_2)}{[(x_1-x_2)^2+c_C^{*2}(t_1-t_2)^2]^{g_C^*/4}[(x_1-x_2)^2+c_S^{*2}(t_1-t_2)^2]^{g_S^*/4}}, \tag{1.15}$$

where we kept only the leading contributions $G=0$, $\pm 2\pi n$ and used the definitions (1.5). This expression is valid when the denominators are large. The amplitude of the oscillations decays as a power law with distance and time differences (and thus quite slowly relative to an exponential decay), and is called algebraic order (Kosterlitz and Thouless, 1973; Kosterlitz, 1974; Landau and Lifshitz, 1980). The exponent of the long-distance (time) behavior of equal-time (space) correlation functions is governed by the sum $(g_C^* + g_S^*)/2$.

To find the behavior of the correlation function in the presence of a spin-density gap, we have to look at Eq. (1.14) again. Now the average $\langle e^{-iG(S_1-S_2)}\rangle$ is finite in the limit of large separation between the points (x_1,t_1) and (x_2,t_2). Thus, in this case, we get

$$\langle d_\uparrow(x_1,t_1)d_\uparrow(x_2,t_2)\rangle_s - n^2 \propto \frac{\cos 2\pi n(x_1-x_2)}{[(x_1-x_2)^2+c_C^{*2}(t_1-t_2)^2]^{g_C^*/4}}, \tag{1.16}$$

which can be obtained formally from Eq. (1.15) by setting $g_S^* = 0$; here $\langle\cdots\rangle_\nu$ means that there is a gap in subsystem ν.

The evaluation of the function (1.14) in the phase having a charge-density gap gives rise to the expression

$$\langle d_\uparrow(x_1,t_1)d_\uparrow(x_2,t_2)\rangle_C - n^2 \propto \frac{\cos 2\pi n(x_1-x_2)}{[(x_1-x_2)^2+c_S^{*2}(t_1-t_2)^2]^{g_S^*/4}}. \tag{1.17}$$

Obviously we can replace the $\uparrow$ spins by $\downarrow$ spins in Eqs. (1.15)–(1.17).

Let us now consider the function $\langle d_\uparrow(x_1,t_1)d_\downarrow(x_2,t_2)\rangle$, which contains information about the correlations of particles of opposite spins. Using Eqs. (1.9) and (1.10), one gets

$$\langle d_\uparrow(x_1,t_1)d_\downarrow(x_2,t_2)\rangle = \sum_{G,G'} d_G d_{G'}, e^{iGx_1+iG'x_2} \times\langle e^{-iGC_1-iG'C_2}\rangle \times\langle e^{-iGS_1+iG'S_2}\rangle. \tag{1.18}$$

First we assume that we are in the normal-metal phase, where both C and S are gapless fields. As before we conclude that the first average in (1.18) singles out the contributions with $G=-G'$, while the second one does that for $G=G'$. The two conditions can be satisfied simultaneously only for $G=G'=0$, which means that only the homogeneous term of the sum (1.18) survives. Therefore we get

$$\langle d_\uparrow(x_1,t_1)d_\downarrow(x_2,t_2)\rangle = n^2. \tag{1.19}$$

Thus we obtain the result that electrons of opposite spin are not correlated at large distances (times) in the normal-metal phase. Of course, there is some short-ranged correlation lost in going to the long-wavelength approximation.

In the spin-density wave phase there is a spin-density gap, and only the variable C in Eq. (1.18) is gapless. The first average in (1.18) singles out the terms with $G=-G'$, with the result that the function (1.18) has exactly the same asymptotic dependence as the function (1.16), thus implying that there is a correlation between particles having opposite spins, which decays algebraically with distance and time.

In the phase having only a charge-density gap, the variable S is gapless and the second average in (1.18) singles out the terms with $G=G'$. Therefore we find that

$$\langle d_\uparrow(x_1,t_1)d_\downarrow(x_2,t_2)\rangle_c - n^2 \propto \frac{\cos[2\pi n(x_1+x_2)+\phi]}{[(x_1-x_2)^2+c_S^{*2}(t_1-t_2)^2]^{g_s^*/4}}, \tag{1.20}$$

where the constant ϕ arises because the Fourier coefficients d_G in Eq. (1.8) are in general complex. We see that there is a correlation between particles of opposite spin and that translational invariance is broken inside this phase, since the correlation function between the points (x_1,t_1) and (x_2,t_2) is not expressed entirely in terms of the difference x_1-x_2. This implies that the presence of a charge-density gap suffices to produce an insulator.

3. The Green's function

In higher than one dimension, fermion systems are described almost entirely in terms of single-particle properties (as in the Landau Fermi-liquid theory); there the case of noninteracting particles gives a good reference model. The present description, in contrast, is entirely in terms of the system's collective modes, and the Fermi surface does not play any role. In fact, there is no discontinuity in the occupancy of single-particle states at

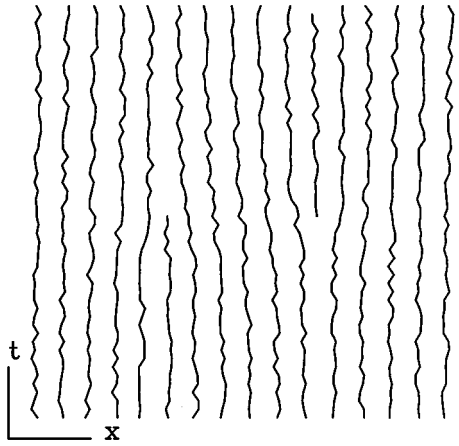

FIG. 2. Dislocation pair in a two-dimensional crystal of world lines. The configuration of the particle world lines is shown in one member of the ensemble. A particle is removed at (x=0, t=0), terminating a line, and another particle is added elsewhere, giving rise to another half-line. The wandering of the lines represents quantum fluctuations.

k_F. This can be shown using the present description (Straley and Kolomeisky, 1995).

To simplify matters, consider a quantum liquid of fermions of one spin type. In our description it will have a macroscopic action

$$A_{\text{harmonic}}=\frac{1}{2}\int dxdt(\mu^*\dot{u}^2+K^*u'^2). \tag{1.21}$$

The quantity we wish to calculate is

$$G(x,t=0)=\langle\psi^\dagger(x,0^+)\psi(0,0)\rangle, \tag{1.22}$$

where $\psi^\dagger(x,t)$ is the operator that creates a fermion. From the point of view of the path-integral formalism that we are using, we must imagine a field of world lines running in the t direction, and the expectation value in Eq. (1.22) measures the average amplitude for having a world line that ends at (0,0) and another that begins at (x,0), within an ensemble with weights determined by Eq. (1.21).

We shall estimate $G(x,0)$ by regarding the imaginary time axis as another space direction, so that the continuum is a two-dimensional crystal of world lines, into which $\psi^\dagger$ inserts a half-line or dislocation, while ψ inserts an opposite dislocation, as sketched in Fig. 2. Each dislocation gives rise to a distortion in the field u which has Burger's vector n^{-1} (because one world line has disappeared); the distortion falls off as x^{-1} and thus gives a logarithmic energy (logarithmic action, in the quantum problem) (Chaikin and Lubensky, 1995)

$$E_{\text{dislocation pair}}=\frac{\sqrt{\mu^*K^*}}{2\pi n^2}\ln(nx)+E_{\text{core}}. \tag{1.23}$$

The core energy E_{core} is large, so that the density of dislocations is small; in fact we shall assume that there is just one pair present. The wave function for the quantum problem is the partition function at "temperature" $\hbar$ for the world-line crystal, and so the probability that they are found at a distance x from each other is then proportional to

$$\text{Prob}(x)\propto\exp(-E_{\text{dislocation pair}}/\hbar)\propto(nx)^{-1/2g^*}, \tag{1.24}$$

where g^* is defined similarly to (1.5),

$$g^*=\frac{\pi\hbar n^2}{\sqrt{\mu^*K^*}}. \tag{1.25}$$

Equation (1.24) gives the scaling behavior of the Green's function for a bosonic system. There is a second phenomenon that has to be taken into account to evaluate $G(x,0)$ for the fermion problem: its sign depends on the number of fermion lines that have been jumped over to get from 0 to x. For a perfect crystal of lines, this would be just nx [$G\propto(-1)^{nx}$], but in the presence of quantum fluctuations there is an averaging over contributions of varying sign. We can estimate this part as $\langle\exp\{i\pi n[x+u(x)-u(0)]\}\rangle$. This is another Gaussian average and gives $\cos(\pi nx)x^{-g^*/2}$. Combining these two factors gives the estimate

$$G(x,0)\propto\cos(\pi nx)x^{-(g^*/2+1/2g^*)}. \tag{1.26}$$

The Fourier transform of this gives the single-particle momentum distribution $\langle n_k\rangle$, and near $k_F=\pi n$ has the form

$$\langle n_k\rangle=\text{const}-\text{sgn}(k-k_F)|k-k_F|^\alpha, \tag{1.27}$$

where $\alpha=g^*/2+1/2g^*-1$. In the argument for the spin-$\frac{1}{2}$ case the spin and charge degrees of freedom are uncoupled; the exponent α becomes $\alpha = g_C^*/8 + g_S^*/8 + g_C^{*-1}/2 + g_S^{*-1}/2 - 1$. For the free-fermion case this gives α=0; for any other combination of the g_ν^* it is positive, giving a smoother descent of $\langle n_k\rangle$ at k_F.

This is not a rigorous derivation, since we have put in the fermion character of the problem by hand; however, it is possible to represent the fermion field operators in terms of bosonic operators (Schotte and Schotte, 1969; Schotte, 1970; Blume, Emery, and Luther, 1970; Luther and Emery, 1974; Mandelstam, 1975) and thereby obtain the results of this section, and calculate other two-point correlation functions (Emery, 1979a, 1979b).

E. Commensuration and near commensuration

When the particle spacing is incommensurate with the external potential, nb is irrational, and for no order l of umklapp scattering and Fourier component k of the external potential does $\rho=|nl-k/b|$ vanish. On length scales large compared with $1/\rho$, the anharmonic terms in the action (1.3) involving the charge degrees of freedom are oscillatory; they are then irrelevant in the sense that they cannot halt transport and there is no gap in the spectrum of the field C, if even the ρ=0 system has a gap. Physically this occurs because there is a finite density (measured by ρ) of discommensurations at which there is a shift in registry of the pattern of long-range order that is present at ρ=0.

In the presence of a spin-sensitive external field (such as the magnetic field), there is a similar situation for the spin field S: the density $(n_\uparrow, n_\downarrow)$ of the up and down spins (and thus average spacing) may be different, leading to discommensurations in the spin ordering of density $n_\uparrow - n_\downarrow$.

Since every number nb is close to many rational values, one might be concerned that disentangling the various commensurabilities will be a difficult process. However, we shall see below (Sec. V) that umklapp scattering of order l is not important for $g_C \gg 1/l^2$, so that rational fractions with small denominators are of the greatest interest.

In an ordered phase (having a gap in any spectrum), there is some form of long-range order, and the correlation functions behave as if the corresponding g_ν^* were zero. The correlation exponents attain this value discontinuously, however, and the discontinuity depends on how the ordered phase is approached. At commensuration (for example, by varying the strength of the external potential) there is a minimum universal value $g_{\nu,\min}$; when one varies the density or magnetization, the limiting value of the renormalized exponent g_ν^* is exactly half as large. The latter exponents characterize ordered phases via the correlation properties of an infinitely dilute gas of discommensurations, which are the solitons of the corresponding fields, and behave like a gas of particles with short-range repulsive interactions.

F. Correlations and nomenclature

Since we shall frequently be referring to the various correlated phases, we shall give them names suggestive of their characteristics.

Any phase not having a charge-density gap is a conductor, and the conductance is given by $g_C^* e^2/h$ (Mattis, 1974; Luther and Peschel, 1974; Apel and Rice, 1982; Kane and Fisher, 1992a). It should be noted that the conductivity of the $T=0$ material is either zero or infinity, since there is no dissipative mechanism. There are three cases, depending on the sign and relevance of the unlike-spin interaction (parametrized by U): the superconductor, the conducting antiferromagnet, and the normal metal.

A conductor having a spin-density gap and no net spin at any place will be referred to as a superconductor, because it has Cooper pairs—but the diamagnetism is not perfect, and the conductance is finite (still $g_C^* e^2/h$). The other phase having a spin-density gap has antiferromagnetic order and will be referred to as an antiferromagnet. This can be a conductor if there is no charge-density gap. Attractive unlike-spin interactions will promote superconductivity, while repulsive interactions will favor antiferromagnetic order.

The normal metal has no gap in either spectrum.

This nomenclature is a simplified version of the conventional one (Emery, 1979a; Solyom, 1979) which distinguishes the possible conducting phases by the presence or absence of a spin-density gap and further by the behavior of certain correlation functions. According to this scheme, there are at least four different conducting phases: (1) metallic with dominant spin-density fluctuations but no spin-density gap and $g_C<2$; (2) metallic with dominant triplet pairing fluctuations but no spin-density gap and $g_C>2$; (3) metallic with dominant charge-density fluctuations in the presence of a spin-density gap and $g_C<2$; and (4) metallic with dominant singlet pairing fluctuations in the presence of a spin-density gap and $g_C>2$. Type (3) we have called an antiferromagnetic conductor, and type (4) is our superconductor. We have not distinguished between types (1) and (2), which we just call a normal metal, because there is no phase transition at $g_C=2$.

Any phase having a charge-density gap is an insulator. There are four insulating phases (again depending on the sign of U): the nonmagnetic insulator with a spin-density gap (which can be visualized as pinned Cooper pairs); the antiferromagnetic insulator without a spin-density gap and having only algebraic antiferromagnetic order [with correlation function given by Eq. (1.20)]; the antiferromagnetic insulator, which has a spin-density gap and long-range antiferromagnetic order; and for odd order of umklapp scattering (which can occur when $nb = k/l$ with l odd) there can be a dimerized insulator, in which the spins are unevenly spaced.

This classification singles out phases that can be described in terms of the charge- and spin-density correlation functions. There can be ordered phases in which the correlations are more subtle—for example, the bond ordering that occurs in the fermionic version of the XXY model (Emery and Noguera, 1988; Noguera and Emery, 1989), in which adjacent pairs of sites are occupied by a singlet wave function: it has a gap in the charge-density wave spectrum, but gives no signature in the charge-density correlations. Since our phase diagrams emphasize the presence or absence of gaps in the spectra, these phases will be distinguished from the disordered phases, but the possibility of more than one kind of ordered phase may be overlooked.

G. The renormalization-group language

Our intention is to determine which phases will arise for various regimes of large and small quantum fluctuations (as parametrized by g_C and g_S) and various choices for other parameters. We shall be using renormalization methods to determine the phase diagram and physical behavior, which involves the study of a set of differential equations describing the consequences of a sequential integrating-out of the shortest-wavelength fluctuations. In special limits these differential equations can be constructed and are quite useful in elucidating the behavior near phase transitions and other singular limits.

Important conceptual tools will be flow diagrams, which represent the assumed result of an exact renormalization treatment. These consist of lines describing how the parameters of the model evolve, according to the renormalization differential equations; each line can

be read as specifying the combinations of parameters that define a family of models that are physically equivalent. The end point of the renormalization yields the macroscopic physical properties.

We do not actually know how to construct the general renormalization differential equations, but argue that symmetry and exact solutions for special cases, as well as what we can learn from perturbation about various limits, so constrain the flow diagram that we can claim to know it. The elements that go into the construction are the perturbative renormalization-group results appropriate to the cases of weak and strong Hubbard interaction; these limits are connected by the results for the continuum Hubbard model, which has been exactly solved.

In the discussion of phase transitions using the renormalization group, a marginal renormalization-group trajectory (or separatrix) is of special interest. It may correspond to the locus of a special physical model whose microscopic Hamiltonian has an extra symmetry; such models are especially amenable to being exactly solved. This can have implications that go beyond the perturbative renormalization group. The Hubbard model will play an important role in what follows, because it lies exactly on the separatrix of the renormalization-group flow.

II. IN THE VICINITY OF HALF-FILLING

We begin with the case of the half-filled band and its vicinity, because this case introduces many of the general ideas, while remaining well connected to exact results. The lattice models at half-filling have particle-hole symmetry, which simplifies the discussion. This is physically important, because the effects of the periodic potential are quite pronounced.

A one-dimensional electronic system with a half-filled band is the case $l=2$ of the action (1.3). The spin and charge degrees of freedom are uncoupled and can be discussed separately. The Γ_2 term is always more relevant than the Γ_3 term in Eq. (1.3d), so that the latter can be discarded; the action (1.3a)–(1.3d) reduces to

$$A=\frac{1}{2}\int dxdt(\mu_S\dot{S}^2+K_S S'^2)+2n^2U\int dxdt\,\cos 4\pi nS+\frac{1}{2}\int dxdt(\mu_C\dot{C}^2+K_C C'^2)$$
$$+2n^2V\int dxdt\,\cos(2\pi\rho x-4\pi nC). \tag{2.1}$$

The prefactors of the cosine terms are given for the limit of weak Hubbard interaction (for U not small, the coefficients would be functions of U) and $a=0$; the parameter V is proportional to both the amplitude of the periodic potential and the Hubbard parameter U (see Appendix). The derivation given in the Appendix is valid only for a weak periodic potential. However, the same functional form with $V=U$ appears upon direct bosonization of the weakly interacting lattice version of the Hubbard model near half-filling (Giamarchi, 1991). The parameter $\rho=|2n-1/b|$ measures the deviation from the exactly half-filled band case $nb=\frac{1}{2}$. Equivalent quantum Hamiltonians have been given previously (Emery, 1979a, 1979b; Solyom, 1979; Schulz, 1990, 1991; Giamarchi, 1991). The $2n^2U$ term corresponds to the backward-scattering amplitude, while $2n^2V$ is the amplitude of the $4\pi n=4k_F$ umklapp scattering.

The amplitude U of the interaction between particles of opposite spin plays several roles in Eq. (2.1): it contributes to the values of K_C and K_S, as described by (A16) and (A17); it determines the coefficient of the anharmonic term for the spin separation variable and contributes to the corresponding coefficient for the charge variable. We shall treat these different terms as independent, because in what follows we shall be using renormalization methods to determine the phase diagram and physical behavior. The renormalization equations describe the mutual evolution of the parameters of the harmonic part and the amplitude of the anharmonic terms; the microscopic value U plays a role in setting the initial values for all of these, but we shall choose to refer to the amplitude of one of the anharmonic terms in terms of a renormalized U, as if this were the only way U entered the theory. In writing (2.1) we have promoted this distinction by explicitly displaying only some of the U dependence.

In the following sections we develop the flow diagram relevant to half-filling. In Sec. II.A we explore the limit of weak Hubbard interaction and show that the lattice model corresponds to the separatrix of the continuum translationally invariant problem. In Sec. II.B we trace the dependence of g_C on the strength of the Hubbard parameter, which then determines the locus of initial conditions for the renormalization study of the lattice model. This section also discusses the vicinity of $g_C=1$, which is an invariant line of the flow, and corresponds to the exactly solved Emery-Luther-Peschel model. Section II.C discusses the vicinity of $g_C=4$, which is another invariant line of the flow, and corresponds to the Efetov-Larkin model. In Sec. II.D we bring all these ideas together to construct the flow diagram for g_C versus V. In Sec. II.E we carry over some of these results to g_S^*.

A. Weak Hubbard interaction

1. Point interactions ($a=0$)

When the Hubbard interaction that couples particles of opposite spin is small, it is relevant to compare it to the case of noninteracting spin populations. To this end we introduce the spinless analog of Eq. (1.5b) (Kane and Fisher, 1992a, 1992b), which we already met in Eq. (1.25)

$$g=\frac{\pi\hbar n^2}{\sqrt{mnK(n)}}. \tag{2.2}$$

This parameter characterizes the degree of quantum fluctuation for noninteracting spin populations, with $K(n)$ given by the analog of Eq. (1.7),

$$K(n)=n^2\,\frac{\partial\mu(n,U=0)}{\partial n}. \tag{2.3}$$

In the continuum Hubbard model, electrons of the same spin do not interact with each other; therefore $\mu_0=\mu(n,U=0)=\pi^2\hbar^2n^2/2m$, and we find from Eqs. (2.2) and (2.3) that $g=1$. It can be seen that $g<1$ for the case of like-spin repulsion and $g>1$ if there is a like-spin attraction (Kane and Fisher, 1992a, 1992b). In the limits $|u|=n^2|U|/K(n)\ll 1$, and $a=0$, the bare values of g_ν (1.5) can be expressed (see Appendix) in terms of g (2.2) and the dimensionless strength of the Hubbard interaction u:

$$g_S=2g(1+u/2), \tag{2.4}$$

$$g_C=2g(1-u/2). \tag{2.5}$$

For the continuum Hubbard model, $g=1$, and the parameter u reduces to $u=mU/\pi^2\hbar^2n=U/\pi\hbar v_F$, where v_F is the Fermi velocity; Eqs. (2.4) and (2.5) then reproduce the known results (Emery, 1979a; Solyom, 1979; Schulz, 1990, 1991; Giamarchi, 1991).

The model (1.1) and subsequent discussion were all in terms of a continuum model. However, the lattice model is similar in important ways: the parameters μ_ν, v_F, and K_ν are different, but they combine to give Eqs. (2.4) and (2.5) again, with $g=1$ and $u=U/\pi\hbar v_F$ for the Hubbard model.

We have introduced the parameter g_C in Eq. (1.5b) to describe the case of half-filling; when we generalize from the half-filled band ($l=2$) to general commensuration (in Sec. V), we shall find a quite similar description in terms of the parameter $l^2g_C/4$ for even l, or l^2g_C for odd l.

2. Perturbative renormalization group ($|u|\ll 1$): spin degrees of freedom

The spin and charge degrees of freedom are already decoupled in the action (2.1), and for the weakly interacting case $|u|\ll 1$ each is of sine-Gordon type. Perturbative renormalization-group analysis (Wiegmann, 1978) can be used to describe the phase transitions between different ground states. The perturbative renormalization-group equations describe the effect of integrating out the short-wavelength components of the field (up to some length scale L), and take the form of differential equations describing how the parameters of the action evolve as this integration is done (Ma, 1976), in terms of an independent variable $\tau=\ln(nL)$.

The equations for the "spin" parameters of the action, valid for g_S close to 2, are the Kosterlitz equations (Kosterlitz, 1974; Wiegmann, 1978):

$$\frac{du}{d\tau}=(2-g_S)u, \tag{2.6a}$$

$$\frac{dg_S}{d\tau}=-C_1u^2, \tag{2.6b}$$

where C_1 is the first of a series of numerical constants C_i. Equations (2.6a) and (2.6b) describe a generic interacting system in the limit $|u|\ll 1$, but we shall adopt the initial condition (2.4) in addition, which requires $a=0$.

The physical content of these equations is that interaction always causes the macroscopic $g_S(L\to\infty)$ to be less than its initial value and that the effective interaction decreases whenever $g_S>2$ (representing the effect of large quantum fluctuations) but increases in the more classical case $g_S<2$. Thus there are two general types of trajectories: those which tend asymptotically towards the Kosterlitz fixed line, $g_S\geqslant 2$, $u=0$, and those for which g_S goes below 2 and $|u|$ increases without bound. They are separated by the special lines $g_S=2\pm\sqrt{C_1}u$.

The continuum Hubbard model with no periodic potential present is a part of the general picture described by Eqs. (2.4) with $g=1$ and (2.6a) and (2.6b). It is a very simple case in that it is specified by the one dimensionless parameter u, the amplitude of the zero-range interaction between particles of the opposite spin. Renormalization cannot generate any other interactions, and so the renormalized Hubbard model is again a Hubbard model, with a different value for the parameter u: the family of Hubbard models lies along a single flow line of the renormalization transformation. This must in fact be the separatrix, because the free-fermion model is contained within the family as the case $u=0$, $g_S=2$. This argument goes beyond the perturbative renormalization group and has several important consequences (Emery, 1979a; Solyom, 1979):

The coefficient C_1 must be unity, so that the line of initial conditions [(2.4) evaluated at $g=1$] is also the separatrix (Emery, 1979a).

For repulsive interactions, $g_S>2$ [again according to Eq. (2.4)], so that under renormalization u is steadily decreasing. We conclude that the anharmonic term in Eq. (2.1) is irrelevant, implying that $A_{\text{correlation}}$ fails to induce antiferromagnetic arrangement of the particles; there is no cutoff to the renormalization, so that for any $u>0$ the measurable exponent g_S^* is given exactly by $g_S^*=2$.

For attractive interactions, $g_S<2$, and $|u|$ is steadily increasing under renormalization. The anharmonic term is relevant, which means that there is a spin-density gap, and indicates the presence of the superconducting phase; however, the renormalization carries us out of the perturbative regime. The perturbative renormalization group does not tell us where the flow goes and thus fails

to determine the value $g_S(U=-\infty)$. We shall give arguments below (Sec. II.E) leading to the conclusion that the flow approaches a fixed point $g_S(U=-\infty)=1$.

The conclusion that there is a phase transition between superconductor and normal metal at $U=0$ is supported by the exact solutions of the continuum Hubbard model by Gaudin (1967, 1983) and Yang (1967). However, these results do not help us trace the separatrix, because the renormalization always carries us to one of the fixed points without stopping.

3. Perturbative renormalization group ($|u|\ll 1$): charge degrees of freedom

The anharmonic terms involving the charge degrees of freedom have their origin in the periodic potential; the charge part of the translationally invariant Hubbard model has a purely harmonic action. The resulting relationship between g_C and the Hubbard interaction u can be found from the exact solutions of Gaudin (1967, 1983) and Yang (1967), which describe the continuation of the perturbative description (2.5) (with $g=1$).

The long-wavelength behavior of the lattice Hubbard model is described by Eq. (2.1); the lattice is represented by a special value for the parameter V that measures the strength of the periodic potential. We can again argue that this model should go into itself under renormalization and thus must lie on the separatrix of the renormalization equations. Exactly at half-filling ($\rho=0$), the equations for the "charge" parameters of the action, valid for g_C close to 2, are the Kosterlitz equations (Kosterlitz, 1974; Wiegmann, 1978):

$$\frac{dv}{d\tau}=(2-g_C)v, \tag{2.7a}$$

$$\frac{dg_C}{d\tau}=-C_1v^2, \tag{2.7b}$$

where $v=mV/\pi^2\hbar^2n$ is the dimensionless amplitude of the periodic potential.

The coefficient C_1 is again unity; the initial conditions relating g_C to u for the Hubbard model are given by Eq. (2.5) with $g=1$. Comparing these, we see that the requirement that the Hubbard model lie along the separatrix $g_C=2+v$ implies $u=v$. This argument establishes the value of V in Eq. (2.1) for which the continuum model in a periodic potential is equivalent to the lattice model, in agreement with Giamarchi's result (1991).

For attractive interactions, $g_C>2$ [again according to Eq. (2.5), with $g=1$], so that under renormalization v is steadily decreasing. We conclude that the umklapp scattering term in Eq. (2.1) is irrelevant, implying that the periodic potential fails to localize the particles; exactly at half-filling there is no cutoff to the renormalization, and then for any $u<0$ the measurable exponent g_C^* is given exactly by $g_C^*=2$.

For repulsive interactions, $g_C<2$, and v is steadily increasing under renormalization. The umklapp scattering is relevant, which means that there is a charge-density gap; however, the renormalization carries us out of the perturbative regime. The perturbative renormalization group does not tell us where the flow goes and thus fails to determine the value $g_C(V=\infty)$. We shall give arguments below (Sec. II.B) leading to the conclusion $g_C(V=\infty)=1$.

The case in which ρ is small but not zero can also be understood from these equations; as the length scale increases, the spatial oscillations in the interaction terms [the last term of Eq. (2.1)] become more important and cut off the flow for $L\rho\approx 1$ (Horovitz *et al.*, 1983). The final value g_C^* that is reached is the macroscopically measurable one.

B. Strong Hubbard repulsion

We shall now discuss the locus of the separatrix of the exact renormalization-group equations, which will help us to understand the flows in the g_S-u and g_C-v planes. We must note that the resulting flow picture is not the flow diagram for the sine-Gordon action (2.1), because (2.1) is valid only for small u and v. Moreover, higher-order terms that are not written down in Eq. (2.1) will somehow affect the outcome. These nonlinearities lead to some ambiguity in the choice of parameters for comparison of models; we shall assume they can be chosen so that the locus of initial conditions for the lattice Hubbard model will be given by $v=u(g_C)$ for the continuum (translationally invariant) Hubbard model for all g_C, and not just in the perturbative regime. We shall show that this is a sensible assumption.

In the limit of weak interactions $|u|\ll 1$, the separatrix for charge degrees of freedom is given by Eq. (2.5) with $g=1$. In the case $u\gg 1$ the infinitely strong repulsion between particles of opposite spin plays a role similar to the Pauli principle between particles of the same spin, so that the $u=+\infty$ limit of the equation of state is the same as that of spinless free fermions with doubled particle density: $\mu(u=+\infty,n)=\mu_0(2n)=\pi^2\hbar^2(2n)^2/2m$. Substituting this into Eq. (1.7) and using Eqs. (1.4) and (1.5), one gets for the $u=+\infty$ limit of the separatrix $g_C=1$. Corrections of order $1/u$ to this result will be found below.

1. Translationally invariant problem, $u>0$

The translationally invariant version of (1.1) has been studied by Kolomeisky (1992) using a different version of the renormalization group appropriate to the case of a dilute limit. The appropriate variables for this case are the dimensionless quantities

$$u=\frac{mU}{\pi^2\hbar^2n}, \tag{2.8}$$

$$w=\frac{mW}{\pi^2\hbar^2n}. \tag{2.9}$$

In the dilute limit the spin direction is irrelevant, as already argued [see the n dependence of Eqs. (2.8) and (2.9)], and the problem reduces to free fermions. The lowest-order correction to the free-fermion result for the equation of state can be found (Kolomeisky, 1992):

$$\mu=\frac{\pi^2\hbar^2(2n)^2}{2m}\left[1+(2C_2/3)\left(na-\frac{1}{u}-\frac{1}{w}\right)\right]. \quad (2.10)$$

With Eqs. (1.5b) and (1.7), this implies

$$K_C=\frac{8\pi^2\hbar^2n^3}{m}\left[1+C_2\left(na-\frac{1}{u}-\frac{1}{w}\right)\right], \quad (2.11a)$$

$$g_C=1-C_2\left(na-\frac{1}{u}-\frac{1}{w}\right), \quad (2.11b)$$

which is valid if the correction to unity on the right-hand side is small. The Hubbard model is the special case $a=0$, $w=\infty$, so that its locus (and therefore the locus of the separatrix) in the limit $u\to+\infty$ is given by

$$g_C=1+C_2/u. \quad (2.12)$$

The same result can be obtained from the Bethe ansatz equations of Gaudin (1983) and Yang (1967). However, our method also allows us to find the loci of more general short-ranged models in the limit $u\to+\infty$. When a is finite and $w=\infty$, then for $na\approx 1/u$ the correction in Eq. (2.11) vanishes in all orders (Kolomeisky, 1992). For $mUa/\hbar^2>1$ the correction in (2.11) changes sign. Allowing w to be finite corresponds to the presence of a short-ranged attraction between electrons of the same spin.

The fact that the separatrix of the exact renormalization-group equations as well as the loci of short-ranged fermion models approach the same universal limit $g_C=1$ for $u\to+\infty$ and $na\to 0$ strongly suggests that the line $g_C=1$ itself is a special line of the exact renormalization group.

2. Free fermions on the lattice and the invariant line

We have been able to make analytic progress in the case $u\gg 1$ because this limit reduces to a system of free fermions. It is useful to calculate the exponent g_C^* for the system of free spinless fermions on a lattice of period b, which can be regarded as a special case of the more general problem (1.1). The chemical potential for a system of lattice fermions of density $2n$ is $\mu=(\hbar^2/mb^2)(1-\cos 2\pi nb)$, from which the coefficient K_C^* (1.7) can be calculated. Since translational symmetry is broken, we must use the expression for the sound velocity $c_C^*=(\hbar/mb)\sin 2\pi nb$ and Eqs. (1.6) and (1.7) to evaluate the coefficient μ_C^*. The result is that again $g_C^*=1$ independent of density and other parameters. This implies that there is no renormalization of the continuum g_C, the renormalization-group trajectory at $g_C=1$ is strictly vertical, and the direction of the flow is upwards, since the half-filled-band infinitely repulsive Hubbard model is an ordinary band insulator.

3. Finite ρ and soliton gas

That $g_C=1$ is an invariant upgoing line of the exact renormalization-group equations is a very important claim, because it locates the stable fixed point corresponding to the Mott insulating phase, which will be important for a wide range of systems. We can arrive at this same limiting behavior by consideration of small finite ρ in Eq. (2.1), for the case of arbitrary $U>0$.

For finite ρ the action (2.1) is translationally invariant. Umklapp scattering is irrelevant but still leads to a renormalization of μ_C and K_C. The effect of finite ρ can also be understood in terms of the flow picture of a system with $\rho=0$ (Horovitz *et al.*, 1983): starting at some initial point of the flow diagram, one follows some trajectory, stopping when the scale $\rho L^*\approx 1$ is reached. On larger length scales the cosine function in the charge part of the action is rapidly oscillating and the renormalization coming from the umklapp term is cut off; the corresponding value of $g_C^*(L^*\approx 1/\rho)$ can be read off the flow diagram. The value of the scale parameter τ corresponding to the interruption point is $\tau^*\approx\ln(n/\rho)$, to logarithmic accuracy. This shows that $\tau^*\to\infty$ as $\rho\to 0$, thus telling us that the finite value $g_C(v\to\infty)$ is the limiting value of the correlation exponent as one approaches exact commensuration by changing the particle density.

In the present case there will be a charge-density gap, so that there is long-range order in the charge subsystem on scales exceeding a correlation length ξ, which is the spatial extent of the solitons, the elementary excitations of the insulator phase. Up to model-dependent numbers, the soliton energy can be estimated as follows:

$$E_s\approx\int dx K_C C'^2\approx K_C\xi(1/n\xi)^2\approx K_C\xi(b/\xi)^2 = K_C b^2/\xi. \quad (2.13)$$

For $\rho=0$, the solitons can be excited only in the form of soliton-antisoliton pairs and therefore the charge-density gap is twice the soliton energy. The parameter ρ in Eq. (2.1) is defined in such a way that it gives us the net soliton density imposed by the deviation from half-filling.

Since there are two length scales, the soliton width ξ and intersoliton distance ρ^{-1}, two qualitatively different regimes are possible. For $\rho\xi\gg 1$, the solitons overlap and are not well defined objects. In this case the dependence $g_C^*(\rho)$ can be extracted from the perturbative renormalization-group equations by the prescription of Horovitz *et al.* (1983) only if the correlation length is large enough: $\xi n\approx\xi/b\gg 1$. The case $\rho\xi\ll 1$ is beyond the range of validity of the perturbative renormalization group, and a new universal picture occurs: we have a very low density of solitons with short-range repulsion between them, which can be approximated by treating the solitons as a gas of spinless noninteracting free fermions (Pokrovsky and Talapov, 1979; Schulz, 1980, 1990, 1991).

The exponent g_C^* can be calculated in the limit $\rho\xi\ll 1$ as follows (Kolomeisky, 1993): let us introduce the auxiliary soliton displacement field $f(x,t)$ in terms of which the long-wavelength version of the charge part of (2.1) has the form

$$A_C=\frac{1}{2}\int dx dt(\lambda_1\dot{f}^2+\lambda_2 f'^2). \quad (2.14)$$

Galilean invariance fixes $\lambda_1=\beta\rho$, where β is the soliton mass; and λ_2 is determined by the compressibility of the soliton (free-fermion) gas $\lambda_2=\pi^2\hbar^2\rho^3/\beta$. The fields C in Eq. (2.1) and f in Eq. (2.14) are related by $\rho\partial f=2n\partial C$. This transforms Eq. (2.14) into the harmonic terms of the charge part of (2.1) with

$$\mu_C^*=\beta\rho(2n/\rho)^2, \tag{2.15}$$

$$K_C^*=\frac{\pi^2\hbar^2\rho^3}{\beta}(2n/\rho)^2. \tag{2.16}$$

The parameters K_C^* and μ_C^* give us via Eqs. (1.4) and (1.7) the critical behavior of compressibility and effective mass, respectively, as $\rho\to 0$. We note that Eqs. (2.15) and (2.16) contain a single model-dependent parameter, the soliton mass β. When one evaluates g_C^* from Eq. (1.5) with these μ_C^* and K_C^*, all the parameters cancel each other and one gets again $g_C^*=1$. Since taking the limit $\rho\to 0$ is equivalent to the macroscopic limit $\tau\to\infty$ of the renormalization group, we conclude that on the scales $n\xi e^{-\tau}\ll 1$ (which is the same as $\rho\xi\ll 1$) any renormalization-group trajectory approaches the stable fixed point $g_C^*=1, v^*=\infty$.

Renormalization-group equations valid on the scales $n\xi e^{-\tau}\ll 1$ can be derived by using a more accurate description of the intersoliton interactions, namely, that solitons behave like finite-ranged repulsive bosons. The ground-state properties of a dilute system of bosons with interparticle repulsion of the form $W\delta_a(x)$ have been studied (Kolomeisky and Straley, 1992) and the ground-state properties found to be governed by the flow of the dimensionless pseudopotential $w\approx m_b Wa/\hbar^2$ (m_b is the bosonic mass) towards a stable fixed point, which corresponds to the free-fermion answer $g_C^*=1$ we just derived. The corrections to this result follow from a diluteness condition. The connection with the present problem is as follows: an intersoliton repulsion of the form $E_s\exp(-x/\xi)$ can be presented as $E_s\xi\delta_\xi(x)$ with the correspondence $E_s\xi\to W$, $\xi\to a$; the soliton mass is given by $\beta\approx E_s/c_C^2=\mu_C E_s/K_C$, so $m_b\to\mu_C E_s/K_C$; the diluteness condition is the same as $\rho\xi\ll 1$, and the interruption condition coincides with that of Horovitz *et al.* (1983). Using the correspondence outlined as well as the definition (1.5) and the estimate (2.13), one finds that up to a factor of order unity the pseudopotential w transforms into something proportional to $1/g_C^2$. Substituting this into the renormalization-group equation for the pseudopotential given by Kolomeisky and Straley (1992), one obtains the renormalization-group equation replacing Eq. (2.7b) on the scales $n\xi e^{-\tau}\approx(\xi/b)e^{-\tau}\ll 1$:

$$\frac{dg_C^2}{d\tau}=1-g_C^2. \tag{2.17}$$

What actually comes from the renormalization-group equation of Kolomeisky and Straley (1992) has some unknown numerical constant instead of unity on the right-hand side of Eq. (2.17): we cannot trace the exact correspondence between the pseudopotential of Kolomeisky and Straley (1992) and g_C and recover unity from the free-fermion arguments.

The minimal spatial scale in Eq. (2.17) is $L\approx\xi$, and for nonzero ρ the dependence $g_C^*(\rho)$ follows from the solution of (2.17) interrupted on a scale τ^* such as $\rho\xi e^{\tau^*}=F_1$, where F_1 is the first of a series of dimensionless functions of interaction, F_i, the precise form of which cannot be captured accurately by the renormalization-group method. Thus we obtain

$$(g_C^*)^2=1+\frac{(g_C)^2-1}{F_1}\rho\xi. \tag{2.18}$$

An analogous result has been found by Schulz (1980) and Haldane (1982) via exact solutions of the sine-Gordon model with nonzero soliton density. The model-dependent parameters in Eq. (2.18) are g_C, F_1, and ξ.

The answer (2.18) is valid for any physical model if the insulator phase existing at half-filling is approached by changing the particle density (Giarmarchi, 1991); this result also depends on the assumed accuracy of separation of spin and charge degrees of freedom. The bare values for g_C come from Eq. (2.11) in the limit $u\gg 1$ and from (2.5) for $|u|\ll 1$ and $a=0$. Equation (2.18) is valid in the vicinity $g_C^*=1$ and thus can be rewritten as

$$g_C^*=1+\frac{g_C-1}{F_1}\rho\xi \tag{2.19}$$

if the initial g_C is close to unity. This equation can be used to find the strong-coupling analog of Eq. (2.7a). The idea is that Eqs. (2.18) and (2.19) describe a family of models including the Hubbard model for which the locus of initial values is simultaneously the renormalization-group trajectory. To find the measurable g_C^* starting from some initial point with coordinates $(g_C, v=u)$, we substitute Eq. (2.12) into Eq. (2.19) and obtain

$$g_C^*=1+\frac{C_2}{uF_1}\rho\xi, \tag{2.20}$$

where for the Hubbard model the function F_1 depends only on u. On the other hand, the interruption point (g_C^*, v^*) belongs to the same curve (2.12):

$$g_C^*=1+\frac{C_2}{v^*}.$$

Comparing this with Eq. (2.20), we conclude that $v^*=uF_1/\rho\xi$, which via the connection $\tau^*=\ln(F_1/\rho\xi)$ implies that v evolves as

$$\frac{dv}{d\tau}=v, \tag{2.21}$$

which is the same as (2.7a) evaluated at $g_C=1$. The system of Eqs. (2.17) and (2.21) was suggested by Straley and Kolomeisky (1993) to describe the strong-coupling regime of the sine-Gordon theory.

C. Strong Hubbard attraction

We now turn to the case in which the Hubbard interaction is strong and attractive: $|u|\gg 1, u<0$. In the limit

of infinitely strong attraction, particles of opposite spin will form strongly coupled pairs distributed with the density n. This system is isomorphic to a free-fermion gas of particles of mass $2m$; the chemical potential is $\pi^2\hbar^2n^2/4m$. To find the $u=-\infty$ limit of the equation of state of the original system, we note that removing a single electron from the system will cost half of the pair binding energy and half of its kinetic energy, so that the equation of state is $\mu(u=-\infty,\ n)=\text{const}+\pi^2\hbar^2n^2/8m$, where the const stands for half of the binding energy and is density independent. Substituting this into Eq. (1.7) and using Eqs. (1.4) and (1.5), we find that the $u=-\infty$ limit of the Hubbard line is $g_C=4$. A correction of order $1/u$ to this result can be found from the Bethe ansatz equations (Gaudin, 1967, 1983), implying that the equation of the separatrix of the exact renormalization-group equations has the asymptotic form

$$g_C=4+C_3/u. \tag{2.22}$$

1. Translationally invariant problem, $u<0$

The loci of various physical models in the vicinity of the point $g_C=4$, $u=-\infty$ can be inferred from the results of Kolomeisky (1992), who studied the translationally invariant version of the original action (1.1) in the dilute limit. In the present context this corresponds to large absolute values of the dimensionless amplitude of the Hubbard interaction $u=Um/\pi^2\hbar^2n$. For $u\to+\infty$ the long-distance properties of the system are governed by the flow of the renormalization-group equations of Kolomeisky (1992) to a stable free-fermion fixed point underlying the result (2.12). For large negative u, the macroscopic behavior of the system is determined by the flow towards another stable fixed point ($u^*=-\infty$, $w^*\approx1$), which corresponds to the result (2.22). We can deduce that this fixed point describes a system of pairs because the divergence of the flow in the variable u indicates the formation of a two-particle bound state; simultaneously the flow is stable along the w direction and directed towards a positive finite value of w^*, thus implying that the system of pairs is stable and behaves like a free-fermion system in the dilute limit. The presence of this fixed point implies that the locus of any physical model approaches the limit $g_C=4$ for $U<0$ and $na\to0$. Since the fixed-point value w^* can be approached from both above and below, we conclude that the same is true for the limiting value $g_C=4$.

2. $g_C=4$ is also an invariant line

Similar to what was found for the limit of strong repulsive interaction, the line $g_C=4$ is an invariant line of the exact renormalization-group equations. We can show this by using the argument we already gave to calculate the exponent g_C^* for a lattice system of free fermions (see Sec. II.B.2). Noting that now the particle density is n, the particle masses are $2m$, and each particle consists of a pair of the original particles (of opposite spins), we conclude that g_C^* for the lattice system is not renormalized from its continuum value $g_C=4$. The direction of the flow on the line $g_C=4$ is opposite to that on the invariant line $g_C=1$, since free spinless fermions at half-filling are in a conductive phase. The direction of the flow in the vicinity of the line $g_C=4$ is also opposite to that in the vicinity of the line $g_C=1$ and can be inferred from the results of Yang and Yang (1966) and Haldane (1980), which also imply that the line $g_C=4$ is an invariant line. Some additional evidence will be presented below.

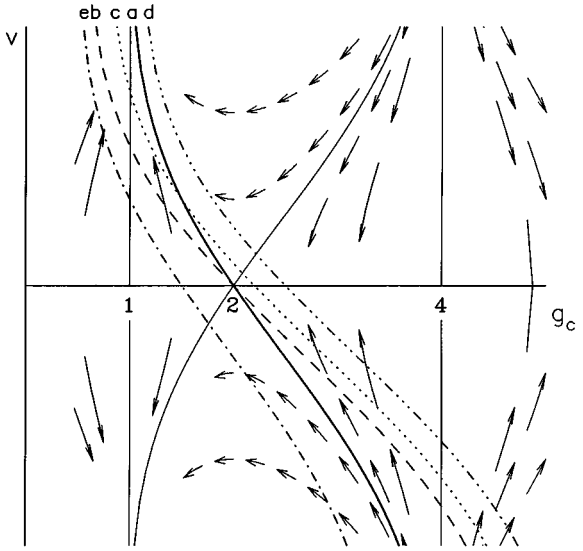

FIG. 3. Flow diagram describing the behavior of the charge degrees of freedom for the case of half-filling in terms of the dimensionless strength of the Hubbard interaction $v=u=n^2U/K(n)$ [see Eq. (2.3)] and the quantum correlation parameter g_C [see Eq. (1.5b)]. The arrows indicate the direction of the flow and the lines labeled a through e show schematically the loci of initial conditions corresponding to various physical models of short-ranged interacting spin-$\frac{1}{2}$ fermions. The two invariant lines at $g_C=1$ and $g_C=4$ correspond to the Emery-Luther-Peschel and Efetov-Larkin exact solutions, respectively. The notation is as follows: (a) the Hubbard model, which is simultaneously the separatrix of the exact renormalization-group equations; (b) a fermion model with a finite-range interaction between particles of opposite spin (extended Hubbard model) that approaches the Hubbard model (the curve a) in the limit of point interaction; (c), (d) fermion models with a finite-range interaction between particles of opposite spin and an attractive finite-range interaction between particles of the same spin. The attraction strength is larger for curve (d), which simultaneously has the topology of the extended Hubbard model with nearest-neighbor attraction; (e) this curve has the topology of the extended Hubbard model with nearest-neighbor repulsion.

D. The flow diagram and loci of physical models

1. The flow diagram

Now we are ready to produce a flow diagram describing the behavior of the charge degrees of freedom (Fig. 3). Its components are a flow pattern and a locus of initial conditions. The flow pattern (represented by the

arrows) is a property of the system with general interactions; it describes how its descriptive parameters evolve under renormalization. The microscopic parameters of a particular model fix a point on this diagram; following the arrows leads us to a different set of parameters, which characterize the macroscopic behavior. In an attempt to show how various initial conditions might be achieved, we have drawn in lines representing the loci of some specified one-parameter families of models.

The key feature of the flow diagram is the Hubbard line, which is the locus of initial conditions for the lattice Hubbard model and also the trajectory of its flow. In the weak-coupling regime it is given by Eq. (2.5) with $g=1$; for the case of large Hubbard repulsion it behaves according to Eq. (2.12) and in the limit of strong Hubbard attraction according to Eq. (2.22). These three limiting behaviors can be connected into a smooth curve a shown in Fig. 3. We assume that the whole curve can be obtained from the Bethe ansatz equations of Gaudin (1967, 1983) and Yang (1967). Its significance is that it determines one of the separatrices; the symmetry with respect to the reversal of the sign of v (the particle-hole symmetry of the lattice Hubbard model) produces the second separatrix.

The behavior of the lattice Hubbard model (already known from the solution of Lieb and Wu, 1968) can be interpreted as follows: Under renormalization, this family of models stays on the separatrix. For attractive Hubbard interaction ($g_C>2$), the periodic potential (that is, the lattice itself) is not a relevant perturbation and the system is translationally invariant macroscopically (we need to look at the behavior of the spin degrees of freedom to determine that it is a superconductor); at half-filling the renormalization does not stop and arrives at $g_C^* = 2$ exactly. For repulsive interactions, the lattice is a relevant perturbation; except at half-filling, the renormalization is stopped by the incommensuration of lattice and interelectron spacing, yielding a metal, while at half-filling an insulating phase (an antiferromagnet) results.

The loci of other physical models are shown by dashed lines $b-d$.

Curve b describes a system of fermions interacting via a finite-range unlike-spin interaction (the Hubbard model has a δ-function interaction of zero range). For $u\to+\infty$ its locus is given by Eq. (2.11) with infinite w. For small u its locus can be understood as follows: since electrons of the same spin do not interact with each other, Eq. (2.5) would imply that $g_C=2-u$ as for the Hubbard model. However, Eq. (2.5) is only the $a=0$ limit, and continuity then implies that for a not equal to zero one must have $g_C=2-uf(na)$ where $f(x)$ is some function having the property $f(x\to0)\to1$. We expect that in general $f(x)\geq1$, since the model under consideration is more repulsive than the positive u Hubbard model and more attractive than the negative u Hubbard model. Accordingly, curve b goes below the Hubbard line for $u>0$ and above the Hubbard line for $u<0$; the two curves intersect only at $u=0$. For $u\to+\infty$ there is a limiting value $g_C<1$ that approaches the universal limit $g_C=1$ linearly in density, as can be seen from Eqs. (2.8) and (2.11). For $u\to-\infty$ there exists a limiting value $g_C>4$ that approaches the universal limit $g_C=4$ as $na\to0$. The results of Kolomeisky (1992) do not tell us how the universal value $g_C=4$ is achieved in the dilute limit for negative u. For the Hubbard model we have a linear dependence [see Eqs. (2.22) and (2.8)], and we assert that this is the case in general.

For finite W one has an extra attraction between electrons of the same spin, and the locus of the corresponding models is presented schematically by curves c ($mWa/\hbar^2\geq1$) and d ($0<mWa/\hbar^2\leq1$). The $u\to+\infty$ limit is given by Eq. (2.11). As in the case of curve b, the small u limit is given by $g_C=2g-guf(na)$ [compare with Eq. (2.5)] with $g>1$. The curves c and d are shown for the special case $1<g<2$; in principle the crossing with the g_C axis can be anywhere to the right of $g_C=2$.

It is useful to understand how the models described by the action (1.1) are related to the extended Hubbard model (Emery, 1979a; Solyom, 1979). The extended Hubbard model is intrinsically a lattice model, and so there cannot be a one-to-one correspondence with the translationally invariant part of (1.1). However, the trend can be traced by noting that the finite range of interparticle interaction will lead to a nearest-neighbor interaction in the lattice problem. Therefore curve b of Fig. 3 can be roughly associated with the locus of the extended Hubbard model with nearest-neighbor repulsion for $u>0$, whereas the curves $b-d$ can be considered as leading under the renormalization group to macroscopic behavior similar to that of extended Hubbard models with nearest-neighbor attraction for $u<0$. In view of these observations, we believe that the locus of the extended Hubbard model always goes below the Hubbard line for the case of nearest-neighbor repulsion and always above the Hubbard line for the case of nearest-neighbor attraction. The former is presented schematically by curve e of Fig. 3 and the latter has the same typical behavior as curve d.

2. Generality

In concluding this section we want to comment on the generality of the flow diagram derived here. Over an important range of parameters, the interacting electron problem is strongly similar to the sine-Gordon problem, which then serves as a pertinent reference model, although we cannot connect the locus of the separatrix of the renormalization-group equations describing the sine-Gordon system with any specific exactly soluble model. In the perturbative limit, the renormalization argument was developed for the sine-Gordon theory (Wiegmann, 1978; Kosterlitz, 1974). The soliton arguments used to elucidate the features associated with the invariant line $g_C=1$ are model independent and therefore apply to any model exhibiting soliton excitations, including the sine-Gordon system. Thus the presence of the invariant line at $g_C=1$ with the associated features of the renormalization-group flow is another universal part of the sine-Gordon model not captured by the Kosterlitz perturbative renormalization group, as was recognized

by Straley and Kolomeisky (1993). The situation is less clear with regard to the presence of the invariant line g_C=4: renormalization arguments applied to the sine-Gordon theory (Horovitz *et al.*, 1983) imply that the dependence of the correlation exponent on density at commensuration should always exhibit a residual singularity which becomes increasingly weak in the strong quantum (large g_C) limit. However, there are exactly solvable lattice models (Gaudin, 1973; Haldane, 1988; Shastry, 1988; Sutherland, 1989) that would seem to be describable in terms of sine-Gordon models (Kolomeisky, 1993) and that indicate that the ground-state energy is analytic in this regime. This might indicate a distinction between the various models in this limit or reveal another general feature of quantum systems with a periodic perturbation. We shall not claim that the feature at g_C=4 is universal, but that it is specific for the one-dimensional electron gas model.

E. The exponent g_S^*

The spin part of the action (2.1) is also a sine-Gordon system, and the study of its behavior in many respects is just a transcription of the ρ=0 case of g_C. The flow diagram strongly resembles Fig. 3, with horizontal axis g_S and vertical axis u. Note that the coefficient of the anharmonic term for the spin variable has its origin in the Hubbard interaction itself, rather than from the periodic potential. Because there is no x dependence in the spin-dependent anharmonic term of Eq. (2.1), there is no cutoff to the renormalization, in the absence of a net magnetic moment. Another difference may arise: we do not know whether g_S=4 is an invariant line. The locus of initial conditions for the Hubbard models (lattice and continuum) is the ascending separatrix, as suggested by Eq. (2.4), so that attractive and repulsive Hubbard interactions play reversed roles from the case of g_C.

We conclude from this flow diagram that the exponent g_S^* approaches the universal limit $g_S^*=1$ for any attractive Hubbard model. This value can be measured in the presence of a perturbation that violates the spin up-down symmetry of the action (1.1), for example, when an external magnetic field produces a small magnetization and thus a finite density of spin solitons. The line g_S=1 itself corresponds to the family of models solved by Luther and Emery (1974).

III. COMPARISON WITH OTHER APPROACHES

The aim of this section is to point out the relationship of the flow picture to previous results and to convince the reader that our point of view provides a natural context for previous results.

A. Repulsive Hubbard interaction

The limit of strong interactions has been studied using several approaches, in particular the connections to exactly soluble models. Emery, Luther, and Peschel (1976), following the ideas of Luther and Emery (1974), found an exact solution of the lattice one-dimensional electron gas at half-filling for a special value of the interparticle repulsion at which the problem becomes equivalent to a free-fermion problem with a gap. Then they used renormalization-group arguments to look at other values of couplings at which the problem is not exactly soluble. We identify this special value with the crossing of the locus of the repulsive extended Hubbard model (curve e in Fig. 3) with the invariant line g_C=1, the Luther-Emery line (Luther and Emery, 1974). Since the Luther-Emery line is attractive, the conclusion derived from the exact solution for a specific coupling (Emery, Luther, and Peschel, 1976), that there is a charge-density gap, can be extended for any model within the basin of attraction of the fixed points $g_C^*=1$, $v^*=\pm\infty$. We see from Fig. 3 that the extended Hubbard model with nearest-neighbor repulsion and any sign of Hubbard interaction falls into this category. To calculate the charge-density gap via Eq. (2.13) we have to understand how to define the correlation length ξ in terms of the flow picture. In the theory of critical phenomena (Ma, 1976), the correlation length is defined as a scale on which an initially small coupling strength renormalizes up to a value of order unity. Applying this definition to the range of small positive u and g_C in the interval between 1 and 2, we can see from Fig. 3 that we must get a formula for the energy gap in which g_C enters as a parameter because flow becomes more and more vertical as one moves away from the value g_C=2. This is in qualitative agreement with arguments based on the connection with the partition function of the classical two-dimensional Coulomb gas (Emery, Luther, and Peschel, 1976) as well as with a connection with the XYZ model (Luther, 1976, 1977). Quantitative agreement can be obtained if we assume that for $g_C \approx 1$ the variable v evolves according to Eq. (2.7a) on scales larger than the mean interparticle distance n^{-1}—what we actually demonstrated was that the variable v obeys Eq. (2.21) for scales much larger than the correlation length ξ and $g_C \approx 1$.

B. Strong Hubbard attraction

For the case of strong Hubbard attraction, Efetov and Larkin (1975) have found an exact solution of the problem for a special value of a dimensionless combination involving both Hubbard and nearest-neighbor attraction: here the system turned out to be isomorphic to a free-fermion system of pairs comprised of the original particles of opposite spin. This solution corresponds to the crossing of the lines $b-d$ of Fig. 3 with the invariant line g_C=4, and the Efetov-Larkin result $g_C^* = 4$ can be read off the flow diagram.

A more general problem of the extended Hubbard model with strong Hubbard attraction was considered by Emery (1976) by means of a mapping onto the exactly soluble (Luther and Peschel, 1975) quantum XXZ spin chain. For a range of parameters Emery produced an exact expression for the exponent as a function of interactions. In terms of our flow picture (Fig. 3), this range of parameters corresponds to the initial conditions

between the Hubbard separatrix a and the Efetov-Larkin line in the limit $v=u=-\infty$. The flow carries those initial values onto the segment [2;4] of the Kosterlitz fixed line $g_C \geqslant 2$, $v=0$, and the boundary values 2 and 4 are achieved for the Hubbard model and on the Efetov-Larkin line, respectively, in correspondence with Emery (1976).

A connection with the XXZ quantum spin chain has been further exploited by Fowler (1978) to gain understanding of the ground state of the extended Hubbard model with strong Hubbard attraction and nearest-neighbor repulsion: this is the region below the Hubbard separatrix a and $v=u=-\infty$ in Fig. 3. The flow picture implies that there is a long-range order in the charge variables, and in the limit of weak nearest-neighbor repulsion the expression for the correlation length must have a form typical for a Kosterlitz-Thouless phase transition (Kosterlitz and Thouless, 1973; Kosterlitz, 1974), with the distance from the phase transition point proportional to the amplitude of the nearest-neighbor repulsion; this is in agreement with Fowler (1978).

We note that all the cases for which exact results are available correspond to the loci of initial conditions directly related to special trajectories of the renormalization-group equations. This may be a generic property of the phenomenon of exact solubility (Kolomeisky, 1994).

IV. APPLICATIONS

The results of previous sections can be used to find the dependence of the correlation exponent g_C^* on the electron density and interactions. The idea is that the initial point of the flow is given by the locus of the continuum problem and the presence of a small finite ρ sets an interruption scale. Far from half-filling, the flow should stop almost immediately; in particular, in the limit of vanishing filling one should come back to the continuum g_C. Several generic types of behavior for g_C are considered below.

A. The Hubbard model

The lattice version of the Hubbard model has been exactly solved and the correlation exponents for it evaluated (Bogoliubov and Korepin, 1988, 1989; Schulz, 1990, 1991; Frahm and Korepin, 1990, 1994; Kawakami and Yang, 1990) using the exact Bethe ansatz equations of Lieb and Wu (1968); however, the renormalization-group treatment sheds new light on the meaning of the exact results and allows generalization to more complex models. The locus of initial values for the Hubbard model is the separatrix a of Fig. 3. The direction of the flow tells us that the value of g_C^* is never larger than the bare (continuum) g_C; the separatrix is confined between the Luther-Emery and the Efetov-Larkin lines, which implies the inequalities

$$1 \leqslant g_C^* \leqslant 2 \tag{4.1}$$

for repulsive interactions and

$$2 \leqslant g_C^* \leqslant 4 \tag{4.2}$$

for attractive interactions.

1. Repulsive interaction

For repulsive interaction the initial point of the flow is on the unstable part of the separatrix. As can be seen from Fig. 3 and the definition (2.8), the universal value $g_C^* = 1$ is achieved for any Hubbard repulsion in the limit of half-filling, for any filling in the limit of infinite Hubbard repulsion, and for any Hubbard repulsion in the dilute limit $n \to 0$.

Near half-filling, the relationship between g_C^*, g_C, and ρ is given by Eq. (2.18), where the coefficient of ρ involves a function F_1 of the dimensionless interaction.

$$u' = u(nb=1) = mUb/\pi^2\hbar^2. \tag{4.3}$$

The correlation length ξ is anomalously large in the limit $u' \to 0$, since $u'=0$ is a metal-insulator phase-transition point for the Hubbard model. To satisfy the scaling hypothesis (Ma, 1976), ξ must be the only length scale for $u' \to 0$; using this constraint and substituting Eq. (2.5) evaluated at $g=1$ into Eq. (2.18), we obtain $F_1(u' \to 0) \to$ const and, correspondingly,

$$g_C^* = 1 + C_4 \rho \xi. \tag{4.4}$$

In the limit of strong repulsion $u' \to +\infty$ and near half-filling, we can rewrite Eq. (2.20) as

$$g_C^* = 1 + \frac{C_2}{2u' F_1(u')} \rho \xi. \tag{4.5}$$

In the limit of strong repulsion and not very close to half-filling, we can use the continuum result (2.12), which can be presented in the form

$$g_C^* = 1 + \frac{C_2}{u'} nb. \tag{4.6}$$

This makes it easier to guess a functional form that summarizes both Eq. (4.5) and Eq. (4.6) in the limit of strong repulsion $u' \to +\infty$ and any filling. A lattice expression for g_C^* will reduce to the continuum result (4.6) when the lattice period b goes to zero. Therefore the combination nb in Eq. (4.6) must be a lowest-order expansion of some bounded periodic function of nb with unit period, having its second zero at the half-filling (4.5). This immediately implies that for $u' \to +\infty$ we shall have, instead of Eq. (4.5),

$$g_C^* = 1 + \frac{C_5}{u'} |2nb - 1| \tag{4.7}$$

and $F_1(u')b/\xi(u') \to$ const as $u' \to +\infty$. The dependence of ξ on u' can be found from Eq. (2.13) because the soliton energy is proportional to the charge-density gap, and the charge-density gap behaves as U/b as $u' \to +\infty$ (Lieb and Wu, 1968; Ovchinnikov, 1969). Estimating K_C in Eq. (2.13) from the continuum free-fermion limit $u' \to +\infty$, we obtain $b/\xi \approx u'$, thus implying that $F_1(u') \approx 1/u'$ as $u' \to +\infty$.

These conclusions are in agreement with the results of the exact calculations of Frahm and Korepin (1990, 1994), who combined the Bethe ansatz solution for the Hubbard model with the principles of conformal field theory. The calculations of Frahm and Korepin (1990, 1994) improve on Eqs. (4.4)–(4.7) by giving all the numerical constants C_i as well as the function $F_1(u')$; however, they do not tell us why the limit of strong repulsion and any filling, any repulsion and small density, and half-filling and any repulsion are the same: the renormalization-group features standing behind these properties are important for a large family of short-range interacting spin-$\frac{1}{2}$ fermions.

The behavior of g_C^* for $u'\to 0$ ($u\to 0$) can be found from the perturbative renormalization-group equations (2.7a) and (2.7b) whenever the interruption point of the flow is within their range of validity. Solving Eqs. (2.7a) and (2.7b), one gets

$$g_C^* = 2 - \frac{u}{1 - u\,\ln(C_6 n/\rho)}, \tag{4.8}$$

which is valid whenever

$$u\,\ln(C_6 n/\rho) \ll 1. \tag{4.9}$$

As half-filling ($\rho\to 0$) is approached with arbitrarily small fixed u, this inequality is eventually violated and g_C^* crosses over to the dependence (4.4). The range of validity of (4.8) is thus extremely small for small u. No direct analytical expression is known describing the vicinity of $g_C^* \approx 2$ for $u\,\ln(C_6 n/\rho) \gg 1$ and $u \ll 1$; as can be seen from Fig. 3, this is a singular limit, since the starting point of the flow is asymptotically close to the unstable fixed point ($g_C=2$, $v=0$), while the interruption point is asymptotically close to the stable fixed point ($g_C=1$, $v=+\infty$).

2. Attractive interaction

For the case of the attractive Hubbard model, the physics is governed by the flow towards the stable fixed point ($g_C=2$, $v=0$); upon approaching half-filling for any attraction strength, the interruption point eventually enters the range of validity of the perturbative renormalization group. For small negative u the second term in Eq. (4.8) is not singular, and we can continue to use it to describe the limit $\rho\to 0$. We can rewrite Eq. (4.8) in a form similar to that of Horovitz *et al.* (1983),

$$g_C^* = 2 + 1/\ln(F_2(u) n/\rho), \tag{4.10}$$

which is valid for any $u<0$ and $\rho\to 0$ with some unknown function $F_2(u)$. In the limit of weak attraction, the form of $F_2(u)$ can be deduced by comparison of Eqs. (4.8) and (4.10): $F_2(u\to -0)\approx \exp(-1/u)$. For the case of the half-filled infinitely attractive Hubbard model, the renormalization-group flow starts at ($g_C=4$, $v=u=-\infty$) and ends at ($g_C=2$, $v=0$), which means that, near half-filling and infinite Hubbard attraction, the interruption point of the flow will be slightly above the value $g_C=2$, thus implying that $F_2(u\to -\infty)\to$const.

For the case of strong Hubbard attraction and far from half-filling we can use the continuum result (2.22), which can be written to resemble Eq. (4.6) as follows:

$$g_C^* = 4 + \frac{C_3}{u'}\, nb. \tag{4.11}$$

The first impression is that Eq. (4.11) might be valid for small nb and $u'\to -\infty$ but this is not the case. Indeed for $u'=-\infty$ Eq. (4.11) predicts that $g_C^* = 4$, whereas direct inspection of the flow diagram (Fig. 3) shows that starting at $g_C=4$, $v=u=-\infty$ depending on the filling factor one ends up at any value of g_C^* between 2 and 4 but always below 4. This argument implies that the $1/u'$ dependence in Eq. (4.11) is not the limit of $u'\to -\infty$ in the lattice problem but rather is the limit of weak attraction $|u'| \ll 1$. Further, we must have both $nb/|u'| \ll 1$ and $nb \ll 1$. We can write down instead of Eq. (4.11)

$$g_C^* = 4 + F_3(u')nb \tag{4.12}$$

with a wider range of validity: fixed u', $nb\to 0$, and $nb/u'\to 0$. For $u'\to -0$, the function F_3 behaves as $1/u'$, while for $u'\to -\infty$ it approaches a negative constant, as implied by the picture of the renormalization-group flow.

Our conclusions about the attractive Hubbard model are in agreement with the results of exact calculations of Bogoliubov and Korepin (1988, 1989). We must note that their calculations go beyond what we find, in that they give all the functions F_i as well as the numerical constants. Our expression for the function F_2 matches their $u\to -0$ result only with exponential accuracy. This could be corrected by starting from the third-order perturbative renormalization-group equations of Emery, Luther, and Peschel (1976).

A convenient way to present the results is to show the dependence of g_C^* on nb for various interaction strengths (4.3). In extracting these dependences from Fig. 3, one must take into account that for a given u' the corresponding initial value of $v=u=u'/nb$ [see Eqs. (2.8) and (4.3)] ranges between ∞ (or $-\infty$, depending on the interaction sign) and $2u'$ as the filling factor changes from zero to half-filling. The degree of downwards renormalization of the corresponding bare g_C will progressively grow upon approaching half-filling. The results are shown in Fig. 4: the behavior in the dilute limit as well as in the vicinity of half-filling is known analytically, and the rest follows from the flow diagram qualitatively. Various parts of this figure have been given previously (Bogoliubov and Korepin, 1988, 1989; Schulz, 1990, 1991; Frahm and Korepin, 1990, 1994; Kawakami and Yang, 1990) using the exact Bethe ansatz equations of Lieb and Wu (1968).

Figure 4 was constructed by numerical integration of a set of differential equations, which are generalizations of (2.7a) and (2.7b) that include the invariant lines at $g_C=1$ and $g_C=4$ and have the appropriate behavior in the soliton regime [where they reduce to (2.17) and (2.21)]:

$$\frac{dv}{d\tau} = (2 - g_C)v, \tag{4.13}$$

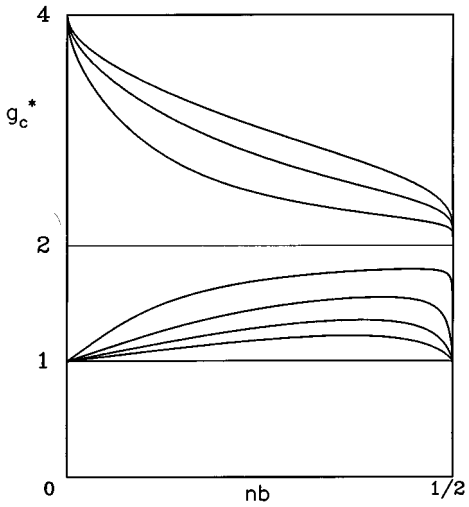

FIG. 4. Schematic plot of the correlation exponent g_C^* for the Hubbard model as a function of band filling for different values of $mUb/\pi^2\hbar^2$. The top curve is for infinite attraction, the bottom straight line g_C=1 is for infinite repulsion, and the interaction grows from the top to the bottom. The straight line g_C=2 describes free lattice fermions.

$$\frac{dg_C}{d\tau}=(1-g_C)(4-g_C)\,\frac{v^2}{1+v^2}\,F(\rho be^{\tau}), \tag{4.14}$$

where $F(x)$ is a function that goes to zero rapidly for $x>1$ and has the limit $F(0)=\frac{1}{3}$; this serves to cut off the flow when $\rho=(1/b)-2n$ is not zero. The separatrix for this set of equations can be found analytically. For Fig. 4, initial values for v and g_C were chosen to lie along the separatrix, and the differential equation followed until g_C had stopped changing, either due to its arrival at a fixed point or to the function $F(x)$ having cut it off. The solid lines in this figure give the final values g_C^* as a function of nb for fixed $u'=unb$. The two subsequent figures were constructed the same way, using other loci of initial conditions. The resulting pictures are schematic representations that incorporate the proper asymptotic behaviors.

The behavior shown in Fig. 4 for $nb\to\frac{1}{2}$ requires some comment. As described by Eq. (4.10), g_C^* always goes to 2 with a nonanalytic singularity for attractive interactions (which is the case $g_C^*>2$). For repulsive interactions, $g_C^*\to 1$ linearly in $\frac{1}{2}-nb$ (which is the case $g_C^*<2$). However, for small u' the slope (which is determined by ξ) is very large.

B. Beyond the Hubbard model

Direct inspection of the flow diagram of Fig. 3 shows that the Hubbard model is a marginal model. Even a small change can lead to significant differences in terms of the renormalized g_C^*. We shall illustrate this using the loci of models (curves e and d of Fig. 3) associated with the extended Hubbard model; other models can be analyzed similarly.

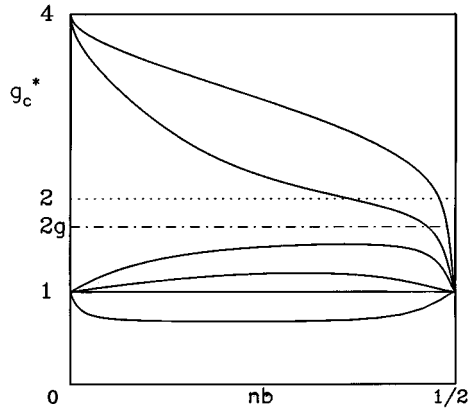

FIG. 5. Schematic plot of the correlation exponent g_C^* for the extended Hubbard model with fixed nearest-neighbor repulsion characterized by $1<2g<2$ as a function of band filling for different values of the Hubbard interaction $u'=mUb/\pi^2\hbar^2$; the top curve is for $u'=-\infty$, the bottom curve is for $u'=+\infty$, and the interaction grows from the top to the bottom. The straight line at $g_C^*=1$ corresponds to the crossing of curve e of Fig. 3 with the Luther-Emery line.

1. The extended Hubbard model with nearest-neighbor repulsion

The extended Hubbard model with nearest-neighbor repulsion (curve e of Fig. 3) always lies below the Hubbard separatrix, indicating the presence of a charge-density gap exactly at half-filling independent of the sign of the Hubbard interaction. For other fillings the measurable g_C^* ranges between 4 and 1 for negative Hubbard interaction and $2g>1$ and can go below unity for positive Hubbard interaction, as can be inferred from Fig. 3. Using the same rules as for the Hubbard model and noting that in the dilute limit the locus of any short-ranged model approaches the limits g_C=1 or g_C=4, we can readily construct the analog of Fig. 4. The results are shown in Fig. 5. We see that now g_C^* can go below unity if the locus of initial conditions is below the Luther-Emery line of Fig. 3. Moreover, we cannot transform Fig. 5 onto Fig. 4 by continuously tuning the strength of the nearest-neighbor repulsion to zero ($g\to 1$) because the Hubbard model is marginal. We also note that the dot-dashed line of Fig. 5, $g_C^*=2g$, which supposedly describes noninteracting spin populations, is an artifact of the approximation (spin-charge separation) used in deriving the action (1.3). For zero Hubbard interaction, the terms that were neglected in Eqs. (1.3) (see Appendix) will renormalize the continuum value $g_C=2g$. However, for $1<2g<2$, the renormalization is significant only in the limit of the completely filled band and will be discussed later along with the case $2g<1$.

2. The extended Hubbard model with nearest-neighbor attraction

The extended Hubbard model with nearest-neighbor attraction (curve d of Fig. 3) always lies above the Hubbard separatrix. Thus it crosses an attractive separatrix,

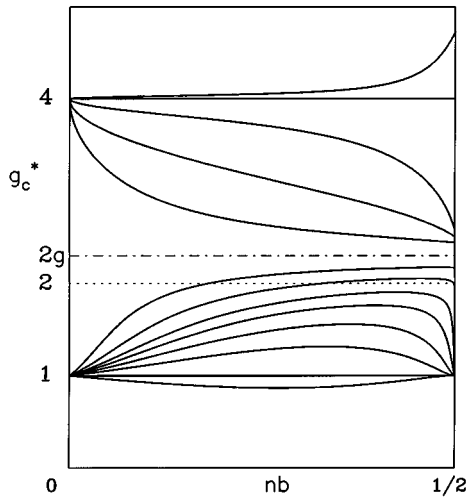

FIG. 6. Schematic plot of the correlation exponent g_C^* for the extended Hubbard model with fixed nearest-neighbor attraction characterized by $2<2g<4$. The straight line at $g_C^*=4$ corresponds to the crossing of curve d of Fig. 3 with the Efetov-Larkin line. The curve that starts at $g_C^*(0)=1$ and ends at $g_C^*(\frac{1}{2})=2$ corresponds to the critical point of the metal-insulator phase transition occurring at half-filling.

which implies that for some finite value of the Hubbard repulsion there is a metal-insulator phase transition at half-filling belonging to the Kosterlitz-Thouless universality class. To the right of the intersection (see Fig. 3), the flow carries any initial point onto the Kosterlitz fixed line $g_C \geqslant 2$, $v=0$, restoring the translational symmetry. In the vicinity of half-filling, the dependence $g_C^*(\rho)$ follows from the interrupted perturbative renormalization-group equations (2.7a) and (2.7b) (see Horovitz *et al.*, 1983):

$$g_C^*(\rho)=g_C^*(0)+(\rho/n)^{2[g_C^*(0)-2]}F_4, \tag{4.15}$$

where $g_C^*(0) > 2$ and F_4 is some unknown function of interactions that changes sign at $g_C^*(0) = 4$: $F_4>0$ for $2 < g_C^*(0) < 4$ and $F_4<0$ for $g_C^*(0) > 4$. The residual singularity (4.15) does not occur within the Hubbard model at all.

Exactly at the crossing (phase transition) point we shall have, instead of (4.13), the analog of Eq. (4.10):

$$g_C^*=2+1/\ln(F_5 n/\rho) \tag{4.16}$$

with some unknown function F_5. For $g\to 1+0$ it behaves with exponential accuracy like $F_5 \approx \exp[1/(g-1)]$.

To the left of the crossing point a charge-density gap opens up exactly at half-filling, and upon approaching the insulator by changing the filling factor we eventually reach the universal regime given by Eqs. (2.15), (2.16), and (2.18). The filling dependence of g_C^* is constructed using the same rules that led us to Figs. 4 and 5. The results are shown in Fig. 6. We note that now g_C^* can go above 4 if the locus of initial conditions is above the Efetov-Larkin line of Fig. 3. There are residual singularities at half-filling for $g_C^*(nb = \frac{1}{2}) \geqslant 2$. They are given by Eq. (4.15) for $g_C^*(nb = \frac{1}{2})>2$ and by Eq. (4.16) for $g_C^*(nb = \frac{1}{2}) = 2$. As in the case of the extended Hubbard model with nearest-neighbor repulsion, Fig. 6 cannot be transformed continuously into Fig. 4 by going to the limit of vanishing nearest-neighbor repulsion, and the dot-dashed line $g_C^* = 2g$ is an artifact of the approximation based on the separation of charge and spin degrees of freedom.

V. UMKLAPP SCATTERING OF ARBITRARY ORDER

Up to now we have studied the effect of the $4k_F$ umklapp scattering on the correlation properties of a one-dimensional quantum liquid, asserting that this process is the most important one near half-filling. Here we shall investigate the role of higher-order umklapp scattering (relevant for $nb=k/l$ with $l\neq 2$), which will justify some results and modify others. We shall find that higher-order umklapp scattering will lead to insulating phases for sufficiently large repulsion between particles of the same spin, but that the Hubbard model and its near neighbors are not significantly affected. We shall also find that spin and charge separation will fail for very strong interactions between particles of the same kind.

The action (1.3a)–(1.3d) takes on essentially different forms depending on the parity of the denominator of the filling factor, which implies that the results for even and odd l will be substantially different; for odd l, the separation of spin and charge fails in many regimes.

A. Umklapp scattering of even order

For even l, there is no coupling between spin and charge degrees of freedom, to the accuracy of the approximations underlying Eqs. (1.3a)–(1.3d). There is some coupling, however, which will be discussed in Sec. V.B. The action takes the form

$$A=\frac{1}{2}\int dxdt(\mu_S\dot{S}^2+K_S S'^2)+\Gamma_1\int dxdt\ \cos 4\pi nS$$
$$+\frac{1}{2}\int dxdt(\mu_C\dot{C}^2+K_C C'^2)$$
$$+\Gamma_2\int dxdt\ \cos 2\pi(\rho x-nlC), \tag{5.1}$$

where the Γ_3 contribution was dropped as being less relevant than the Γ_2 term. The spin parts of this equation are the same as before [Eq. (2.1)], and so we shall focus on the charge part of Eq. (5.1). This is still a sine-Gordon action, with the significant difference that the periodicity of the cosine function has changed.

1. The flow diagram

The flow will have features near $l^2 g_C/4=2$ associated with the Kosterlitz-Thouless phase transition and other features near $l^2 g_C/4=1$ associated with the Luther-Emery line (Luther and Emery, 1974), as in Fig. 3. Also as in Fig. 3, the corresponding flow diagram can be presented in terms of v and g_C, since $\Gamma_2 \propto u$, which sets the initial value for v. It should be pointed out that Γ_2 is not

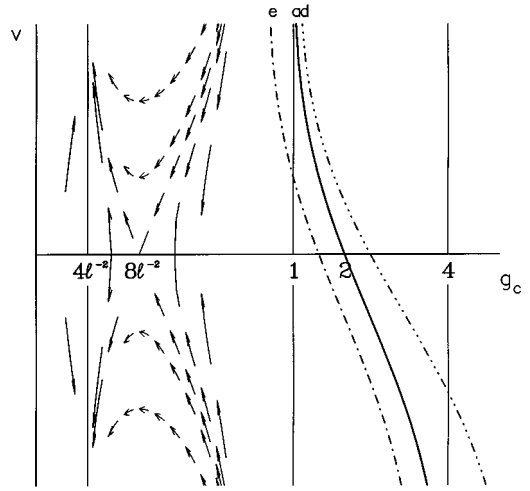

FIG. 7. Flow diagram describing the effect of $2k_Fl$ umklapp scattering for even $l>2$. Only a few trajectories are shown. The curves a, d, and e taken from Fig. 3 correspond to the loci of initial conditions for the Hubbard model (a) and extended Hubbard models with nearest-neighbor attraction (d) and repulsion (e).

the same number that occurred in Eq. (2.1)—this is a different term of an expansion and owes its existence to a different Fourier component of the external potential. It is shown schematically in Fig. 7, together with the loci of initial conditions for the extended Hubbard model taken from Fig. 3.

The flow diagram is not necessarily symmetric with respect to reversal of sign of v, because there is no particle-hole symmetry (but it does have this symmetry to perturbative accuracy). The $v\to+\infty$ limit of the attractive separatrix must lie below $g_C=1$. There cannot be a crossing point between the attractive separatrix and the locus of initial conditions for the Hubbard model (curve a of Fig. 7), because that would imply a phase transition into an insulating phase with filling factor k/l and $l>2$, thus contradicting the exact result of Lieb and Wu (1968) that only the half-filled Hubbard model undergoes a metal-insulator transition. We have no arguments to place this limit more accurately.

The arguments of Sec. II based on the correlation properties of free lattice fermions can again be applied to show that the renormalization-group trajectories at $g_C=1$ and $g_C=4$ are vertical. The trajectories for $1<g_C<4$ are directed towards the $v=0$ axis and presumably almost vertical, since here we are very far away from the Kosterlitz end point at $l^2g_C/4=2$ for even $l>2$. In fact, it seems likely that they are strictly vertical for $g_C\geqslant 1$. Otherwise the effect of the $2k_Fl$ umklapp scattering in the limit $\rho\to 0$ would be manifested in a residual singularity (Horovitz *et al.*, 1983) generalizing Eq. (4.15)

$$l^2g_C^*(\rho)/4=l^2g_C^*(0)/4+F_6(\rho/n)^{2[l^2g_C^*(0)/4-2]} \tag{5.2}$$

whenever $l^2g_C^*(0)/4>2$. This would include the Hubbard model for $l>2$, since for $nb=k/l$, the Hubbard model has g_C^* in the interval [1; 4], thus contradicting the exact results (Lieb and Wu, 1968; Ovchinnikov, 1969; Frahm and Korepin, 1990, 1994; Kawakami and Yang, 1990), which do not indicate residual singularities of this form. This conflict can be resolved if $F_6\equiv 0$ inside the interval [1; 4]. Then there is no physical reason for F_6 to be nonzero to the right of $g_C=4$, since this region of strong quantum fluctuations is very distant from the end point $l^2g_C/4=2$ of the Kosterlitz fixed line. Therefore $2k_Fl$ scattering does not affect our previous results for either the Hubbard model or the extended Hubbard model with nearest-neighbor attraction (curve d of Fig. 7).

We can infer from Fig. 7 that, for even $l>2$, residual singularities of the sort represented by Eq. (5.2) can occur for the extended Hubbard model with nearest-neighbor repulsion, should the locus of initial conditions reach the region where the flow is no longer vertical. For sufficiently large nearest-neighbor repulsion, curve e of Fig. 7 can cross the attractive Kosterlitz separatrix, indicating a phase transition into an insulator with filling factor k/l. In the limit $\rho\to 0$ we shall have at the crossing point instead of Eq. (5.2) an analog of Eq. (4.16),

$$l^2g_C^*/4=2+1/\ln(F_7n/\rho). \tag{5.3}$$

As can be seen from Fig. 7, for initial values at and above the crossing of curve e and the attractive separatrix, the measurable $l^2g_C^*/4$ for the extended Hubbard model with nearest-neighbor repulsion ranges between 2 and some value not larger than l^2. The universal phase transition value $l^2g_C^*/4=2$ is achieved exactly at commensuration $nb=k/l$; for the case of infinite Hubbard repulsion, the exact upper boundary for $l^2g_C^*/4$ is $l^2g_C/4=l^2/4$ (or $g_C=1$) for any filling.

For initial values to the left of the crossing of curve e and the separatrix, the measurable value of $l^2g_C^*/4$ ranges, depending on filling, from unity to the bare value $l^2g_C/4$ representing the crossing point. The former universal limit is achieved as $\rho\to 0$; this is completely analogous to the soliton regime in the vicinity of half-filling (see Sec. II.B.3).

2. The metal-insulator transition (general even l)

The physical picture of the metal-insulator transition that occurs on approach to the commensuration $nb=k/l$ when the particle density is changed is analogous to that in the vicinity of half-filling. There is a very low density of solitons, which are the elementary excitations of the commensurate phase with $nb=k/l$. An estimate of the soliton energy is given by a generalization of Eq. (2.13):

$$E_s\approx K_C\xi/(nl\xi)^2=K_C/(nl)^2\xi\equiv K_Cb^2/k^2\xi. \tag{5.4}$$

Other formulas can be derived straightforwardly (see Kolomeisky, 1993, for details). Instead of Eqs. (2.15), (2.16), and (2.18), we shall have

$$\mu_C^*=\beta\rho(nl/\rho)^2, \tag{5.5}$$

$$K_C^*=\frac{\pi^2\hbar^2\rho^3}{\beta}(nl/\rho)^2, \tag{5.6}$$

$$(l^2 g_C^*/4)^2 = 1 + \frac{[(l^2 g_C/4)^2 - 1]}{F_8}\,\rho\xi. \tag{5.7}$$

Equation (5.7) reproduces a result of Schulz (1980) and Haldane (1982) for the sine-Gordon action.

In view of these considerations, the results of the previous section need to be modified only for $g_C^* < 1$, and it is relevant (as can be seen from Figs. 5 and 6) only for the extended Hubbard model with sufficiently strong nearest-neighbor repulsion. In this region of parameters, instead of the smooth curves shown in Fig. 5 we shall have nonanalytic features of the form (5.2), (5.3), or (5.7) associated with each rational filling k/l. Which of the singularities (5.2), (5.3), or (5.7) is realized depends on whether we are above, at, or below the transition from metal to an insulator with filling k/l, as was explained previously. We note that the singularities at half-filling that are already present in Figs. 5 and 6 are special cases of the more general expressions (5.2), (5.3), and (5.7). The behavior in the dilute limit $nb \to 0$ is not changed, since here we have to get back to the continuum problem.

The density dependence of the correlation exponent below the Luther-Emery line of Fig. 5 can be imagined as follows. When we are above the transition point into the $l=4$ phase—the next important even commensurate phase after the $l=2$ phase—we have residual singularities of the sort represented by Eq. (5.2) for $l \geqslant 4$ and a real singularity (2.18) at half-filling. We note that the residual singularities are weaker both in the dilute and in the almost half-filled limits, since the corresponding fractions involve increasingly large denominators l. As the nearest-neighbor repulsion is increased, the phase-transition point into the $l=4$ phase is eventually reached, and the behavior in the vicinity of $nb=\frac{1}{4}$ is described by Eq. (5.3) with $l=4$. The singularities at $l>4$ are still given by Eq. (5.2). Slightly below the phase-transition point a real singularity (5.7) with $l=4$ shows up and persists for stronger nearest-neighbor repulsion. Upon further increase of the nearest-neighbor repulsion, the $l=6$ phase becomes relevant and the type of singularity at $nb=\frac{1}{6}$ changes from (5.2) via (5.3) to (5.7) as the phase transition is passed. Then the scenario repeats for $l>6$ upon further increase of the nearest-neighbor repulsion.

As will become clear shortly, for the case of odd denominators the scenario described is the same if there is a spin-density gap; when there is no spin-density gap, another type of residual singularity replacing Eq. (5.2) occurs.

Both a qualitative and a quantitative change in the dependence $g_C^*(nb)$ is predicted below for sufficiently strong like-spin repulsion ($2g<1$), as a result of the failure of the approximation based on spin-charge separation at half-filling.

3. The quarter-filled band

The quarter-filled band ($l=4$) extended Hubbard model with infinite Hubbard repulsion can be exactly solved (Schulz, 1990, 1991), providing us with an expression for g_C^*. These exact results are in agreement with those extracted from the flow diagram shown in Fig. 7.

This model has also been studied numerically by Mila and Zotos (1993), and Fig. 7 could again be used to demonstrate that the value of the charge exponent g_C^* at the metal-insulator transition (the crossing of curve e with the attractive separatrix of the flow) equals $8/4^2=\frac{1}{2}$. One can also infer from Fig. 7 that in the conductive phase in the range $\frac{1}{2} \leqslant g_C^* \leqslant 1$ the charge exponent g_C^* is a decreasing function of nearest-neighbor repulsion, and that this is going to change for $g_C^* > 1$. These conclusions are in agreement with Mila and Zotos (1993). There are two features of these numerical results that we cannot recover: (i) a tendency towards phase separation for very repulsive nearest-neighbor interaction and intermediate Hubbard repulsion, and (ii) a metal-insulator boundary at infinite nearest-neighbor interaction. We attribute this to the difference in the models (see the discussion in Sec. II.D.1).

B. Beyond spin-charge separation

Up to now our results have been based on the assumption of spin-charge separation in the action (5.1). However, this is not an exact property: the nonlinear terms of (5.1) were singled out as being the most relevant (in the renormalization-group sense) contributions destabilizing the harmonic part of (5.1), and other terms that couple spin and charge degrees of freedom were dropped as being irrelevant (see Appendix). All of our conclusions based on the soliton picture correspond to the strong-coupling regime of (5.1), where the nonlinear terms are strongly relevant. In general, at this point we cannot neglect the spin-charge interaction.

An indication of the failure of the approximation based on spin-charge separation is already present in Figs. 5 and 6, which predict that for noninteracting spin populations [$\Gamma_1=\Gamma_2=0$ in Eq. (5.1)] the value of the correlation exponent is the same as for the translationally invariant problem. This is physically incorrect; the noninteracting spin populations behave as independent spinless sets of interacting particles moving in a periodic potential that renormalizes the exponent and will give rise to a metal-insulator phase transition at a sufficiently low level of quantum fluctuations. The contributions responsible for this transition do not couple the fields $u_\downarrow$ and $u_\uparrow$ describing the displacements of electrons of two spin directions with respect to their classical positions, and the resulting phases are not describable in terms of the spin and charge variables C and S [see Eq. (1.2)]. The outcome can be understood by combining the results of Kolomeisky (1993), describing spinless interacting particles moving in a periodic potential, with those implied by the properties of the action (5.1). The results for possible phases and correlation exponents of spinless fermions moving in periodic potential with filling factor k/l are accumulated in Table II. The value of the correlation exponent is given both in terms of g (2.2) and g_ν

TABLE II. Possible phases of noninteracting spin populations (spinless fermions) having filling factor $nb=k/l$.

Phase	Correlation exponents	Charge-density gap	Spin-density gap	Elementary excitations
Normal metal	$l^2g^*\geq 2$, or $l^2g_S^*=l^2g_C^*\geq 4$	no	not applicable	charge phonons
Mott insulator	$l^2g^*=1$, or $l^2g_S^*=l^2g_C^*=2$	yes	not applicable	soliton-antisoliton pairs

(1.5) to make it easier to compare with the cases in which there is an unlike-spin interaction. We start from the case of half-filling.

1. The flow diagram for half-filling

The flow picture is shown in Fig. 8, and the possible phases are described in Table III. The flow takes place in a multidimensional space of parameters g_ν and Γ_i and what is shown in Fig. 8 is just a projection onto the g_C-g_S plane. For small u, however, we can read off the initial value $v=u$ with the aid of Eqs. (2.4) and (2.5):

$$ug=g_C-g_S \tag{5.8}$$

(initially $v=u$). This describes the region of the multidimensional space referred to above, which is accessible by the generalized Hubbard models. In the sectors for which spin-charge separation is a good approximation, the flows along the two axes are practically independent, and each can be understood by reference to the flow along the g_C axis in Fig. 3. This consideration generates several of the special lines of Fig. 8, as follows: the lines g_C=2 and g_S=2 give us the limit of stability of the charge and spin subsystems, correspondingly, with respect to the appearance of charge- and spin-density gaps. These are implications of the Kosterlitz theory applied separately to the spin and charge parts of the action (5.1) for l=2. The lines g_C=1 and g_S=1 are the Luther-Emery invariant lines, the satellites of the Kosterlitz-Thouless phase transitions.

The dashed curve schematically represents the locus of initial values for the Hubbard model: for small u it is given by

$$g_C+g_S=4 \tag{5.9}$$

[according to Eqs. (2.4) and (2.5) with g=1]. Above the noninteracting line $g_C=g_S$ it approaches the limit g_C=4, g_S=1, while below the noninteracting line it approaches the limit g_C=1, g_S>2, as implied by Fig. 3 and Eq. (2.4). The symmetry of the problem suggests that the limit for infinite repulsion is g_S=4, and the figures have been drawn this way, but there is no firm reason for believing this. Several characteristic renormalization-group trajectories are shown: starting on the Hubbard line one always ends up at the point $g_S^*=1, g_C^*=2$ for the case of attractive interactions, and at the point $g_S^*=2, g_C^*=1$ for the case of repulsive interactions. These two points are the end points of the Kosterlitz-Thouless-Luther-Emery fixed lines $g_S^*=1, g_C^*\geq 2$, and $g_S^*\geq 2, g_C^*=1$ shown by the bold lines. The former describes a superconductor, while the latter corresponds to an antiferromagnetic insulator having only a charge-density gap (antiferromagnetic insulator I of Table III). The values $g_C^*=1$ and

TABLE III. Possible phases of half-filled interacting spin-$\frac{1}{2}$ electronic system. Any phase has its counterpart through spin-charge symmetry (normal metal transforms onto itself); in terms of the correlation exponents it corresponds to the permutation of g_C^* and g_S^*.

Phase	Correlation exponents	Charge-density gap	Spin-density gap	Elementary excitations
Normal metal	$g_C^*\geq 2, g_S^*\geq 2$	no	no	charge and spin phonons
Superconductor	$g_C^*\geq 2, g_S^*=1$	no	yes	charge phonons, spin soliton-antisoliton pairs
Antiferromagnetic insulator I	$g_C^*=1, g_S^*\geq 2$	yes	no	charge soliton-antisoliton pairs, spin phonons
Nonmagnetic "pair" insulator I (U<0)	$g_C^*=g_S^*=1$	yes	yes	charge and spin soliton-antisoliton pairs
Antiferromagnetic insulator II (U>0)	$g_C^*=g_S^*=1$	yes	yes	charge and spin soliton-antisoliton pairs
Nonmagnetic "pair" insulator II (U<0)	$g_C^*=g_S^*=\frac{1}{2}$	yes	yes	soliton-antisoliton pairs of noninteracting spin populations
Antiferromagnetic insulator III (U>0)	$g_C^*=g_S^*=\frac{1}{2}$	yes	yes	soliton-antisoliton pairs of noninteracting spin populations

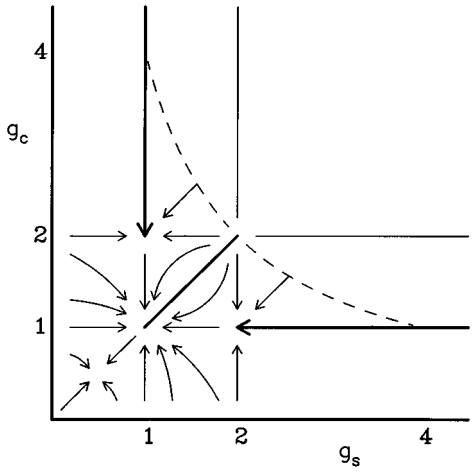

FIG. 8. Schematic flow picture for a half-filled band problem beyond the approximation based on spin-charge separation. The bold segments indicate the stable parts of the Kosterlitz fixed lines corresponding to an antiferromagnetic insulator having only a charge-density gap ($g_C^* = 1, g_S^* \geq 2$), to a superconductor ($g_S^* = 1, g_C^* \geq 2$), and to translationally invariant noninteracting spin populations ($g_C^* = g_S^* \geq 1$). The locus of the Hubbard model is shown by the dashed line, and a few trajectories are indicated by arrows.

$g_S^*=1$ can be attained only in the limits of half-filling and zero magnetization, respectively. The sufficient conditions for being a superconductor or an antiferromagnet without a spin-density gap are as follows: any physical model situated between the attractive (upper dashed) part of the Hubbard line and the line g_S=2 will be a superconductor with the exponents $g_S^*=1$ and $g_C^*\geq 2$, whereas models located between the repulsive (lower dashed) part of the Hubbard line and the line g_C=2 are antiferromagnetic insulators with the exponents $g_C^* = 1, g_S^* \geq 2$. The necessary conditions are actually less restrictive and have to be found separately for each specific model. There is no point in looking for them unless the locus of initial values is known accurately.

Figure 8 demonstrates that the Hubbard model is a marginal system, so that generalized Hubbard models having loci below the Hubbard line (but not very far from it) will end up at the fixed point $g_C^*=g_S^*=1$ describing two different insulator phases: from the attractive side it is a nonmagnetic insulator comprised of evenly distributed pairs of the original particles (nonmagnetic "pair" insulator I of Table III), whereas from the repulsive side it is an antiferromagnetic insulator with each minimum of the periodic potential occupied (antiferromagnetic insulator II of Table III); these insulating phases have both charge- and spin-density gaps.

It is tempting to consider still more general models, in which the initial g_C, g_S, and v can be chosen independently. These can also be understood, in that the Hubbard model lies along a surface in this higher-dimensional problem which contains the three fixed points (g_C=2, g_S=1), (g_C=1, g_S=2), and (g_C=2, g_S=2). This surface separates the region of parameters that corresponds to models with gaps in both spectra from the region in which one or both spectra are gapless.

2. Half-filling: effects of the failure of spin-charge separation

Up to now we have not found any qualitative differences from the physical picture based on spin-charge separation. However, along the noninteracting line $g_C=g_S$ a new phenomenon appears: the behavior for interacting spin populations does not correctly extrapolate to the noninteracting case.

If one starts on the noninteracting line one should always stay there, i.e., the noninteracting line is an invariant line, and the two spin populations will order independently if at all. As in our previous results there are two features of the renormalization-group flow associated with the noninteracting line $g_C=g_S$: there is a Kosterlitz-Thouless metal-insulator phase transition at $g^*=2/l^2=\frac{1}{2}$ or $g_C^* = g_S^* = 2g^* = 1$ (Kolomeisky, 1993); all the trajectories for $g_C^* = g_S^* < 1$ approach a stable fixed point $g_C^* = g_S^*=\frac{1}{2}$ given by the Luther-Emery condition (Kolomeisky, 1993; Straley and Kolomeisky, 1993). The flow diagram is further constrained by the implications of Eq. (5.1) for l=2 that the lines g_C=1 and g_S=1 are invariant lines having some range of attraction.

What is new in Fig. 8 is the stable fixed point at $g_C^* = g_S^*=\frac{1}{2}$, which is beyond the approximation based on spin-charge separation. This is the Luther-Emery stable fixed point of the noninteracting spin populations, but the picture of the flow outside the noninteracting line implies that it must be an attractor within the whole region $g_S<1, g_C<1$. The insulating phases described by this new fixed point are again the nonmagnetic insulator (nonmagnetic "pair" insulator II of Table III) and the antiferromagnetic insulator (antiferromagnetic insulator III of Table III) having both charge and spin-density gaps; from the point of view of the noninteracting spin populations, the two phases differ in whether the two spin types happen to order in the same or different minima of the potential. As in the previous case, the value $g_C^*=g_S^*=\frac{1}{2}$ can be probed in the limits of half-filling and zero magnetization.

The two fixed points at $g_C^* = g_S^*=\frac{1}{2}$ and $g_C^* = g_S^* = 1$ correspond to different phases in that the elementary excitations of the former are close to being solitons of the noninteracting spin populations, whereas the elementary excitations of the latter are spin and charge solitons of the spin and charge parts of the action (5.1) for l=2.

Putting the locus of initial values $g_C+g_S=4g$ [implied by (2.4) and (2.5)] on Fig. 8, we conclude that in the limit of weak Hubbard repulsion the physics is determined by the Luther-Emery fixed point $g_C^*=g_S^*=\frac{1}{2}$ of the noninteracting spin populations if the like-spin repulsion is sufficiently large so that $g<\frac{1}{2}$.

Figure 8 also demonstrates why it was permissible to neglect the coupling between spin and charge variables for weak like-spin repulsion: an external periodic potential does not localize the noninteracting spin populations

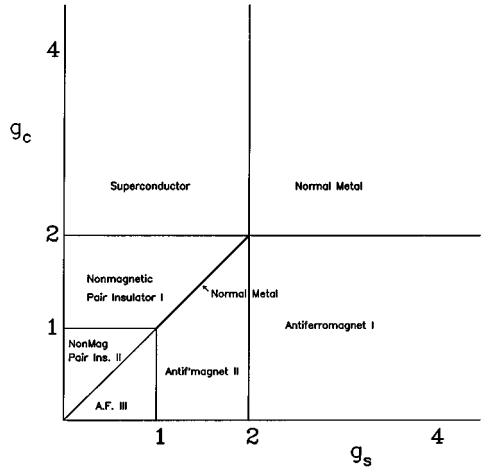

FIG. 9. Phase diagram for half-filling. Here we have labeled the various regions of the (g_C, g_S) plane to indicate which phase results from each combination of microscopic values, assuming the anharmonicity to be small. Each region is thus the basin of accumulation of the fixed points and lines of Fig. 8.

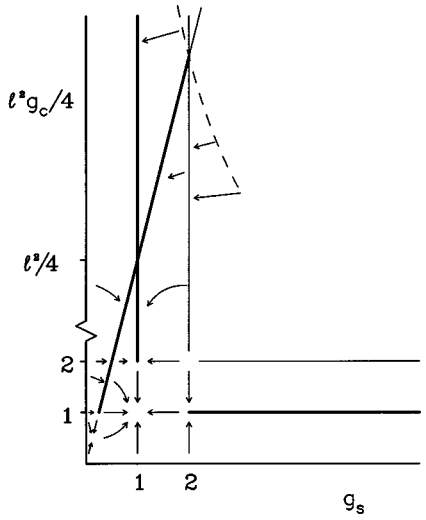

FIG. 10. Schematic flow picture for a less than half-filled band problem with even $l>2$ beyond the approximation based on spin-charge separation. The bold segments indicate the stable parts of the Kosterlitz fixed lines corresponding to an antiferromagnetic insulator having only a charge-density gap ($l^2g_C^*/4 = 1, g_S^* \geq 2$), to either a superconductor or a conductive antiferromagnet ($g_S^* = 1, l^2g_C^*/4 \geq 2$), and to translationally invariant noninteracting spin populations ($g_C^* = g_S^* \geq 4/l^2$). The locus of the Hubbard model is shown by the dashed line, and a few trajectories are indicated by arrows.

for $g_C^* = g_S^* \geq 1$. This stable segment up to the free-fermion point $g_C = g_S = 2$ is shown by the bold line. However, within the same range of parameters, the introduction of an arbitrarily small Hubbard interaction changes the physical picture completely, thus creating a gap in at least one of the collective modes.

There is one more feature specific to the half-filled band problem: the position of the end point of the Kosterlitz fixed line for noninteracting spin populations $g_C^* = g_S^* \geq 1$ coincides with the crossing of the Luther-Emery lines $g_C=1$, $g_S=1$ that determine the physics whenever the approximation based on spin-charge separation is accurate. These points will be distinct for other fillings.

Figure 9 presents the consequences of Fig. 8 in another way. Here we imagine that the anharmonic parts of the action (5.1) are small, and indicate what phase results from various combinations of the microscopic g_C and g_S. The positions of the boundaries between the various phases depend on the values of Γ_1 and Γ_2 (in a way that can be deduced from the directions of flow in Fig. 8); in drawing this figure we have assumed that the Γ_i are small (which is physically correct only in the vicinity of the noninteracting line $g_C = g_S$).

3. Less than half-filling: even denominators

The arguments already presented for the case of half-filling will work in very much the same way for less than half-filling with even denominators. Therefore we shall focus on the differences that arise because the noninteracting line $g_C = g_S$ is no longer a symmetry line between spin and charge degrees of freedom when $l>2$. The results are shown in Fig. 10, and the possible phases are listed in Table IV.

As in Fig. 8, the range of stability of the harmonic parts of the action (5.1) with respect to the appearance of density gaps is given by the straight lines $l^2g_C/4=2$, $g_S=2$. The Luther-Emery lines associated with those are $l^2g_C/4=1$, $g_S=1$; their crossing produces the stable fixed point $l^2g_C^*/4 = g_S^* = 1$. The stable Kosterlitz-Thouless-Luther-Emery fixed line $l^2g_C^*/4 = 1, g_S^* \geq 2$ describes an antiferromagnetic insulator having only a charge-density gap (antiferromagnetic insulator I of Table IV, generalizing that of Table III for any even l). Likewise, the stable line $g_S^* = 1, l^2g_C^*/4 \geq 2$ corresponds to a phase having only a spin-density gap. This phase is superconductive and has the exponents $g_S^* = 1, g_C^* \geq 1$ for the case of an attractive Hubbard interaction (superconductor I of Table IV, analogous to that of Table III). As can be seen from Fig. 10, this is not the only regime that yields a superconductor; for $2 \leq l^2g_C/4 \leq l^2/4$, a Hubbard attraction also leads to a superconductor, for which the exponents lie along the noninteraction line $g_C = g_S$ (superconductor II of Table IV). We expect that this superconductive phase is different from superconductor I, since it corresponds to the final points of the flow located on the noninteracting line $g_C = g_S$ rather than on the Luther-Emery line $g_S=1$. Therefore we cannot say much about its elementary excitations (question mark in Table IV). Naively, one can expect that the particles of opposite spin forming Cooper pairs are more weakly coupled to each other than in superconductor I. This phase does not have an analog in the half-filling case. Its nature and even its existence need to be further studied.

In addition to these superconducting phases, there is another phase with a spin-density gap: a conductor with an antiferromagnetic configuration of electrons of opposite spin. This will be the case for the repulsive Hubbard

TABLE IV. Possible phases of a less than half-filled interacting spin-$\frac{1}{2}$ electronic system having filling factor k/l with even $l>2$. The phases marked with an asterisk * also exist for odd l with exactly the same properties. The question mark corresponds to phases for which we do not know the elementary excitations; moreover, their existence is not firmly established.

Phase	Correlation exponents	Charge-density gap	Spin-density gap	Elementary excitations
Normal metal	$l^2g_C^*/4\geqslant 2, g_S^*\geqslant 2$	no	no	charge and spin phonons
Superconductor I*	$g_C^*\geqslant 1, g_S^*=1$	no	yes	charge phonons, spin soliton-antisoliton pairs
Superconductor II*	$g_C^*=g_S^*, 2\leqslant l^2g_C^*/4\leqslant l^2/4$	no	yes	?
Antiferromagnetic conductor I*	$2\leqslant l^2g_C^*/4\leqslant l^2/4, g_S^*=1$	no	yes	charge phonons, spin soliton-antisoliton pairs
Antiferromagnetic conductor II*	$g_C^*=g_S^*, 1\leqslant g_C^*\leqslant 2$	no	yes	?
Nonmagnetic "pair" insulator I*	$g_C^*=g_S^*, 1\leqslant l^2g_C^*/4\leqslant 2$	yes	yes	?
Nonmagnetic "pair" insulator II*	$l^2g_C^*=l^2g_S^*=2$	yes	yes	soliton-antisoliton pairs of noninteracting spin populations
Antiferromagnetic insulator I	$l^2g_C^*/4=1, g_S^*\geqslant 2$	yes	no	charge soliton-antisoliton pair, spin phonons
Antiferromagnetic insulator II	$l^2g_C^*/4=g_S^*=1$	yes	yes	charge and spin soliton-antisoliton pairs

interaction and $2\leqslant l^2g_C^*/4\leqslant l^2/2$. The locus of the exponents for this phase is $g_S^*=1$, for $2\leqslant l^2g_C^*/4\leqslant l^2/4$ (antiferromagnetic conductor I of Table IV), and the segment of the noninteracting line $g_C=g_S$ for $1\leqslant g_C^*\leqslant 2$ (antiferromagnetic conductor II of Table IV). This latter phase is a repulsive analog of superconductor II of Table IV. Its nature and elementary excitations need to be further studied. The conductive antiferromagnet phases occur only for less than half-filling.

For general l, the periodic potential does not localize the noninteracting spin populations as long as $l^2g^*\geqslant 2$ or $l^2g_C^*/4\geqslant 1$ (Table II). This gives the locus of the stable part of the Kosterlitz fixed line; the associated Luther-Emery fixed point is located at $l^2g_C^*/4=\frac{1}{2}$, $l^2g_S^*=2$ and determines the physics for $l^2g_C/4<1$ and attractive unlike-spin interactions. The corresponding phase is a nonmagnetic insulator formed from uniformly spaced pairs of the original particles of opposite spin and having both charge- and spin-density gaps (nonmagnetic "pair" insulator II of Table IV). Figure 10 shows that another, somewhat "weaker," nonmagnetic insulator phase is possible, with the exponents located on the noninteracting line $g_C=g_S$, and $1\leqslant l^2g_C/4<2$ (nonmagnetic "pair" insulator I of Table IV). This phase can be considered a result of localization of the superconductor II phase by a periodic potential. Once again, the properties of this phase need to be further explored.

The fixed point $l^2g_C^*/4=\frac{1}{2}, g_S^*=2/l^2$ is unstable for repulsive interactions, and the physics is determined by the flow to the stable fixed point $l^2g_C/4^*=g_S^*=1$ describing an antiferromagnetic insulator having both charge- and spin-density gaps (antiferromagnetic insulator II of Table IV). For a large level of quantum fluctuations in the spin subsystem, such that $g_S^*\geqslant 2$, an antiferromagnetic insulator ($l^2g_C^*/4=1$) may be formed, having only a charge-density gap (antiferromagnetic insulator I of Table IV, generalizing that of Table III for even denominators). Some of the phases of Table IV are highlighted by the mark *. These phases are insensitive to the parity of the umklapp scattering and exist for both even and odd l.

Now that we have described the possible ground states, we need to determine under what circumstances they can occur. The Hubbard model itself is either a gapless normal metal with $g_S^*=2, 1\leqslant g_C^*\leqslant 2$ (for the case of repulsive interactions) or a superconductor with $g_S^*=1, 2\leqslant g_C^*\leqslant 4$. The generalized Hubbard models with weak Hubbard interaction have loci of initial conditions parallel to this: $g_C+g_S=4g$ [according to Eqs. (2.4) and (2.5)]. When a like-spin attraction is turned on ($g>1$), the range of superconductivity will shrink. When a like-spin repulsion is turned on ($g<1$), there will appear a range of stability of the conductive antiferromagnet. This conductive antiferromagnet transforms into an antiferromagnetic insulator described by the fixed point $l^2g_C^*/4=g_S^*=1$ as the degree of interparticle repulsion is further increased. Likewise, to transform superconductor I into the nonmagnetic "pair" insulator II (passing by superconductor II, and the nonmagnetic "pair" insulator I) described by the fixed point $l^2g_C^*/4=\frac{1}{2}, g_S^*=2/l^2$, one should further increase the like-spin repulsion keeping the Hubbard interaction attractive. The antiferromagnetic insulator I described by the fixed line $l^2g_C^*/4=1$,

$g_S^* \geq 2$ can be realized if the level of quantum fluctuations is small in the charge subsystem and large for the spin variable. Such conditions could possibly be satisfied for sufficiently strong Hubbard repulsion and could more probably be satisfied in the presence of a finite range of interaction, but we cannot make reliable predictions without knowing accurate loci.

We remind the reader that in all the cases when there is a density gap in a subsystem ν, the corresponding nonzero value of g_ν^* given in the tables needs to be understood as a limiting value upon approaching this density phase by turning the filling factor towards $nb=k/l$, and (or) magnetization to zero.

C. Umklapp scattering of odd order

For fractional fillings $nb=k/l$ with odd l, there is a complete failure of the separability of the spin and charge degrees of freedom, represented by the Γ_2 term in Eq. (1.3d). Let us introduce the dimensionless fields

$$\psi = 2nS, \quad \varphi = 2nlC. \tag{5.10}$$

These cause the action to take the form

$$A = \frac{1}{2}\int dxdt\left(\frac{\mu_S}{4n^2}\,\dot{\psi}^2 + \frac{K_S}{4n^2}\,\psi'^2\right) + \Gamma_1\int dxdt\,\cos 2\pi(2\delta x - \psi) + \frac{1}{2}\int dxdt\left(\frac{\mu_C}{4l^2n^2}\,\dot{\varphi}^2 + \frac{K_C}{4l^2n^2}\,\varphi'^2\right)$$
$$+\Gamma_2\int dxdt\,\cos\pi(2\rho x - \varphi)\cos\pi(2\delta x - \psi) + \Gamma_3\int dxdt\,\cos 2\pi(2\rho x - \varphi) \tag{5.11}$$

in which an auxiliary parameter δ has been introduced, which plays a role similar to that of finite ρ in Eqs. (1.3) and (5.1) and will help us to understand the strong-coupling regime of (5.11) for $\rho=\delta=0$. Physically, finite δ corresponds to an excess of particles of one spin direction over the other, and thus is proportional to the magnetization. The coupling of the charge and spin degrees of freedom arises because the antiferromagnetic arrangement of the spins cannot be commensurate with the external potential. In the presence of this coupling, the Γ_3 term must be included; its more rapid spatial variation will lead to the appearance of factors l^2 (e.g., $l^2 g_C$ instead of $l^2 g_C/4$), where just $l^2/4$ appeared previously.

The action (5.11) is invariant with respect to the transformation

$$\psi \leftrightarrow \varphi, \quad \mu_S \leftrightarrow \mu_C/l^2, \quad K_S \leftrightarrow K_C/l^2, \quad \Gamma_1 \leftrightarrow \Gamma_3, \quad \rho \leftrightarrow \delta, \tag{5.12}$$

which maps the charge and spin degrees of freedom onto each other. For nonzero ρ and δ the action (5.11) is also invariant with respect to infinitesimal shifts of the fields ψ and φ; for $\rho=\delta=0$, Eq. (5.11) has the transformational property

$$\psi \to \psi + 1 \ \ (\text{or} \ \ \varphi \to \varphi + 1), \ \ \Gamma_2 \to -\Gamma_2. \tag{5.13}$$

The stationary manifold of the transformation (5.12),

$$\mu_S = \mu_C/l^2, \quad K_S = K_C/l^2, \quad \Gamma_1 = \Gamma_3, \tag{5.14}$$

defines the invariant line in the (g_S, g_C) plane:

$$l^2 g_C = g_S, \tag{5.15}$$

which coincides with that of noninteracting spin populations $g_C = g_S$ for $l=1$.

First we analyze the action (5.11) for $\rho=\delta=0$ perturbatively, i.e., we consider all the Γ terms to be small perturbations with respect to the harmonic part of the action. This perturbative renormalization-group analysis is in the spirit of the standard treatment of the sine-Gordon action (Wiegmann, 1978). Working to second order in the Γ's, we get the set of the renormalization-group equations

$$\frac{d\Gamma_1}{d\tau} = \Gamma_1(2 - g_S) + \Gamma_2^2(g_S - l^2 g_C), \tag{5.16}$$

$$\frac{d\Gamma_3}{d\tau} = \Gamma_3(2 - l^2 g_C) + \Gamma_2^2(l^2 g_C - g_S), \tag{5.17}$$

$$\frac{d\Gamma_2}{d\tau} = \Gamma_2\left(2 - \frac{g_S + l^2 g_C}{4}\right) - \Gamma_2(\Gamma_1 g_S + \Gamma_3 l^2 g_C), \tag{5.18}$$

$$\frac{dg_S}{d\tau} = -\Gamma_1^2 C_7 g_S^3 - \frac{\Gamma_2^2 C_7}{4}\, g_S^2(g_S + l^2 g_C), \tag{5.19}$$

$$\frac{d(l^2 g_C)}{d\tau} = -\Gamma_3^2 C_7 (l^2 g_C)^3 - \frac{\Gamma_2^2 C_7}{4}\,(l^2 g_C)^2(l^2 g_C + g_S). \tag{5.20}$$

Here the Γ's are the dimensionless analogs of the original Γ's in Eq. (5.11). In terms of the parameters g_S and $l^2 g_C$, the transformation (5.12) reduces to the permutation $g_S \leftrightarrow l^2 g_C$, $\Gamma_1 \leftrightarrow \Gamma_3$. Equations (5.16)–(5.20) have this symmetry as well as the symmetry $\Gamma_2 \to -\Gamma_2$, which derives from Eq. (5.13). We note that off the invariant line $g_S = l^2 g_C$ the $\Gamma_{1,3}$ contributions are always generated under renormalization, even if they were originally absent. However, if one starts from noninteracting sets of particles, an unlike-spin interaction (the $\Gamma_{1,3}$ terms) is not generated under renormalization. For $l>1$, all the Γ's are zero on the noninteracting line $g_C = g_S$ and Eqs. (5.16)–(5.20) do not generate the $\Gamma_{1,3}$ terms. For $l=1$ and $u=0$, the initial $\Gamma_{1,3}$ are zero while Γ_2 is finite; the unlike-spin

interaction terms, $\Gamma_{1,3}$, are not generated in this case, since the positions of the noninteracting line $g_C=g_S$ and the invariant line (5.15) coincide for $l=1$.

The main conclusion of the study of this set of equations is that sufficiently far into the region

$$g_S \geqslant 2, \tag{5.21}$$

$$l^2 g_C \geqslant 2, \tag{5.22}$$

$$g_S + l^2 g_C \geqslant 8, \tag{5.23}$$

the interactions Γ_i are irrelevant, and the flow fails to carry us out of this region. This is the normal metal. If the flow goes out of this region, there is a Kosterlitz-Thouless transition to a different phase having a gap in the spectrum for at least one of the fields S or C; however, further analysis is beyond the range of the perturbative treatment.

The strong-coupling regime of the action (5.11) can be understood from a different viewpoint. First, we assume that we are inside a phase having only a spin-density gap. This will always be the case if $\delta=0$ and ρ is finite in Eq. (5.11) and either $g_S<2$ or $l^2 g_C + g_S<8$. We can integrate out the noncritical spin-density degrees of freedom (the field ψ). After that the φ-dependent part of the action (5.11) acquires the form

$$A_C = \frac{1}{2}\int dx dt \left(\frac{\mu_C}{4l^2 n^2}\,\dot{\varphi}^2 + \frac{K_C}{4l^2 n^2}\,\varphi'^2 \right) + \Gamma_2' \int dx dt\, \cos\pi(2\rho x - \varphi) + \Gamma_3 \int dx dt\, \cos 2\pi(2\rho x - \varphi). \tag{5.24}$$

Here Γ_2' comes from a Gaussian averaging of $\cos\pi\psi$ over the zero-point motion:

$$\Gamma_2' = \Gamma_2 \exp\left(-\frac{\pi^2}{2}\langle \psi^2 \rangle \right), \tag{5.25}$$

where the presence of the spin-density gap guarantees that $\langle\psi^2\rangle$ is finite. Dropping the last (less relevant) term of Eq. (5.24) and going back to the variable C (5.10), we recover an action that has the same functional form as the charge part of Eq. (5.1) with Γ_2 replaced by Γ_2' (5.25). Therefore we can immediately translate most of the results for the present purposes.

First of all for $\rho=0$ the Γ_2' term in (5.24) is irrelevant for $l^2 g_C^*/4 \geqslant 2$, and we have a phase having only a spin-density gap. Combined with the perturbative condition $g_S^* < 2$ [compare with Eq. (5.21)], this gives us the range of stability of the spin-density wave phase. Inside this phase the presence of the irrelevant umklapp scattering term Γ_2' in (5.24) could manifest itself in residual singularities of the form (5.2) or (5.3). For $l^2 g_C^*/4 < 2$ and $\rho=0$ an extra charge-density gap opens up, and in the vicinity of commensuration $\rho\to 0$ the critical behavior is governed by the presence of the Luther-Emery line at $l^2 g_C^*/4 = 1$. This is given by Eqs. (5.5)–(5.7) with different nonuniversal parameters.

Then there can be a regime in which there is no spin-density gap; this will always be the case if δ in Eq. (5.11) is nonzero. After we integrate out the spin-density degrees of freedom, the φ-dependent part of the action (5.11) acquires the form

$$A_C = \frac{1}{2}\int dx dt \left(\frac{\mu_C}{4l^2 n^2}\,\dot{\varphi}^2 + \frac{K_C}{4l^2 n^2}\,\varphi'^2 \right) + \Gamma_3 \int dx dt\, \cos 2\pi(2\rho x - \varphi). \tag{5.26}$$

This is again a sine-Gordon action, and for $\rho=0$ the Γ_3 term is irrelevant if $l^2 g_C^* \geqslant 2$. Inside this phase the presence of the irrelevant umklapp scattering term Γ_3 in (5.26) could manifest itself, similarly to Eqs. (5.2) and (5.3), in residual singularities of the form

$$l^2 g_C^*(\rho) = l^2 g_C^*(0) + F_9 (\rho/n)^{2[l^2 g_C^*(0) - 2]} \tag{5.27}$$

above the phase transition and

$$l^2 g_C^* = 2 + 1/\ln(F_{10} n/\rho) \tag{5.28}$$

at the phase transition.

Below the phase transition point a charge-density gap opens up, and the critical behavior for $\rho\to 0$ is governed by the presence of the Luther-Emery line at $l^2 g_C=1$. It is given, analogously to Eq. (5.7), as

$$(l^2 g_C^*)^2 = 1 + \frac{(l^2 g_C)^2 - 1}{F_{11}}\,\rho\xi. \tag{5.29}$$

Up to now we have considered the charge degrees of freedom while integrating out the spin modes. We can repeat the same analysis for the spin subsystem by integrating out the charge modes. The results can be written down immediately with the help of the transformational property (5.12). We shall have two extra invariant lines at $g_S=1$ and $g_S=4$. The critical behavior in the vicinity of the former (i.e., in the limit of zero magnetization) is

$$g_S^{*2} = 1 + \frac{g_S^2 - 1}{F_{12}}\,\delta\zeta, \tag{5.30}$$

where ζ is the width of the spin soliton, while in the vicinity of the latter one has

$$g_S^{*2} = 16 + \frac{g_S^2 - 16}{F_{13}}\,\delta\zeta. \tag{5.31}$$

We note that the nonuniversal charge (ξ) and spin (ζ) soliton widths in Eqs. (5.7), (5.29), and (5.30), (5.31), respectively, are different. Similarly to Eqs. (5.2), (5.3), (5.27), and (5.28), the effect of irrelevant backward scattering, depending on the presence of the charge-density gap, could be manifested in residual singularities having one of the following forms:

$$g_S^*(\delta) = g_S(0) + F_{14}(\delta/n)^{g_S^*(0)/2 - 4}, \tag{5.32}$$

$$g_S^* = 8 + 1/\ln(F_{15} n/\delta), \tag{5.33}$$

$$g_S^*(\delta) = g_S^*(0) + F_{16}(\delta/n)^{2[g_S^*(0) - 2]}, \tag{5.34}$$

$$g_S^* = 2 + 1/\ln(F_{17} n/\delta). \tag{5.35}$$

The crossings of the invariant lines $l^2 g_C=4$, $l^2 g_C=1$, $g_S=4$, and $g_S=1$ produce fixed points that govern the physics in the strong-coupling regime. As was explained previously, this is the same as the limit $\rho, \delta \to 0$.

The case $l=1$ and $l>1$ will be considered separately, because only for $l=1$ does the invariant line (5.15) of the transformation (5.12) coincide with the noninteracting line $g_C=g_S$. Also note that the action (5.11) is more accurate for $l=1$. Then we have $\Gamma_{1,3}=0$ and $\Gamma_2 \neq 0$ on the noninteracting line, whereas for $l>1$ we have $\Gamma_i=0$, and to provide physical renormalization of g_ν due to the presence of external periodicity we shall need to take into account terms that are not present in Eq. (5.1) (see Appendix). Starting on the noninteracting line $g_C=g_S$, one must always stay on this line, i.e., the noninteracting line is simultaneously the renormalization-group trajectory.

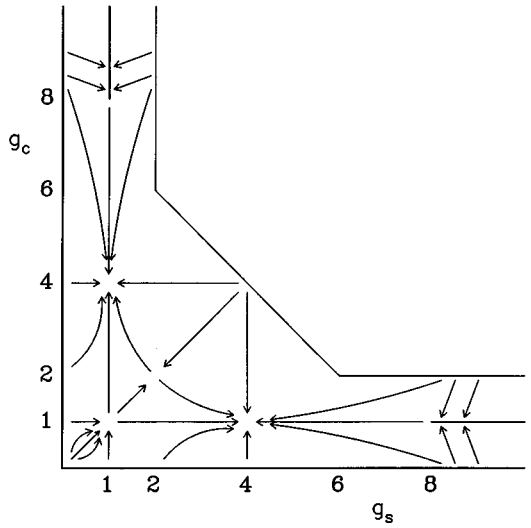

FIG. 11. Schematic renormalization-group diagram describing the flow of the parameters g_ν for $l=1$; only the strong-coupling regime given by the conditions opposite to Eqs. (5.21)–(5.23) is shown.

1. Completely filled band and its vicinity

For a continuum model with a periodic potential, the completely filled band (that is, $nb=1$) is not at all trivial in the case of strong quantum fluctuations: interband mixing can eliminate the charge-density gap altogether, giving a conductor. Even for a lattice model, which for the filled band is an insulator, the vicinity of this limit is of interest, because we can verify that we obtain the physical behavior predicted (through hole-particle symmetry) for a dilute system.

In the absence of any unlike-spin interaction for $l=1$, the action (5.1) splits into two independent sine-Gordon actions describing each spin population moving in a periodic potential. This potential is irrelevant if $g_C^* = g_S^* \geqslant 4$. If this condition is violated, the particles will be localized. In terms of the flow picture, we shall have a Kosterlitz-Thouless transition at $g_C=g_S=4$ and a Luther-Emery feature at $g_C=g_S=2$. From these considerations we deduce the flow picture, Fig. 11; the results on possible phases are assembled in Table V. The behavior in the perturbative regime (5.21)–(5.24) is described by the renormalization-group equations (5.16)–(5.20) and is not shown. The boundary between weak-coupling and strong-coupling behavior is given by the envelope of the lines $g_S=2$, $g_C+g_S=8$, and $g_C=2$. Outside this envelope the system is in a normal-metal phase (first entry of Table V). To understand the direction of the flow in the strong-coupling regime, we take into account the implications of the perturbative equations (5.16)–(5.20), the fact that invariant manifolds associated with the Luther-Emery condition have some range of attraction, and the continuity arguments.

We see from Fig. 11 that the exponents g_ν are not independent and there are several possible strong-coupling outcomes, depending on the initial conditions.

When the macroscopic behavior is governed by the fixed line $g_C^* = 1, g_S^* \geqslant 8$, we have an antiferromagnetic insulator (this is the region of the Hubbard repulsion) having only a charge-density gap; the value $g_C^* = 1$ is probed upon approaching the commensuration $\rho \to 0$.

When the macroscopic behavior is governed by the stable fixed point $g_C^* = 1, g_S^* = 4$, the ground-state configuration is that of evenly spaced "dimers" formed from the original particles of opposite spin. Here we shall have both charge- and spin-density gaps (dimer insulator I of Table V). The values $g_C^* = 1$ and $g_S^* = 4$ are probed upon approaching the commensuration $\rho \to 0$ and in the limit of zero magnetization $\delta \to 0$.

For noninteracting spin populations, the outcome depends on the degree of like-spin interaction. Here the locus of initial conditions is given by $g_C=g_S=2g$ [compare Eqs. (2.4) and (2.5) for $u=0$] so that for $1<2g<4$ the physics is governed by the flow towards the noninteracting free-fermion fixed point $g_S^* = g_C^* = 2$. For noninteracting spin populations, Fig. 11 seems to predict that there is one more special feature (in addition to those of Kosterlitz and Thouless, for $g=2$, and Luther and Emery, at $g=1$) for spinless particles moving in a periodic potential, that the point $2g=1$ might be an attractor for $2g \leqslant 1$. We think that this feature is an illusion, since Fig. 11 is not a literal flow diagram but a slice from a multidimensional flow diagram involving also the parameters Γ_i. Exact results of Haldane (1982) on the sine-Gordon model tell us that there are no extra features of the system beyond those of Kosterlitz and Thouless and Luther and Emery. In other words, starting anywhere on the noninteracting line $g_C=g_S$ in the strong-coupling regime, one ends up at the Luther-Emery (free-fermion) fixed point $g_C^* = g_S^* = 2$. One may speculate that the fixed point $g_C^* = g_S^* = 1$ does attract physical models in the presence of finite Hubbard interaction for $g_C \leqslant 1$ and $g_S \leqslant 1$. Then the resulting phases are as follows: for an attractive Hubbard interaction, one has a nonmagnetic insulator formed from evenly distributed pairs of the original particles of opposite spin (the nonmagnetic "pair" insulator II of Table V), whereas for a repulsive

TABLE V. Possible phases of a completely filled interacting spin-$\frac{1}{2}$ electronic system. Any phase has its counterpart through the spin-charge permutational symmetry of g_C^* and g_S^*. The question mark has the same meaning as in Table IV.

Phase	Correlation exponents	Charge-density gap	Spin-density gap	Elementary excitations
Normal metal	$g_C^* \geq 2, g_S^* \geq 2,$ $g_C^* + g_S^* \geq 8$	no	no	charge and spin phonons
Superconductor	$g_C^* \geq 8, g_S^* = 1$	no	yes	charge phonons, spin soliton-antisoliton pairs
Antiferromagnetic insulator	$g_C^* = 1, g_S^* \geq 8$	yes	no	charge soliton-antisoliton pairs, spin phonons
Nonmagnetic "pair" insulator I	$g_C^* = 4, g_S^* = 1$	yes	yes	charge and spin soliton-antisoliton pairs
"Dimer" insulator I	$g_C^* = 1, g_S^* = 4$	yes	yes	charge and spin soliton-antisoliton pairs
Nonmagnetic "pair" insulator II ($U<0$)	$g_C^* = g_S^* = 1$	yes	yes	?
"Dimer" insulator II ($U>0$)	$g_C^* = g_S^* = 1$	yes	yes	?

Hubbard interaction we have a "dimer" insulator having both charge- and spin-density gaps (dimer insulator II of Table V). The existence of insulators governed by the fixed point $g_C = g_S = 1$ is under question, as are their properties. We think that there is reason to believe that the fixed point $g_C = g_S = 1$ is real, because it attracts physical models with $g_C \leq 1$ and $g_S \leq 1$. For the same range of g's the approximation based on spin-charge separation fails in the case of half-filling (see Sec. V.B.1). We expect that this fact can manifest itself in a change of physics for the completely filled band.

When the macroscopic behavior is governed by the stable fixed point $g_C^* = 4$, $g_S^* = 1$, the ground-state configuration is that of evenly distributed pairs formed from the original particles of opposite spin. Here we shall have both charge- and spin-density gaps (nonmagnetic "pair" insulator I of Table V). The values $g_C^* = 4$, $g_S^* = 1$, can be probed in the limits $\rho, \delta \to 0$.

Finally, when the macroscopic behavior is governed by the fixed line $g_S^* = 1, g_C^* \geq 8$, we have a collection of pairs forming a superconductor. The value $g_S^* = 1$ is probed only in the limit of vanishing magnetization $\delta \to 0$.

The noninteracting line $g_C = g_S$ for $1 < g_S = g_C < 4$ and the lines $g_C = 1$ and $g_S = 1$ for $g_S < 1$ and $g_C < 1$, respectively, are phase transition lines between various insulator phases having both charge- and spin-density gaps.

In drawing Fig. 11 we assumed that the locus of the Hubbard model coincides with the marginal trajectory that connects the free-fermion point ($g_C = 2$, $g_S = 2$) to the stable fixed points ($g_C = 4$, $g_S = 1$) and ($g_C = 1$, $g_S = 4$). For either sign of the Hubbard interaction the system is an insulator having both charge- and spin-density gaps. However, the ground-state configuration generally depends on the sign of the interaction. For the case of a repulsive interaction (below the noninteracting line $g_C = g_S$), we have a "dimer" insulator I, while for the case of an attractive interaction we shall have a "pair" insulator I (see Table V). For lattice models in which the particles are allowed to occupy only the lattice sites, there is no clear spatial distinction between "dimer" and "pair" insulators, since for a completely filled band in the absence of vacant sites each lattice site will be occupied by two electrons of opposite spin. However, the distinction between the two phases manifests itself in different values of correlation exponents as complete filling is approached and (or) magnetization is tuned to zero.

The Hubbard model has particle-hole symmetry around half-filling, thus giving us an independent way of checking the flow of Fig. 11. For a repulsive Hubbard interaction and an almost filled band, the dependence $g_C^*(\rho)$ is given by Eq. (5.29) with $l = 1$, and the universal value $g_C^* = 1$ is approached linearly in the hole (or soliton) density ρ from above. This dependence can be mapped onto the dilute limit [see Eqs. (2.12) and (4.6) and the repulsive portion of Fig. 4], implying a relationship between the nonuniversal parameters of Eqs. (2.12) and (5.29).

The same is true for an attractive Hubbard interaction. Here the dependence $g_C^*(\rho)$ is given by Eq. (5.7) with $l = 1$, and the universal value $g_C^* = 4$ is approached linearly in the hole density ρ from below, being consistent with the dilute limit [see Eqs. (2.22), (4.11), and (4.12) and the attractive portion of Fig. 4].

There are many systems that do not have particle-hole symmetry. For example, a system of two independent sets of particles having some like-spin interaction does not have this property. For the situations shown in Figs. 5 and 6 by dot-dashed lines, the actual dependence $g_C^*(nb)$ starts from $g_C^*(0) = 2g$ and ends at $g_C^*(1) = 2$, as implied by the flow of Fig. 11.

Figure 12 presents the consequences of Fig. 11 in another way. Here we imagine that the anharmonic parts of the action (5.1) are small, and indicate what phase results from various combinations of the microscopic g_C and g_S. The positions of the boundaries between the

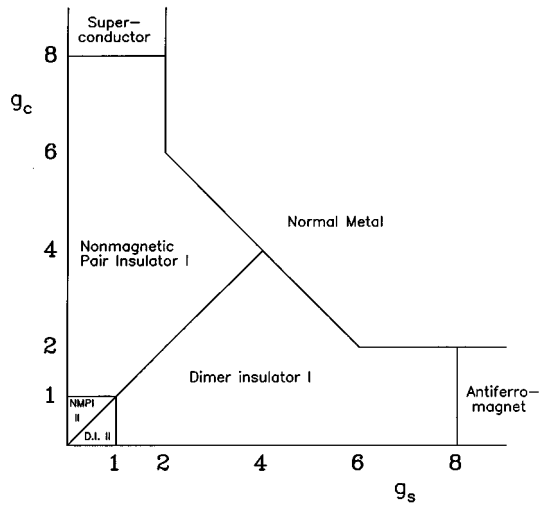

FIG. 12. Phase diagram for a filled band. Here we have labeled the various regions of the (g_C, g_S) plane to indicate which phase results from each combination of microscopic values, assuming the anharmonicity to be small. Each region is thus the basin of accumulation of the fixed points and lines of Fig. 11.

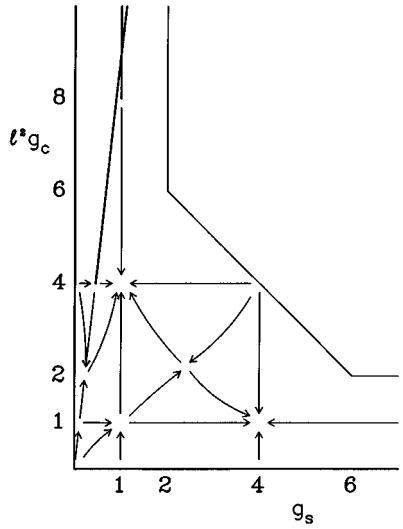

FIG. 13. Schematic renormalization-group diagram describing the flow of the parameters g_ν for odd $l>1$; only the strong-coupling regime, given by the conditions opposite to Eqs. (5.21)–(5.23), is shown. The parts of the flow in common with that of Fig. 10 ($l^2 g_C>7$) or identical to that of Fig. 11 ($g_S>7$) are not shown.

various phases depend on the values of Γ_1 and Γ_2 (in a way that can be deduced from the directions of flow in Fig. 11). In drawing this figure we assumed that the Γ_i are small (which is physically correct only in the vicinity of the noninteracting line $g_C=g_S$).

2. Unfilled band: umklapp scattering of odd order

Now we consider the case of odd denominators with $l>1$. It has already been explained that the action (5.11) fails to describe noninteracting spin populations correctly for $l>1$. However, in the presence of an arbitrarily small unlike-spin interaction, the action (5.11) is a proper long-distance limit at least at some range of parameters, since the contributions important for noninteracting spin populations become irrelevant in the presence of unlike-spin interactions if we are not deeply inside the strong-coupling regime. Similar to the case of even denominators, the outcome can be understood by combining the results of the analysis of the action (5.11) with the implications set by the properties of noninteracting spin populations moving in a periodic potential (Kolomeisky, 1993).

We shall use the flow diagram of Fig. 11 as a starting point for understanding the $l>1$ situation. The arguments followed in the discussion of the $l=1$ case are general and imply that in terms of $l^2 g_C$ versus g_S the flow has invariant lines at $l^2 g_C=1$, $l^2 g_C=4$, $g_S=1$, and $g_S=4$. The line $l^2 g_C=g_S$ is not a trajectory in general, however. The fixed points at $l^2 g_C=1$, $g_S=4$ and $l^2 g_C=4$, $g_S=1$ are stable, implying that there exists an unstable fixed point for $1\leqslant l^2 g_C\leqslant 4$ and $1\leqslant g_S\leqslant 4$ analogous to the Luther-Emery (free-fermion) point of Fig. 11. Also analogously to Fig. 11 there are stable fixed lines at $l^2 g_C=1$, $g_S\geqslant 8$, and $g_S=1$, $l^2 g_C\geqslant 8$. In these respects the phase diagram has the same topology as Fig. 11; the difference comes from the constraint that the noninteracting line $l^2 g_C=l^2 g_S$ must be an invariant line, so that its crossings with the invariant lines $l^2 g_C=1$, $l^2 g_C=4$, and $g_S=1$ will produce extra fixed points. The resulting flow picture is shown in Fig. 13, and the results on possible phases are collected in Table VI. The part of the flow above the noninteracting line $g_C=g_S$ having common features with that of Fig. 10 is not shown. The phases insensitive to the parity of the order of the umklapp scattering are shown only in Table IV, highlighted by an asterisk. The origin of the parity-independent features is that, for the case of an attractive Hubbard interaction, there is a tendency to form pairs that act as a single population of new particles. For these combined particles with no internal (spin) degrees of freedom, the issue of parity does not exist at all. Since the pairs consist of the original particles, this argument is only suggestive. We can see from Fig. 13 that parity manifests itself for $l^2 g_C^* \leqslant 1$ even for an attractive unlike-spin interaction. Here we have a nonmagnetic insulator with the exponents $l^2 g_C^* = l^2 g_S^* = 1$ that has no analog in Fig. 10 (nonmagnetic "pair" insulator III of Table VI, generalizing nonmagnetic "pair" insulator II of Table V for any odd l).

As in Fig. 10, the Luther-Emery fixed point of the noninteracting spin population $l^2 g_C^* = l^2 g_S^* = 2$ is unstable for a repulsive Hubbard interaction, and for some range of parameters the outcome is governed by the flow to the stable fixed point $l^2 g_C^* = 4, g_S^* = 1$, which has its analog in Fig. 10. Two other fixed points of Fig. 13, $l^2 g_C^* = g_S^* = 1$ and $l^2 g_C^* = 1, g_S^* = 4$, do not have any analogs for even l. These two fixed points, as well as $l^2 g_C^* = 4, g_S^* = 1$, describe three different "dimer" insulators (see Table VI). "Dimer" insulators I and II of Table VI

TABLE VI. Possible phases of a partially filled interacting spin-$\frac{1}{2}$ electronic system having filling factor k/l with odd l. Phases of Table IV having an asterisk * are also present but not displayed. The question mark has the same meaning as in Tables IV and V.

Phase	Correlation exponents	Charge-density gap	Spin-density gap	Elementary excitations
Normal metal	$l^2g_C^*\geqslant 2, g_S^*\geqslant 2$ $l^2g_C^*+g_S^*\geqslant 8$	no	no	charge and spin phonons
Nonmagnetic "pair" insulator III	$l^2g_C^*=l^2g_S^*=1$	yes	yes	?
Antiferromagnetic insulator	$l^2g_C^*=1, g_S^*\geqslant 8$	yes	no	charge soliton-antisoliton pairs, spin phonons
"Dimer" insulator I	$l^2g_C^*=1, g_S^*=4$	yes	yes	charge and spin soliton-antisoliton pairs
"Dimer" insulator II	$l^2g_C^*=g_S^*=1$	yes	yes	?
"Dimer" insulator III	$l^2g_C^*=4, g_S^*=1$	yes	yes	charge and spin soliton-antisoliton pairs

generalize those of Table V; "dimer" insulator III of Table VI has no analog for the completely filled (l=1) case (Table V).

Two more phases are possible for a repulsive Hubbard interaction. One of them, existing for $l^2g_C^*\geqslant 8$, is completely analogous to the conductive antiferromagnet we found for even l: they even have the same range of stability. Another phase is an antiferromagnetic insulator having $l^2g_C^*=1$ and $g_S^*\geqslant 8$.

D. The exponent g_C^* and fractional charge

The value of the translational correlation exponent g_C^* can be used to determine the elementary charge of solitons, which turns out to be fractional in general. This is an example of the general idea that topological excitations in broken-symmetry systems carry fractional charge (Heeger *et al.*, 1988).

The exponent g_C^* determines the conductance of a spin-$\frac{1}{2}$ quantum liquid according to the rule

$$\mathcal{G}=g_C^*e^2/h \tag{5.36}$$

(Apel and Rice, 1982; Kane and Fisher, 1992a, 1992b). For noninteracting fermions, this reduces to $\mathcal{G}=2e^2/h$ [see Eq. (2.5) for g=1 and u=0], which is Landauer's rule $\mathcal{G}=e^2/h$ per channel (Landauer, 1970), since the two spin states provide two channels. In the present language, the derivation of this expression is as follows: Let the right and left extremities of our one-dimensional system be in equilibrium with reservoirs with chemical potentials differing by $e\mathcal{V}$, where $\mathcal{V}$ is the applied voltage. There will be an excess of $2e\mathcal{V}\,\partial n/\partial\mu$ states filled on one side (the right side, for definiteness) relative to the other, of which half are excitations moving to the left, with velocity $c_C^*=\sqrt{K_C^*/\mu_C^*}$ (1.6). Thus there is a current $\mathcal{I}=e^2c_C^*\partial n/\partial\mu\mathcal{V}$ flowing across the system, and the conductance is $\mathcal{G}=\mathcal{I}/\mathcal{V}=e^2c_C^*\partial n/\partial\mu$. Rewriting this in terms of $K_C^*=2n^2\partial\mu/\partial n$ [Eq. (1.7)] reproduces (5.36) with g_C^* given by $4\pi n^2\hbar/\sqrt{\mu_C^*K_C^*}$, in agreement with Eq. (1.5b). The essential point is that the density of states $\partial n/\partial\mu$ is the same as the compressibility in one dimension.

As we have seen, the insulator phases of our system are characterized by the value of the exponent g_C^* asymptotically close to commensuration. In this regime the system is conductive and can be described as a dilute gas of solitons, which are isomorphic to free fermions. We can also define a soliton charge Q by applying Landauer's rule to the gas of solitons. When the charge-carrying solitons are the nonlinear excitations of the field C [Eq. (1.2)], they are spinless, so that $\mathcal{G}=Q^2/h$. There are also cases for which the solitons have spin $\frac{1}{2}$, so that $\mathcal{G}=2Q^2/h$. This occurs when the solitons are the nonlinear excitations of the fields $u_\downarrow$ and $u_\uparrow$ (1.2); this situation can be realized only when the physics is determined by the Luther-Emery fixed point of noninteracting spin populations. Comparing the two expressions for the conductance gives

$$Q=e\sqrt{g_C^*} \tag{5.37}$$

for charge-carrying solitons of the field C (1.2), or

$$Q=e\sqrt{g_C^*/2} \tag{5.38}$$

for solitons of noninteracting spin populations.

The cases of even- and odd-order umklapp scattering are best treated separately.

1. Umklapp scattering of even order

For half-filling, the insulating phases having soliton excitations give exponent values $g_C^*=1$ and $g_C^*=\frac{1}{2}$ (see Fig. 8). The former describes antiferromagnetic insulators I and II, and nonmagnetic "pair" insulator I of Table III. From Eq. (5.37) we find that the solitons of those phases carry charge e and zero spin, as was found previously by Su, Schrieffer, and Heeger (1980).

The value $g_C^*=\frac{1}{2}$ (see Fig. 8) describes nonmagnetic "pair" insulator II and antiferromagnetic insulator III of Table III, and the corresponding fixed point coincides with that of Luther and Emery of the noninteracting

spin populations. From (5.38) we find that the solitons of the noninteracting spin populations at half-filling carry the charge $e/2$ in accordance with existing results (Jackiw and Rebbi, 1976; Rice *et al.*, 1976; Su and Schrieffer, 1981; Heeger *et al.*, 1988).

For less than half-filling, there are again two possible outcomes pertinent to charged solitons: $l^2 g_C^*/4 = 1$ and $l^2 g_C^*/4 = \frac{1}{2}$ (see Fig. 10). The former describes antiferromagnetic insulators I and II of Table IV, and from Eq. (5.37) we find that solitons of these insulators carry the charge

$$Q = 2e/l, \tag{5.39}$$

in agreement with the counting arguments of Su and Schrieffer (1981). For half-filling (l=2), this is the case $Q = e$ already described. From the present point of view, getting the electronic charge e (and not some fraction of it) is practically an accident.

The value $l^2 g_C^*/4 = \frac{1}{2}$ describes the nonmagnetic "pair" insulator II of Table IV; its elementary excitations are soliton-antisoliton pairs of the noninteracting spin populations. From Eq. (5.38), we find that the solitons of the noninteracting spin populations carry the charge $Q = e/l$, in accordance with Rice *et al.* (1976), Jackiw and Rebbi (1976), and Heeger *et al.* (1988).

2. Umklapp scattering of odd order

For a completely filled band, there are three values of g_C^* corresponding to insulators with soliton excitations (see Fig. 11): $g_C^* = 4$, $g_C^* = 1$, and $g_C^* = 2$. The first describes the nonmagnetic "pair" insulator I of Table V. From Eq. (5.37) we find the soliton charge $Q = 2e$. This is the special (l=1) case of the more general result (5.39), since particles of opposite spin form pairs, thus making the issue of parity of the order of umklapp scattering irrelevant. The value $g_C^* = 1$ corresponds to an antiferromagnetic insulator and the "dimer" insulator I of Table V. From Eq. (5.37) we find that the solitons of these phases carry charge e. The value $g_C^* = 2$ describes the Mott insulator of the noninteracting spin populations (Table II). From (5.38) we find $Q = e$, which is a special (l=1) case of the more general result $Q = e/l$ for spinless particles (Jackiw and Rebbi, 1976; Rice *et al.*, 1976; Heeger *et al.*, 1988).

For an incompletely filled band, there are also three values of g_C^* corresponding to insulators with soliton excitations (see Fig. 13): $l^2 g_C^* = 2$ (nonmagnetic "pair" insulator II of Table IV), $l^2 g_C^* = 4$ ("dimer" insulator III of Table VI), and $l^2 g_C^* = 1$ ("dimer" insulator I, antiferromagnetic insulator of Table VI). The first value needs to be substituted into Eq. (5.38), since we are at the fixed point of noninteracting spin populations. This gives $Q = e/l$, as we already found for even orders of umklapp scattering. This result is parity-insensitive, since the ground-state configuration is a collection of periodically distributed pairs of the original particles. The value $l^2 g_C^* = 4$ belongs to the case of Eq. (5.37) and reproduces Eq. (5.39) found for even l. Here the "dimer" ground-state configuration has no analog for even l, but the corresponding solitonic charge is still given by the common formula (5.39).

A new result is found if one substitutes the third value $l^2 g_C^* = 1$ into Eq. (5.37):

$$Q = e/l. \tag{5.40}$$

This result does not have an analog for even l. We conclude that solitons of "dimer" insulator I and antiferromagnetic insulators of Table VI carry the charge given by Eq. (5.40). A special case of this general expression was found above for l=1. The result (5.40) might be better written $Q = 2e/2l$, since it is the subharmonic of order $2l$ [the Γ_3 term of (1.3)], or $4lk_F$ umklapp scattering is responsible for the formation of the "dimer" insulator I and the antiferromagnetic insulator of Table VI. The result (5.40) could have been guessed directly from this observation as well as from the counting arguments of Su and Schrieffer (1981), which depend on nothing more than charge conservation. Then, reversing the logic of this section, the connection with the Landauer rule provides us with an independent and elementary derivation of the correlation exponents g_C^* confirming the renormalization-group results.

VI. CONCLUSION

In this paper we have constructed a general unifying approach for the study of the ground-state properties of interacting spin-$\frac{1}{2}$ fermions moving in a periodic potential. We were able to classify many of the possible types of ground states as well as to determine the correlation exponents associated with these phases. In particular, we found that filling factors with even and odd denominators form distinct universality classes which can be characterized according to the form of the long-wavelength action. In the case of even denominators, the spin and charge variables are separated in the long-wavelength action, while for odd denominators spin-charge separation is not achieved in the long-distance limit, thus leading to different physical behavior. The physical reason for this selectivity is perhaps not parity but the degeneracy factor: for particles of arbitrary spin S, the physical behavior for filling factors with denominators that are a multiple of $2S+1$ is expected to be different from that for other denominators.

The theory we have developed is phenomenological in spirit and therefore determines which answers can be found in principle. A further study of microscopic models is necessary to find the actual conditions of realization for various regimes of physical behavior as well as to understand the detailed spatial organization of "dimer" phases.

We have left some questions open. As noted by the question marks on Tables III and V, there are a number of phases whose existence is indicated by the renormalization flows, but which are not clearly characterized.

We hope that the general ideas developed in this paper can be used to analyze problems such as the case of the presence of a magnetic field and the combined effect

of impurities and periodic potential. We think that these methods can be used to look at the case in which underlying particles have an arbitrary number of internal degrees of freedom (for instance, arbitrary spin). The simplest problem of this sort—classification of the ground states of a translationally invariant many-component quantum liquid—was solved recently (Kolomeisky and Straley, 1994).

ACKNOWLEDGMENTS

We acknowledge illuminating discussions with G. Gómez-Santos, F. Guinea, A. P. Levanyuk, A. Luther, L. V. Mikheev, and A. A. Nersesyan. Special thanks go to J. P. Sethna for a careful reading of the manuscript and useful conversations. This work was supported by the National Science Foundation through the grants DMR-9003698 and DMR-9121654.

APPENDIX: DERIVATION OF THE LONG-WAVELENGTH ACTION (1.3a)–(1.3d)

Here we derive the terms in the action equations (1.3a)–(1.3d) in the limit of weak Hubbard interaction U and weak periodic potential $V(x)$. We represent the positions of the particles in terms of their displacement away from uniform spacing,

$$x_j = jn^{-1} + u_{\uparrow j}; \quad y_j = jn^{-1} + u_{\downarrow j}, \tag{A1}$$

and then use Poisson's summation formula to write

$$\sum_j V(x_j) = n \sum_{q=-\infty}^{\infty} \int V[x+u_\uparrow(x)] e^{2\pi niqx} dx \tag{A2}$$

$$= \sum_{q=-\infty}^{\infty} \int V[x] e^{2\pi niq[x-u_\uparrow(x)]} \times (1-\partial u_\uparrow/\partial x) dx, \tag{A3}$$

where now we are regarding $u_\uparrow(x)$ and $u_\downarrow(x)$ to be continuous (and, in fact, slowly varying) functions of x; in Eq. (A3) we have changed the variables to $\tilde{x} = x + u_\uparrow(x)$, and then ignored the difference between $u_\uparrow(x)$ and $u_\uparrow(\tilde{x})$. This transforms Eq. (1.1) to

$$A = \frac{1}{2} \sum_{S=\uparrow,\downarrow} \int dx dt \left[mn \left(\frac{\partial u_S}{\partial t} \right) + K \left(\frac{\partial u_S}{\partial x} \right)^2 + 2\tilde{\mu} n \frac{\partial u_S}{\partial x} \right] + n \sum_{S=\uparrow,\downarrow} \int dx dt \left(1 - \frac{\partial u_S}{\partial x} \right) \sum_p V(x) e^{2\pi ipn[x-u_S(x)]}$$
$$+ n^2 \int dx dy dt \left(1 - \frac{\partial u_\uparrow}{\partial x} \right) \left(1 - \frac{\partial u_\downarrow}{\partial y} \right) \sum_{p,q} U \delta(x-y) e^{2\pi in[p(x-u_\uparrow(x))+q(y-u_\downarrow(x))]} \tag{A4}$$

where we have used the harmonic liquid approximation ($|\partial u_S/\partial x| \ll 1$) to describe like-spin interactions, and dropped background terms that do not depend on $u_\uparrow$ and $u_\downarrow$.

The compliance K describes the long-wavelength part of the interactions within a single spin population. It can be calculated exactly when the dependence of the chemical potential on particle density is known: $K = n^2 \partial\mu(n, U=0)/\partial n$. This compliance contains not only the interparticle forces but quantum effects coming from the relative accessibility of phase space—entropic effects, in the language of the two-dimensional gas of world lines.

An important example is the case in which the particles constituting each spin population are free fermions [in terms of the Action (1.1), this is the case $W=\infty$, $a=0$, $V=0$, and $U=0$]; then $\mu = \pi^2\hbar^2 n^2/2m$ and $K = \pi^2\hbar^2 n^3/m$. Even though the particles interact only when they touch, we can consistently continue to assume $|\partial u/\partial x|$ and $|\partial v/\partial x| \ll 1$, because the condition that the lines cannot touch anywhere implies that they are held away from each other almost everywhere. For the case of interfermion repulsion [which in terms of (1.1) can be modeled by $W=\infty$, $a \neq 0$, $V=0$, and $U=0$], one has $\mu > \pi^2\hbar^2 n^2/2m$ and $K > \pi^2\hbar^2 n^3/m$. The case of interfermion attraction is included in (1.1) when, for example, $a=0$, $V=0$, $U=0$, and W is finite. Here one has $\mu < \pi^2\hbar^2 n^2/2m$, and $K < \pi^2\hbar^2 n^3/m$, respectively.

In Eq. (A4), $\partial u_\uparrow/\partial x$ and $\partial u_\downarrow/\partial x$ represent the fluctuations in particle density about homogeneity. We must impose $\int dx dt (\partial u_S/\partial x) = 0$ if the particle density is to be correctly specified by n. The parameter $\tilde{\mu} n$ is a Lagrange multiplier which ensures this condition; $\tilde{\mu}$ itself is a contribution to the chemical potential.

Of course, we can do the integration over y in the last term, bringing it to the form

$$n^2 U \int dx dt (1-u'_\uparrow)(1-u'_\downarrow) \sum_{p,q} e^{2\pi inx(p+q) - 2\pi in(pu_\uparrow + qu_\downarrow)}, \tag{A5}$$

where primes stand for spatial derivatives.

To put the action into harmonic liquid form we must eliminate the terms that are linear in the spatial derivatives. Collecting these, we have

$$-n \sum_{S=\uparrow,\downarrow} u'_S V(x) - n^2 U \sum_{S=\uparrow,\downarrow} u'_S + \tilde{\mu} n \sum_{S=\uparrow,\downarrow} u'_S. \tag{A6}$$

In equilibrium these terms must cancel on average; this determines both the chemical potential and the ac-

tual particle distribution, which is modulated by the external potential. We select the parameter $\tilde{\mu}$ to cancel the interaction between unlike spins: $\tilde{\mu}=nU$. This implies a connection between the equations of state of interacting ($U\neq 0$) and noninteracting particles ($U=0$):

$$\mu(n)=\mu_0(n)+nU. \tag{A7}$$

Equation (A7) has a typical perturbative form. We shall specify its range of validity later. The remainder of the linear part in (A6) can be absorbed in the harmonic part of the action by the shift

$$u_\uparrow \to u_\uparrow+\eta, \quad u_\downarrow \to u_\downarrow+\eta \tag{A8}$$

where

$$\eta(x)=\int^x \frac{nV(z)dz}{K+n^2U}. \tag{A9}$$

After this transformation the action acquires the form, to lowest order in the spatial derivatives,

$$A=\frac{1}{2}\int dxdt[mn(\dot{u}_\uparrow^2+\dot{u}_\downarrow^2)+K(u_\uparrow'^2+u_\downarrow'^2)+2n^2Uu_\uparrow'u_\downarrow']+\int dxdt{\sum_p}' V_p(x)e^{2\pi inp(x-u_\uparrow)}$$
$$+\int dxdt{\sum_q}' V_q(x)e^{2\pi inq(x-u_\downarrow)}+\int dxdt{\sum_{p,q}}' W_{p+q}(x)e^{2\pi inx(p+q)-2\pi in(pu_\uparrow+qu_\downarrow)}, \tag{A10}$$

where the dots stand for time derivatives, Σ' means that the homogeneous terms have been removed, and we introduced the following notation:

$$V_p(x)=n\left(1-\frac{nV(x)}{K+n^2U}\right)V(x)e^{-2\pi inp\,\eta(x)}, \tag{A11}$$

$$W_{p+q}(x)=n^2U\left(1-\frac{nV(x)}{K+n^2U}\right)^2 e^{-2\pi in(p+q)\eta(x)}. \tag{A12}$$

This latter expression is misleading in that it suggests that W_{p+q} is nonzero even when the periodic potential is absent, when in fact it is the coefficient of terms in Eq. (A10) that break translational symmetry. The resolution is that the terms in (A12) that are independent of V make no contribution to (A10) and should be dropped. Then for small U and $V(x)$, $W_{p+q}(x)\approx -2n^3UV(x)/K$.

It is useful to extract the $p+q=0$ contribution explicitly from the last term of Eq. (A10) and to introduce the charge and spin fields S and C defined in Eq. (1.2). This transformation diagonalizes the harmonic part of the action (A10), leading to

$$A=\frac{1}{2}\int dxdt[\mu_C\dot{C}^2+\mu_S\dot{S}^2+K_CC'^2+K_SS'^2]$$
$$+2\int dxdt{\sum_q}' V_q(x)e^{2\pi inq(x-C)}\cos 2\pi nqS$$
$$+\int dxdt\sum_{p+q\neq 0} W_{p+q}(x)e^{2\pi in(p+q)(x-C)-2\pi in(p-q)S}$$
$$+\int dxdt{\sum_q}' W_0(x)e^{-4\pi inqS}. \tag{A13}$$

The action (A13) is a general long-wavelength action describing the behavior of a spin-$\frac{1}{2}$ quantum liquid in an external potential of general nature, and the final result (A13) is actually more general than the derivation given. The coefficients of the harmonic part of (A13) are given by

$$\mu_C=2mn, \tag{A14}$$

$$\mu_S=2mn, \tag{A15}$$

$$K_C=2K(1+u), \tag{A16}$$

$$K_S=2K(1-u), \tag{A17}$$

where we have introduced the dimensionless parameter of the interaction between spins

$$u=n^2U/K. \tag{A18}$$

Equations (A14)–(A18), as well as Eqs. (A11) and (A12) for the functions $V_p(x)$ and $W_{p+q}(x)$, are perturbative and valid if

$$|u|\ll 1 \tag{A19}$$

and if the absolute value of the derivative $\eta'(x)$ (A9), which is a local deformation of the harmonic liquid, is small with respect to unity. Beyond this approximation the expressions (A11), (A12), and (A14)–(A18) are no longer valid, even though the long-wavelength action still has the functional form (A13) with undetermined phenomenological parameters. The combination of Eqs. (A14)–(A18) and Eqs. (1.5) and (2.3) gives the results (2.4) and (2.5).

For periodic $V(x)=V(x+b)$, the potentials $V_q(x)$ and $W_{p+q}(x)$ in Eq. (A13) are also periodic functions [see Eqs. (A9), (A11), and (A12)] and can be decomposed into a Fourier series:

$$2V_l(x)=\sum_k V_{l,k}e^{-i(2\pi/b)kx}, \tag{A20}$$

$$W_{p+q}(x)=\sum_k W_{p+q,k}e^{-i(2\pi/b)kx}, \tag{A21}$$

where V_{lk} and $W_{p+q,k}$ are Fourier coefficients satisfying

$$V_{-l,-k}=V_{l,k}^*, \quad W_{-l,-k}=W_{l,k}^*. \tag{A22}$$

Substituting (A20) and (A21) into Eq. (A13), we obtain

$$A=\frac{1}{2}\int dxdt[\mu_C\dot{C}^2+\mu_S\dot{S}^2+K_CC'^2+K_SS'^2]+\int dxdt\sum_{l,k}{}'V_{l,k}e^{2\pi ix[ln-(k/b)]-2\pi ilnC}\cos 2\pi nlS$$
$$+\int dxdt\sum_{p+q\neq 0,k}W_{p+q,k}e^{2\pi ix[n(p+q)-(k/b)]-2\pi i(p+q)nC-2\pi in(p-q)S}+\Gamma_1\int dxdt\ \cos 4\pi nS, \tag{A23}$$

where $\Gamma_1=2n^2U$, and where we have dropped the periodic contribution to the last term of (A23) [the external potential part in the function $W_0(x)$ from (A12)] due to its oscillating behavior, which cannot be affected by changing the particle density. On the other hand, the oscillating dependence of the second and the third sums in (A23) can be altered by changing the particle density. If the filling factor nb is equal to a fraction k/l, the corresponding Fourier harmonic is commensurate with the interparticle distance, and an insulating phase can occur. For incommensurate fillings the oscillating dependences in (A23) are not compensated, and the corresponding terms are irrelevant in the renormalization-group sense.

To find the form of the phase diagram and to describe the phase transitions for the case of a commensurate filling factor, we have to single out the dominant contributions from the sums in (A23). If $nb=k/l$ is an irreducible fraction, the V_{lk} harmonic is the most relevant one that contributes to the first sum. In general all the terms from the second sum in (A23) for which $p+q=l$ will contribute equally. Now we have to determine the most important contribution in view of differing spin parts. Since the presence of the variable S in the form $\cos 2\pi nlS$ in the first sum, or as $e^{-2\pi in(p-q)S}$ in the second sum, increases the effect of quantum fluctuations on the otherwise identical C part, the idea is to select the term that gives the smallest possible contribution. For a fixed denominator l we can do nothing with $\cos 2\pi lnS$, but we are free to minimize the absolute value of the difference $p-q$ inside the exponential $e^{-2\pi in(p-q)S}$ for fixed $l=p+q$. Here the outcome clearly depends on the parity of l. For even l, the minimal absolute value of the difference is zero and is achieved for $p=q=l/2$, whereas for odd l the minimum of $|p-q|$ is unity. We conclude that the contributions we have just identified are more important than those coming from the V term of the action (A23), except at l=1, for which they are equally important. The V contributions are those responsible for physics whenever the approximation based on spin-charge separation is not accurate enough.

In collecting the relevant contributions, we note that the functions $V_l(x)$ and $W_{p+q}(x)$ from Eqs. (A11) and (A12) have common (modulo π) phases. Extracting this phase by a shift in the variable C, we finally get the action (1.3a)–(1.3d), with the following parameters:

$$\Gamma_2=2|W_{1,1}|+2|V_{1,1}| \quad \text{for } l=1,$$
$$\Gamma_2=2|W_{l,k}| \quad \text{for } l>1, \tag{A24}$$
$$\Gamma_3=2|W_{2l,2k}| \quad \text{for } l\geqslant 1.$$

For the case of half-filling, the parameter V appearing in Eq. (2.1) is given by

$$V=\Gamma_2/2n^2=|W_{2,1}|/n^2. \tag{A25}$$

REFERENCES

Apel, W., and T. M. Rice, 1982, Phys. Rev. B **26**, 7063.

Blume, M., V. J. Emery, and A. Luther, 1970, Phys. Rev. Lett. **25**, 450.

Bogoliubov, N. M., and V. E. Korepin, 1988, Mod. Phys. Lett. B **1**, 349.

Bogoliubov, N. M., and V. E. Korepin, 1989, Int. J. Mod. Phys. B **3**, 427.

Chaikin, P. M., and T. C. Lubensky, 1995, *Principles of Condensed Matter Physics* (Cambridge University, Cambridge, England), Sec. 9.3.

Efetov, K. B., and A. I. Larkin, 1975, Zh. Eksp. Teor. Fiz. **69**, 764 [Sov. Phys. JETP **43**, 390 (1976)].

Emery, V. J., 1976, Phys. Rev. B **14**, 2989.

Emery, V. J., 1979a, in *Highly Conducting One-Dimensional Solids*, edited by J. T. Devreese, R. P. Evrard, and V. E. van Doren (Plenum, New York), p. 247.

Emery, V. J., 1979b, in *Proceedings of the Kyoto Summer Institute 1979—Physics of Low-Dimensional Systems*, edited by Y. Nagaoka and S. Hikami (Publication Office, Progress of Theoretical Physics, 1979), p. 1.

Emery, V. J., A. Luther, and I. Peschel, 1976, Phys. Rev. B **13**, 1272.

Emery, V. J., and C. Noguera, 1988, Phys. Rev. Lett. **60**, 631.

Fowler, M., 1978, Phys. Rev. B **17**, 2989.

Frahm, H., and V. E. Korepin, 1990, Phys. Rev. B **42**, 10 553.

Frahm, H., and V. E. Korepin, 1994, Int. J. Mod. Phys. B **8**, 403.

Gaudin, M., 1967, Phys. Lett. **24A**, 55.

Gaudin, M., 1973, J. Phys. (Paris) **34**, 511.

Gaudin, M., 1983, *La Fonction d'Onde de Bethe* (Masson, Paris).

Giamarchi, T., 1991, Phys. Rev. B **44**, 2905.

Gutfreund, H., and M. Schick, 1968, Phys. Rev. **168**, 418.

Haldane, F. D. M., 1980, Phys. Rev. Lett. **45**, 1358.

Haldane, F. D. M., 1981a, Phys. Rev. Lett. **47**, 1840.

Haldane, F. D. M., 1981b, J. Phys. C **14**, 2585.

Haldane, F. D. M., 1981c, Phys. Lett. **81A**, 153.

Haldane, F. D. M., 1982, J. Phys. A **15**, 507.

Haldane, F. D. M., 1988, Phys. Rev. Lett. **60**, 635.

Heeger, A. J., S. Kivelson, J. R. Schrieffer, and W.-P. Su, 1988, Rev. Mod. Phys. **60**, 781.

Hohenberg, P., 1967, Phys. Rev. **158**, 383.

Horovitz, B., T. Bohr, J. M. Kosterlitz, and H. J. Schulz, 1983, Phys. Rev. B **28**, 6596.

Jackiw, R., and C. Rebbi, 1976, Phys. Rev. D **13**, 3398.

Kane, C. L., and M. P. A. Fisher, 1992a, Phys. Rev. B **46**, 15 233.

Kane, C. L., and M. P. A. Fisher, 1992b, Phys. Rev. Lett. **68**, 1220.
Kawakami, N., and S.-K. Yang, 1990, Phys. Lett. A **148**, 359.
Kolomeisky, E. B., 1992, Phys. Rev. B **46**, 13 956.
Kolomeisky, E. B., 1993, Phys. Rev. B **47**, 6193.
Kolomeisky, E. B., 1994, Phys. Rev. Lett. **73**, 1648.
Kolomeisky, E. B., and J. P. Straley, 1992, Phys. Rev. B **46**, 11 749.
Kolomeisky, E. B., and J. P. Straley, 1994, Phys. Rev. B **50**, 8838.
Kolomeisky, E. B., and J. P. Straley, 1995, Phys. Rev. Lett. **74**, 4891.
Kosterlitz, J. M., 1974, J. Phys. C **7**, 1046.
Kosterlitz, J. M., and D. J. Thouless, 1973, J. Phys. C **6**, 1181.
Landau, L. D., and E. M. Lifshitz, 1980, *Statistical Physics*, Vol. 5, Part 1, third edition, revised and enlarged by E. M. Lifshitz and L. P. Pitaevskii (Pergamon), Secs. 137–138, p. 432.
Landauer, R., 1970, Philos. Mag. **21**, 863.
Lieb, E. H., and F. Y. Wu, 1968, Phys. Rev. Lett. **20**, 1445.
Luther, A., 1976, Phys. Rev. B **14**, 2153.
Luther, A., 1977, Phys. Rev. B **15**, 403.
Luther, A., and V. J. Emery, 1974, Phys. Rev. Lett. **33**, 589.
Luther, A., and I. Peschel, 1974, Phys. Rev. Lett. **32**, 992.
Luther, A., and I. Peschel, 1975, Phys. Rev. B **12**, 3908.
Luttinger, J. M., 1963, J. Math. Phys. **4**, 1154.
Ma, S.-K., 1976, *Modern Theory of Critical Phenomena* (Benjamin, Reading).
Mandelstam, S., 1975, Phys. Rev. D **11**, 3026.
Mattis, D., 1974, Phys. Rev. Lett. **32**, 714.
Mermin, N. D., 1967, J. Math. Phys. **8**, 1061.
Mermin, N. D., and H. Wagner, 1966, Phys. Rev. Lett. **27**, 1133.
Mila, F., and X. Zotos, 1993, Europhys. Lett. **24**, 133.
Noguera, C., and V. J. Emery, 1989, Synthetic Metals **29**, F523.
Ovchinnikov, A. A., 1969, Zh. Eksp. Teor. Fiz. **57**, 2137 [Sov. Phys. JETP **30**, 1160 (1970)].
Pokrovsky, V. L., and A. L. Talapov, 1979, Phys. Rev. Lett. **42**, 65.
Popov, V. N., 1972, Teor. Mat. Fiz. **11**, 354 [Theor. Math. Phys. **11**, 65 (1972)].
Rice, M. J., A. R. Bishop, J. A. Krumhansl, and S. E. Trullinger, 1976, Phys. Rev. Lett. **36**, 432.
Schotte, K. D., 1970, Z. Phys. **235**, 155.
Schotte, K. D., and U. Schotte, 1969, Phys. Rev. **182**, 479.
Schulz, H. J., 1980, Phys. Rev. B **22**, 5274.
Schulz, H. J., 1990, Phys. Rev. Lett. **64**, 2831.
Schulz, H. J., 1991, Int. J. Mod. Phys. B **5**, 57.
Schulz, H. J., 1994, in *Strongly Correlated Electronic Materials, Los Alamos Symposium—1993*, edited by K. S. Bedell, Z. Wang, D. E. Melzer, A. V. Balatsky, and E. Abrahams (Addison-Wesley, Reading), p. 187.
Shastry, B. S., 1988, Phys. Rev. Lett. **60**, 639.
Solyom, J., 1979, Adv. Phys. **28**, 209.
Straley, J. P., and E. B. Kolomeisky, 1993, Phys. Rev. B **48**, 1378.
Straley, J. P., and E. B. Kolomeisky, 1995, unpublished.
Su, W.-P., and J. R. Schrieffer, 1981, Phys. Rev. Lett. **46**, 738.
Su, W.-P., J. R. Schrieffer, and A. J. Heeger, 1980, Phys. Rev. B **22**, 2099.
Sutherland, B., 1989, in *Interacting Electrons in Reduced Dimensions*, Vol. 213 of NATO Advanced Science Institutes, Series B: Physics, edited by D. Baeriswyl and D. K. Campbell (Plenum, New York), p. 1.
Wiegmann, P. B., 1978, J. Phys. C **11**, 1583.
Yang, C. N., 1967, Phys. Rev. Lett. **19**, 1312.
Yang, C. N., and C. P. Yang, 1966, Phys. Rev. **150**, 321, 327.